AN ABSTRACT OF THE DISSERTATION OF

Yvonne Chang for the degree of Doctor of Philosophy in Toxicology presented on June 11, 2020.

Title: Toxicogenomic Biomarkers Associated with PAH Carcinogenic Potential in a 3D in Vitro Bronchial Epithelial Model

Abstract approved:

_____

Susan C. Tilton

The environmental health science community recognizes polycyclic aromatic hydrocarbons (PAHs) as a re-emerging class of environmental pollutants due to their persistence and prominence in mixtures of concern. Due to their widespread distribution in the environment, exposure to PAHs often occur as complex chemical mixtures. Exposures are linked to numerous adverse health outcomes in humans, with cancer as the greatest concern. Current assessment of cancer risk for PAHs involves testing individual compounds in a two-year rodent bioassay. These studies are time and resource-intensive, and often lack reproducibility or concordance. Furthermore, they require extrapolation of effects to humans, leading to further uncertainties regarding species-specific biology and chemical mode of action (MOA). The primary method for estimating cancer risk of PAH mixtures is the relative potency factor (RPF) approach in which mixtures are evaluated based on a subset of individual component PAHs compared to benzo[*a*]pyrene (BAP) as a surrogate or reference. However, we and others have found this approach has proved to be inadequate for predicting carcinogenicity of PAH mixtures and certain individual PAHs, particularly those that function through alternate pathways or exhibit greater promotional capacity compared to BAP. Furthermore, the specific mechanisms by which environmental exposures to

PAHs may cause cardio-respiratory diseases and increase cancer risk remains poorly understood.

In this dissertation, we employed a 3D, organotypic human *in vitro* bronchial epithelial culture (HBEC) model to address these gaps in knowledge. First, a comparative transcriptomic evaluation was conducted to assess potential differences in mechanism of toxicity for two PAHs, benzo[*a*]pyrene (BAP) and dibenzo[*def*,*p*]chrysene (DBC), compared to a complex PAH mixture based on short-term biosignatures identified from global gene expression profiling. Comparison of BAP and DBC gene signatures showed that a majority of genes (~60%) were uniquely regulated by treatment, including those enriched for cell cycle, hypoxia, oxidative stress, and inflammation. Gene networks involved in NRF2-mediated oxidative stress detoxification were upregulated by BAP, while DBC downregulated these same targets, suggesting a chemical-specific pattern in transcriptional regulation involved in antioxidant response, potentially contributing to differences in PAH potency. These findings support research scrutinizing the applicability of the RPF, where assumptions of similar MOA are necessary for quantitative PAH cancer risk assessment.

Next, we developed and refined an approach to utilize chemical-specific transcriptional patterns towards accurate classification of carcinogenic potency of PAHs and PAH mixtures. Systems biology information was collected from a human *in vitro* airway epithelial model exposed to a range of non-carcinogenic and carcinogenic PAHs and PAH mixtures. These transcriptional changes were evaluated for differentially enriched biological functions. Individual pathway-based gene sets were tested for optimal classification performance. Posterior probabilities of best performing gene sets were selected and integrated via Bayesian integration resulting in a 91% accurate classifier with four gene sets, including aryl hydrocarbon receptor signaling, regulation of epithelial mesenchymal transition, regulation of angiogenesis, and cell cycle G2-M. In addition, transcriptional benchmark dose modeling of (BAP) showed that the most sensitive gene sets were largely dissimilar from those that best classified

PAH carcinogenicity challenging current assumptions that BAP carcinogenicity (and subsequent mode of action) is reflective of overall PAH carcinogenicity.

Lastly, we evaluated molecular mechanisms related to PAH cancer risk through a two-tiered weighted gene co-expression network analysis (WGCNA) two-tiered approach, first to identify gene sets co-modulated to RPF cancer risk and then to link genes to a more comprehensive list of regulatory values, including inhalation-specific risk values. Over 3,000 genes associated with processes of cell cycle regulation, inflammation, DNA damage, and cell adhesion processes were found to be co-modulated with increasing RPF with pathways for cell cycle S phase and cytoskeleton actin identified as the most significantly enriched biological networks correlated to RPF. These gene sets represent potential biomarkers that can be used to evaluate cancer risk associated with PAH mixtures. In this study, the results illustrated the utility of systems toxicology approaches in analyzing global gene expression towards chemical hazard assessment, and information obtained from these analyses could be used towards future predictive model development. This work expanded current understanding of early mechanisms involved in PAH toxicity and provided novel applications utilizing toxicogenomics and organotypic cell culture models for classification, modelling, and biomarker identification. Together, these advances support further development of alternative approaches for use in predictive and mechanistic toxicology towards chemical hazard assessment.

Toxicogenomic Biomarkers Associated With PAH Carcinogenic Potential in a 3D in Vitro Bronchial Epithelial Model

by
Yvonne Chang

A DISSERTATION

submitted to

Oregon State University

in partial fulfillment of
the requirements for the
degree of

Doctor of Philosophy

Presented June 11, 2020
Commencement June 2021

Doctor of Philosophy dissertation of Yvonne Chang presented on June 11, 2020.

APPROVED:

Major Professor, representing Toxicology

Head of the Department of Environmental and Molecular Toxicology

Dean of the Graduate School

I understand that my dissertation will become part of the permanent collection of Oregon State University libraries. My signature below authorizes release of my dissertation to any reader upon request.

Yvonne Chang, Author

ACKNOWLEDGEMENTS

This journey would not have been possible without the support and guidance of all current and past mentors and friends. I would first like to thank Dr. Susan Tilton for being my research advisor and mentor during my time at Oregon State University. I have tremendous gratitude for her support and encouragement throughout my dissertation research, which has helped me grow into the scientist I am today. I have been inspired by her research vision, and will always be grateful for the opportunity to be her trainee. I would also like to thank all members of my committee: Dr. Robyn Tanguay, Dr. Staci Simonich, Dr. David Williams, Dr. Barbara Taylor, and Dr. Molly Megraw for their contributions and endless support. I am extremely grateful for all faculty, administrative staff, and peers within the Department of Environmental and Molecular Toxicology.

To the past and present members of the Tilton lab (especially Beth, Zhen, Lauren, Brianna, Celine, Kelley, Andrew, and Jamie), I am thankful for all of the support and community we have built. I must also thank Dr. Julia Rager for hosting me at the University of North Carolina, Chapel Hill, and mentoring and providing guidance for my research for Chapter 4. I am so thankful for her patience and infectious enthusiasm towards toxicology research.

To all past mentors that have trusted and believed in me along the way, I express the most gratitude of all. These wonderful leaders and mentors include Katherine Melvin, Scott Dickerman, Kiho Song, Sylwia Fudali, Sara Freeman, Kyla Walter, Galen Miller, Pamela Lein, Jenna Guynn, and Matthew Kelley. I now appreciate the challenges they have laid out for me to overcome, for it was completing those have allowed me to build the confidence to continue tackling greater challenges. I am thankful for every piece of advice they have imparted on me.

I must acknowledge the contributions of my peers in the department. I am thankful for TEAMTox officers and members, for their shared commitment in enhancing science outreach and mentoring to both undergraduate students and K-12 students visiting the Oregon State University campus. These opportunities to encourage young students and early scientists have been among the most rewarding activities of my experience on this campus. I am also thankful for all the fun events and traditions I shared with TEAMTox during graduate school. I am so deeply grateful toward my peers for all the help, kindness, and support they have extended, especially with manuscript edits and presentation feedback. The kindness, generosity, and support of Lindsay Denluck, Mitra Geier, Michael Garland, Raymmah Garcia, Holly Dixon, Prarthana Shankar, Brianna Rivera, Elaine Jennings, Kalilah Hyman, and Burinatt Thanasuwat will not be forgotten.

To the wonderful people I have met in the greater Corvallis community that have supported me through my goals both in and outside of the university, you have my deepest gratitude. To Cindy Martin and Kristin Benson, I have many thanks for their unwavering support of both my career and health goals. They have taught me that fear does not make a goal any less achievable, and that we may just surprise ourselves in our strength and grit if we choose to commit to the process. Lastly, I am very thankful for my family; to my mother Tina, I am most thankful. Her commitment to my education and health continues to keep me grounded. None of this would have been possible without her trust, love, and support.

CONTRIBUTION OF AUTHORS

In all chapters, Dr. Susan Tilton contributed to intellectual formulation, writing, and study design.

Chapter 1: Prepared by Yvonne Chang with editorial comments provided by Susan Tilton.

Chapter 2: Prepared by Yvonne Chang with editorial comments provided by Lindsay Denluck and Susan Tilton. Beth Siddens assisted with cell culture and PAH exposures. David Sampson and Lauren Heine assisted with RNAseq data processing.

Chapter 3: Prepared by Yvonne Chang with editorial comments provided by Mitra Geier, Michael Garland, and Susan Tilton. Beth Siddens assisted with cell culture and PAH exposures. Celine Huynh and Kelley Bastin assisted with data analysis, and Brianna Rivera assisted with sample processing.

Chapter 4: Prepared by Yvonne Chang with editorial comments provided by Julia Rager, Susan Tilton, Mitra Geier, Michael Garland, Jamie Pennington, and Brianna Rivera. Julia Rager assisted with study design, analysis setup, figure formulation, and data interpretation. Susan Tilton assisted with data interpretation.

Chapter 5: Prepared by Yvonne Chang

TABLE OF CONTENTS

TABLE OF CONTENTS (Continued)

LIST OF FIGURES

LIST OF FIGURES (Continued)

LIST OF TABLES

Toxicogenomic biomarkers associated with PAH carcinogenic potential in a 3D in vitro bronchial epithelial model

Chapter 1 – INTRODUCTION

Polycyclic aromatic hydrocarbons as global contaminants

Globally, the environmental health science research community continues to recognize polycyclic aromatic hydrocarbons (PAHs) as a class of environmental contaminants of concern, due to their persistence and environmental pervasiveness. PAHs are a diverse class of chemicals generated through incomplete combustion that may pose environmental, ecological, and human health threats due to their ubiquitous environmental presence and associated carcinogenic activity [1, 2]. Characterized by two to seven fused aromatic rings [3, 4], these chemicals can have numerous substitutions including alkylations and halogenations, leading to a diversity in physical-chemical properties and resulting environmental fate in air, soil, and water [5-7]. Several of these compounds are established carcinogens, and account for 3 of the top 10 pollutants of concern at priority pollutant sites [8-10]. Therefore, ongoing research efforts to better understand PAH environmental levels and biological effects are crucial to protecting environmental and public health.

Air Quality and Human Health

PAHs are widespread in the environment due to their generation and emission from a variety of natural and anthropogenic sources, which include industrial manufacturing processes and combustion of all organic materials, such as fossil fuels. Anthropogenic activity is a major source of PAH emissions in the environment, and this is reflected in the elevated concentrations of PAHs near areas with high industrial and urban development [1, 2, 5, 11-13]. Airborne PAHs can also move across long distances via long-range atmospheric transport, thus their emissions can impact air quality in remote regions far from original sources [14-16]. Poor air quality remains a public health issue in many industrializing countries, particularly in the Western Pacific and South East Asian regions. In

indoor environments, particulate matter (PM2.5) and PAH levels have been reported to exceed international outdoor ambient air guidelines [17]. The World Health Organization (WHO) has also estimated in 2016 that nearly seven million premature deaths are caused each year from the combined effects of household and ambient air pollution, indicating a large global health burden from excessive air pollution [18].

Health effects of PAHs

Inhalation exposure of PAHs is associated with increased risk of acute lower respiratory infections, chronic obstructive pulmonary disease, and lung cancer [19, 20]. However, the mechanisms by which environmental exposures to PAHs may cause or exacerbate cardio-respiratory diseases in children and adults and increase susceptibility to later develop cancer remains poorly understood [17]. The U.S. Agency for Toxic Substances and Disease Registry (ATSDR) has designated 17 PAHs as priority pollutants due to their environmental prevalence and potential toxicity in humans. 16 of these are also designated high priority pollutants by the U.S. EPA. The World Health Organization's International Agency for Research on Cancer (IARC) has designated several PAHs and PAH-containing mixtures, such as diesel exhaust, air pollution, coal and coke mixtures, as either Class 1 known or Class 2A/B probable/possible carcinogens to humans [9, 21-23]. Despite the fact that PAHs were the first class of chemicals identified as chemical carcinogens, little is known about the carcinogenic potential of many of the over 1500 polycyclic aromatic compounds or their potential mechanisms of carcinogenic action.

Challenges to cancer risk assessment of PAHs

One of the most difficult challenges for cancer risk assessment is evaluation of health hazards for chemicals that predominately co-occur in

mixtures like polycyclic aromatic hydrocarbons. Current risk assessment for PAH cancer risk involves testing compounds in a 2-year rodent cancer bioassay. Historically, PAHs have been evaluated as individual chemicals in these assays, primarily through intraperitoneal or dermal routes of administration [24]. However, PAH exposures occur as complex environmental mixtures through inhalation, oral, and dermal routes. These *in vivo* rodent cancer studies are also time and resource-intensive, and inconsistently predictive of responses in humans. Furthermore, they require extrapolation of effects to humans, leading to further uncertainties regarding species-specific biology and chemical mode of action (MOA) [25].

Currently, the accepted method for estimating cancer risk of PAH mixtures is the relative potency factor (RPF) approach, in which mixtures are evaluated based on a subset of individual component PAHs and compared to benzo[*a*]pyrene (BAP) as a surrogate or reference [24]. Because BAP is the index carcinogen to which the potency of other PAHs is compared and estimated to be greater or less than, the first assumption of similar toxicological mode-of-action (MOA) must be true for this approach to accurately estimate cancer risk. While some evidence indicates that the mutagenic and tumor-initiating MOA of BAP (involving aryl hydrocarbon receptor-modulated gene expression and metabolic activation to reactive intermediates) is shared by other PAHs, the structural diversity of PAHs provokes concern for assuming similarities in MOA. The second assumption of this approach is that the sum cancer risk of a mixture can be adequately evaluated based on the sum RPF estimates of individual component PAHs compared to BAP. However, we and others have found this RPF approach inadequate for predicting carcinogenicity of mixtures and also for certain individual PAHs, particularly those that function through alternate pathways or exhibit greater carcinogenic and promotional capacity compared to BAP [26-29].

Chemically induced carcinogenesis is a complex process that involves numerous biological processes and molecular targets during initiation, promotion, and progression. Recent studies using *in vitro* assays and organotypic human *in*

vitro models have identified numerous contributing mechanisms of action in carcinogenic PAHs. Certain PAHs have genotoxic modes of action and induce DNA damage through adduct formation [30-32]. Other carcinogenic PAHs were found to have non-genotoxic modes of action that include estrogenic/antiestrogenic activity [33, 34], inhibition of gap-junctional intercellular communication [26, 35, 36], generation of reactive oxygen species (ROS) and oxidative stress [37-40], and promotional activity via dysregulation of cell proliferation [41, 42].Thus, the complexity in mechanisms of carcinogenicity contributes to difficulty identifying singular endpoints or in vitro assays to predict carcinogenic hazard of chemicals [26, 29, 43-45]. Therefore, it is critical to consider alternative approaches in improving carcinogenic assessment accuracy, speed, and relevance to human health.

Alternative Approaches to Cancer Hazard Assessment of PAHs

Toxicogenomics usage in carcinogenic hazard assessment has progressed considerably in the past two decades; numerous methods have been developed to successfully identify genes linked to specific carcinogenic mechanisms. Applications of transcriptional profiling include correlational analyses and hierarchical clustering to identify genes to describe mechanisms of chemical toxicity [46]. Recent studies have utilized transcriptomics and *in vitro* human cell models to identify gene patterns to discriminate between genotoxic and non-genotoxic carcinogens [47-50] and identify specific pathways that respond differently between genotoxic and non-genotoxic chemicals [51, 52]. The wide range of MOAs identified supports the need for development of a battery of *in vitro* assay endpoints and systems toxicology approaches to evaluate mechanisms and targets involved in chemical carcinogenicity. Therefore, predictive toxicology methods, such as utilizing organotypic models for toxicogenomic profiling and modelling, may reduce the time and resource needed for carcinogenic assessments.

Organotypic 3D human bronchial epithelial cells

Organotypic 3D culture of human bronchial epithelial cells (HBEC) offer a physiologically relevant, sensitive model to evaluating biological perturbations associated with chemical exposure. The human airway epithelium and epithelial lining fluid is the first line of defense against inhaled gaseous and particulate pollutants in the ambient air, and thus a major target zone of toxicity for air pollutants [53]. When differentiated at the air-liquid interface (ALI), primary 3D HBECs develop into a polarized, pseudo-stratified epithelial tissue with tight junctions, basal cells, mucus-secreting goblet cells, and ciliated cells [26, 54, 55]. Transcriptional profiling of a primary *in vitro* airway epithelium also demonstrates a high degree of similarity to healthy human airway epithelia *in vivo* [56]. These findings, in conjunction with the HBEC morphology and differentiated cell types, suggest that primary culture of HBEC can recapitulate the biological responses of the human airway epithelium. Furthermore, the expression of CYP450 metabolizing enzymes in HBECs further increase their utility for evaluating PAH toxicity *in vitro*.

Thesis Objectives

The goal of this dissertation is to advance our understanding of the biological targets and mechanisms of action affected by short-term exposure to carcinogenic PAHs, and to develop a classification model predictive of carcinogenic potency. To achieve this, we performed two studies identifying mechanisms of action through transcriptomic profiling of HBECs (chapters 2 and 4), then tested and developed a classification approach to accurately predict carcinogenic potency of PAHs using gene signatures (chapter 3). Finally, we adapted a coexpression network analysis approach to link gene networks with cancer risk estimates and identify gene networks correlated to increasing cancer risk (chapter 4).

The studies presented in this dissertation demonstrate the utility of employing toxicogenomic approaches in organotypic airway epithelial models to assess the effects of carcinogenic air pollutants and mixtures. A comparative analysis of two carcinogenic PAHs identified dissimilar mechanisms that may mediate enhanced carcinogenicity (chapter 2). For the first time, a classification model to predict carcinogenic potency in human bronchial epithelium was developed, with a 91% integrated accuracy for cancer potency classification (chapter 3). A co-expression network analysis was adapted in a novel approach, and identified over 3,000 co-modulated genes associated to cancer risk and toxicity values (chapter 4). This work expanded current understanding of early mechanisms involved in PAH toxicity, and provided novel applications integrating toxicogenomics and organotypic cell culture models. Together, these advances support further development of alternative approaches for use in predictive and mechanistic toxicology towards chemical hazard assessment.

References

1. Spies, R.B. and D.W. Rice, *Effects of organic contaminants on reproduction of the starry flounder Platichthys stellatus in San Francisco Bay*. Marine Biology, 1988. **98**(2): p. 191-200.
2. Abdel-Shafy, H.I. and M.S.M. Mansour, *A review on polycyclic aromatic hydrocarbons: Source, environmental impact, effect on human health and remediation*. Egyptian Journal of Petroleum, 2016. **25**(1): p. 107-123.
3. Arey, J. and R. Atkinson, *Photochemical Reactions of PAHs in the Atmosphere*. PAHs: An Ecotoxicological Perspective, 2003: p. 47-63.
4. Di Toro, D.M., J.A. McGrath, and D.J. Hansen, *Technical basis for narcotic chemicals and polycyclic aromatic hydrocarbon criteria. I. Water and tissue*. Environmental Toxicology and Chemistry, 2000. **19**(8): p. 1951-1970.
5. Mackay, D. and D. Callcott, *Partitioning and Physical Chemical Properties of PAHs*, in *PAHs and Related Compounds: Chemistry*, A.H. Neilson, Editor. 1998, Springer Berlin Heidelberg: Berlin, Heidelberg. p. 325-345.
6. Sverdrup, L.E., T. Nielsen, and P.H. Krogh, *Soil Ecotoxicity of Polycyclic Aromatic Hydrocarbons in Relation to Soil Sorption, Lipophilicity, and Water Solubility*. Environmental Science & Technology, 2002. **36**(11): p. 2429-2435.
7. IARC Working Group on the Evaluation of Carcinogenic Risks to Humans., World Health Organization., and International Agency for Research on Cancer., *Bitumens and bitumen emissions, and some N- and S-heterocyclic polycyclic aromatic hydrocarbons*. IARC monographs on the evaluation of carcinogenic risks to humans,. 2013, Lyon: IARC Press. v, 342 p.
8. IARC, *Some non-heterocyclic polycyclic aromatic hydrocarbons and some related exposures. Monographs on the evaluation of carcinogenic risks to humans*. IARC MONOGRAPHS ON THE EVALUATION OF CARCINOGENIC RISKS TO HUMANS, 2010. **92**.
9. IARC, *Diesel and gasoline engine exhausts and some nitrarenes*. IARC MONOGRAPHS ON THE EVALUATION OF CARCINOGENIC RISKS TO HUMANS, 2014. **105**.
10. ATSDR, *ATSDR's Substance Priority List: Agency for Toxic Substances and Disease Registry*. ATSDR, 2017.
11. Du, J. and C. Jing, *Anthropogenic PAHs in lake sediments: a literature review (2002–2018)*. Environmental Science: Processes & Impacts, 2018. **20**(12): p. 1649-1666.
12. Pereira, W.E., et al., *Sedimentary record of anthropogenic and biogenic polycyclic aromatic hydrocarbons in San Francisco Bay, California*. Marine Chemistry, 1999. **64**(1): p. 99-113.
13. Arzayus, K.M., R.M. Dickhut, and E.A. Canuel, *Fate of Atmospherically Deposited Polycyclic Aromatic Hydrocarbons (PAHs) in Chesapeake Bay*. Environmental Science & Technology, 2001. **35**(11): p. 2178-2183.

14. Lafontaine, S., et al., *Relative Influence of Trans-Pacific and Regional Atmospheric Transport of PAHs in the Pacific Northwest, U.S.* Environmental Science & Technology, 2015. **49**(23): p. 13807-13816.
15. Killin, R.K., et al., *Transpacific and regional atmospheric transport of anthropogenic semivolatile organic compounds to Cheeka Peak Observatory during the spring of 2002.* Journal of Geophysical Research: Atmospheres, 2004. **109**(D23).
16. Genualdi, S.A., et al., *Trans-Pacific and Regional Atmospheric Transport of Polycyclic Aromatic Hydrocarbons and Pesticides in Biomass Burning Emissions to Western North America*. Environmental Science & Technology, 2009. **43**(4): p. 1061-1066.
17. Oliveira, M., et al., *Children environmental exposure to particulate matter and polycyclic aromatic hydrocarbons and biomonitoring in school environments: A review on indoor and outdoor exposure levels, major sources and health impacts*. Environment International, 2019. **124**: p. 180-204.
18. WHO, *World Health Statistics 2016 data visualizations dashboard: Ambient and household air pollution attributable death rate (2016)*. World Health Organization Global Health Observatory, 2018.
19. Ezzati, M., et al., *Comparative quantification of health risks : global and regional burden of disease attributable to selected major risk factors / edited by Majid Ezzati ... [et al.]*. 2004, World Health Organization: Geneva.
20. Smith, K., S. Mehta, and M. Maeusezahl-feuz, *Indoor Air Pollution from Household Use of Solid Fuels." Comparative Quantification of Health Risks 18:1435–1492*. 2004.
21. Benbrahim-Tallaa, L., et al., *Carcinogenicity of diesel-engine and gasoline-engine exhausts and some nitroarenes*. The Lancet Oncology, 2012. **13**(7): p. 663-664.
22. IARC, *Some non-heterocyclic polycyclic aromatic hydrocarbons and some related occupational exposures*. IARC monographs on the evaluation of carcinogenic risks to humans,. 2010, Lyon, France

Geneva: IARC Press ;

Distributed by World Health Organization. viii, 853 p.
23. Rengarajan, T., et al., *Exposure to polycyclic aromatic hydrocarbons with special focus on cancer*. Asian Pacific Journal of Tropical Biomedicine, 2015. **5**(3): p. 182-189.
24. EPA, U.S., *Development of a Relative Potency Factor (Rpf) Approach for Polycyclic Aromatic Hydrocarbon (PAH) Mixtures (External Review Draft)*, U.S. Environmental Protection Agency, Editor. 2010: Washington, DC

25. Gottmann, E., et al., *Data quality in predictive toxicology: reproducibility of rodent carcinogenicity experiments.* Environmental health perspectives, 2001. **109**(5): p. 509-514.
26. Chang, Y., et al., *Comparative mechanisms of PAH toxicity by benzo[a]pyrene and dibenzo[def,p]chrysene in primary human bronchial epithelial cells cultured at air-liquid interface.* Toxicology and Applied Pharmacology, 2019. **379**: p. 114644.
27. Siddens, L.K., et al., *Polycyclic aromatic hydrocarbons as skin carcinogens: Comparison of benzo[a]pyrene, dibenzo[def,p]chrysene and three environmental mixtures in the FVB/N mouse.* Toxicology and applied pharmacology, 2012. **264**(3): p. 377-386.
28. Courter, L.A., et al., *The influence of diesel exhaust on polycyclic aromatic hydrocarbon-induced DNA damage, gene expression, and tumor initiation in Sencar mice in vivo.* Cancer Letters, 2008. **265**(1): p. 135-147.
29. Tilton, S.C., et al., *Mechanism-Based Classification of PAH Mixtures to Predict Carcinogenic Potential.* Toxicol Sci, 2015. **146**(1): p. 135-45.
30. Topinka, J., et al., *DNA adduct formation in mammalian cell cultures by polycyclic aromatic hydrocarbons (PAH) and nitro-PAH in coke oven emission extract.* Mutation Research/Genetic Toxicology and Environmental Mutagenesis, 1998. **419**(1): p. 91-105.
31. Ross, J.A., et al., *Adenomas induced by polycyclic aromatic hydrocarbons in strain A/J mouse lung correlate with time-integrated DNA adduct levels.* Cancer Res, 1995. **55**(5): p. 1039-44.
32. Baird, W.M. and B. Mahadevan, *The uses of carcinogen-DNA adduct measurement in establishing mechanisms of mutagenesis and in chemoprevention.* Mutation Research/Fundamental and Molecular Mechanisms of Mutagenesis, 2004. **547**(1): p. 1-4.
33. Sievers, C.K., et al., *Differential action of monohydroxylated polycyclic aromatic hydrocarbons with estrogen receptors α and β.* Toxicological sciences : an official journal of the Society of Toxicology, 2013. **132**(2): p. 359-367.
34. Kummer, V., et al., *Estrogenic activity of environmental polycyclic aromatic hydrocarbons in uterus of immature Wistar rats.* Toxicol Lett, 2008. **180**(3): p. 212-21.
35. Bláha, L., et al., *Inhibition of Gap-Junctional Intercellular Communication by Environmentally Occurring Polycyclic Aromatic Hydrocarbons.* Toxicological Sciences, 2002. **65**(1): p. 43-51.
36. Upham, B.L., et al., *Nongenotoxic Effects of Polycyclic Aromatic Hydrocarbons and Their Ozonation By-Products on the Intercellular Communication of Rat Liver Epithelial Cells.* Toxicological Sciences, 1994. **23**(3): p. 470-475.
37. Penning, T.M., et al., *Dihydrodiol Dehydrogenases and Polycyclic Aromatic Hydrocarbon Activation: Generation of Reactive and Redox Active o-Quinones.* Chemical Research in Toxicology, 1999. **12**(1): p. 1-18.

38. Park, J.-H., et al., *Polycyclic Aromatic Hydrocarbon (PAH) o-Quinones Produced by the Aldo-Keto-Reductases (AKRs) Generate Abasic Sites, Oxidized Pyrimidines, and 8-Oxo-dGuo via Reactive Oxygen Species.* Chemical Research in Toxicology, 2006. **19**(5): p. 719-728.
39. An, J., et al., *The combined effects of BDE47 and BaP on oxidatively generated DNA damage in L02 cells and the possible molecular mechanism.* Mutat Res, 2011. **721**(2): p. 192-8.
40. Hanzalova, K., P. Rossner, and R.J. Sram, *Oxidative damage induced by carcinogenic polycyclic aromatic hydrocarbons and organic extracts from urban air particulate matter.* Mutation Research/Genetic Toxicology and Environmental Mutagenesis, 2010. **696**(2): p. 114-121.
41. Plíšková, M., et al., *Deregulation of Cell Proliferation by Polycyclic Aromatic Hydrocarbons in Human Breast Carcinoma MCF-7 Cells Reflects Both Genotoxic and Nongenotoxic Events.* Toxicological Sciences, 2004. **83**(2): p. 246-256.
42. Vondráček, J., A. Kozubík, and M. Machala, *Modulation of Estrogen Receptor-Dependent Reporter Construct Activation and G0/G1–S-Phase Transition by Polycyclic Aromatic Hydrocarbons in Human Breast Carcinoma MCF-7 Cells.* Toxicological Sciences, 2002. **70**(2): p. 193-201.
43. Moffat, I., et al., *Comparison of toxicogenomics and traditional approaches to inform mode of action and points of departure in human health risk assessment of benzo[a]pyrene in drinking water.* 2015. **45**(1): p. 1-43.
44. Chepelev, N.L., et al., *Integrating toxicogenomics into human health risk assessment: lessons learned from the benzo[a]pyrene case study.* Crit Rev Toxicol, 2015. **45**(1): p. 44-52.
45. Labib, S., et al., *Comparative transcriptomic analyses to scrutinize the assumption that genotoxic PAHs exert effects via a common mode of action.* Arch Toxicol, 2016. **90**(10): p. 2461-80.
46. Burczynski, M.E., et al., *Toxicogenomics-Based Discrimination of Toxic Mechanism in HepG2 Human Hepatoma Cells.* Toxicological Sciences, 2000. **58**(2): p. 399-415.
47. Magkoufopoulou, C., et al., *A transcriptomics-based in vitro assay for predicting chemical genotoxicity in vivo.* Carcinogenesis, 2012. **33**(7): p. 1421-1429.
48. van Delft, J.H.M., et al., *Comparison of supervised clustering methods to discriminate genotoxic from non-genotoxic carcinogens by gene expression profiling.* Mutation Research/Fundamental and Molecular Mechanisms of Mutagenesis, 2005. **575**(1): p. 17-33.
49. van Delft, J.H.M., et al., *Discrimination of genotoxic from non-genotoxic carcinogens by gene expression profiling.* Carcinogenesis, 2004. **25**(7): p. 1265-1276.

50. Lee, S.J., et al., *Distinguishing between genotoxic and non-genotoxic hepatocarcinogens by gene expression profiling and bioinformatic pathway analysis.* Scientific Reports, 2013. **3**(1): p. 2783.
51. Kim, J.-Y., et al., *Identification of potential biomarkers of genotoxicity and carcinogenicity in L5178Y mouse lymphoma cells by cDNA microarray analysis.* Environmental and Molecular Mutagenesis, 2005. **45**(1): p. 80-89.
52. Watanabe, T., et al., *Discrimination of genotoxic and non-genotoxic hepatocarcinogens by statistical analysis based on gene expression profiling in the mouse liver as determined by quantitative real-time PCR.* Mutation Research/Genetic Toxicology and Environmental Mutagenesis, 2012. **747**(2): p. 164-175.
53. Mathis, C., et al., *Human bronchial epithelial cells exposed in vitro to cigarette smoke at the air-liquid interface resemble bronchial epithelium from human smokers.* American Journal of Physiology - Lung Cellular and Molecular Physiology, 2013. **304**(7): p. L489-L503.
54. Yamaya, M., et al., *Differentiated structure and function of cultures from human tracheal epithelium.* Am J Physiol, 1992. **262**(6 Pt 1): p. L713-24.
55. Karp, P.H., et al., *An in vitro model of differentiated human airway epithelia. Methods for establishing primary cultures.* Methods Mol Biol, 2002. **188**: p. 115-37.
56. Pezzulo, A.A., et al., *The air-liquid interface and use of primary cell cultures are important to recapitulate the transcriptional profile of in vivo airway epithelia.* Am J Physiol Lung Cell Mol Physiol, 2011. **300**(1): p. L25-31.

CHAPTER 2 – Comparative mechanisms of PAH toxicity by benzo[*a*]pyrene and dibenzo[*def,p*]chrysene in primary human bronchial epithelial cells cultured at air-liquid interface

Yvonne Chang[a,b], Lisbeth K. Siddens[a,b], Lauren K. Heine[a,1], David A. Sampson[a,2], Zhen Yu[a], Kay A. Fischer[c], Christiane V. Löhr[c], Susan C. Tilton[a,b,*]

[a]Environmental and Molecular Toxicology Department, Oregon State University, Corvallis, OR, USA
[b]NIEHS Superfund Research Program, Oregon State University, Corvallis, OR, USA
[c]College of Veterinary Medicine, Oregon State University, Corvallis, OR, USA
*Corresponding author at: Environmental and Molecular Toxicology Department, Oregon State University, Corvallis, OR 97330. *E-mail address*: susan.tilton@oregonstate.edu
[1]Present address: Pharmacology and Toxicology Department, Michigan State University, East Lansing, MI, USA
[2]Present address: Knight Cancer Institute, Oregon Health Sciences University, Portland, OR, USA

Toxicology and Applied Pharmacology.
Reprinted with permission

Abstract

Current assumption for assessing carcinogenic risk of polycyclic aromatic hydrocarbons (PAHs) is that they function through a common mechanism of action; however, recent studies demonstrate that PAHs can act through unique mechanisms potentially contributing to cancer outcomes in a non-additive manner. Using a primary human 3D bronchial epithelial culture (HBEC) model, we assessed potential differences in mechanism of toxicity for two PAHs, benzo[*a*]pyrene (BAP) and dibenzo[*def,p*]chrysene (DBC), compared to a complex PAH mixture based on short-term biosignatures identified from transcriptional profiling. Differentiated bronchial epithelial cells were treated with BAP (100-500 µg/mL), DBC (10 µg/mL), and coal tar extract (CTE 500-1500 µg/mL, SRM1597a) for 48 hrs and gene expression was measured by RNA sequencing or quantitative PCR. Comparison of BAP and DBC gene signatures showed that the majority of genes (~60%) were uniquely regulated by treatment, including signaling pathways for inflammation and DNA damage by DBC and processes for cell cycle, hypoxia and oxidative stress by BAP. Specifically, BAP upregulated targets of AhR, NRF2, and KLF4, while DBC downregulated these same targets, suggesting a chemical-specific pattern in transcriptional regulation involved in antioxidant response, potentially contributing to differences in PAH potency. Other processes were regulated in common by all PAH treatments, BAP, DBC and CTE, including downregulation of genes involved in cell adhesion and reduced functional measurements of barrier integrity. This work supports prior *in vivo* studies and demonstrates the utility of profiling short-term biosignatures in an organotypic 3D model to identify mechanisms linked to carcinogenic risk of PAHs in humans.

Keywords: Benzo[a]pyrene; Polycyclic Aromatic Hydrocarbons; Toxicogenomics; Mixtures; Bronchial Epithelial Cells; Organotypic Culture

1. Introduction

Polycyclic aromatic hydrocarbons (PAHs) are a chemically diverse class of environmental pollutants found in air, water, and soil, emitted by incomplete combustion of natural and anthropogenic sources, with over 1500 species of substituted and unsubstituted PAHs in the environment. Anthropogenic sources of PAHs include fossil fuel burning, vehicle exhaust, wood burning, and coal-tar pitch and asphalt production [1]. As such, inhalation is a primary route of exposure to PAHs in ambient air, indoor air, and cigarette and tobacco smoke. Humans are primarily exposed to PAHs as complex mixtures, which are dependent on the amount and type of combustion. Higher molecular weight PAHs (containing 4 or more fused benzene rings) tend to have lower aqueous solubility and greater lipophilicity [2]. These can be found in the particle phase in ambient air. A number of high MW PAHs are linked to carcinogenic and mutagenic effects in humans, including benzo[*a*]pyrene (BAP; classified by International Agency for Research on Cancer (IARC) as a Class 1 known human carcinogen.) [3-6] Additionally, dibenzo[*def,p*]chrysene (DBC), formerly known as dibenzo[*a,l*]pyrene, is classified as a class 2A probable human carcinogen [4]. Both BAP and DBC are environmental carcinogens linked with multiple cancer types, particularly lung and skin [7].

The U.S. Environmental Protection Agency Integrated Risk Information System's (IRIS) 2010 release of a relative potency factor (RPF) approach for cancer risk assessment of PAH mixtures provided recommendations for quantitative cancer risk assessment by scaling doses and potency relative to benzo[a]pyrene (BAP), the index carcinogen [8]. Because BAP is the index carcinogen to which potency is estimated to be greater or less than, the first assumption of similar toxicological mode-of-action (MOA) must be true for this approach to accurately estimate cancer risk. While some evidence indicates that the mutagenic and tumor-initiating MOA of BAP (involving aryl hydrocarbon receptor-modulated gene expression and metabolic activation to reactive

intermediates) is shared by other PAHs, the structural diversity of PAHs provokes concern for assuming similarities in MOA [9].

The aryl hydrocarbon receptor (AhR) is well established as a key modulator in genotoxic PAH toxicity [10, 11]. The MOA involves binding and activating the AhR, translocation from the cytosol to the nucleus, and subsequent binding to xenobiotic response elements. This activates the transcription of many genes, some of which metabolize xenobiotics. For PAHs containing a "bay" and/or a "fjord" region (as is the case for both BAP and DBC), cytochrome P450 (CYP450)-dependent metabolism into diol epoxides is necessary for the genotoxic and mutagenic effects of PAHs. As diol epoxide metabolites, the PAHs are then able to bind DNA and other cellular constituents, which can lead to DNA strand breakage, protein damage, redox cycling, and/or oxidative stress. While the method of PAH toxicity through DNA damage is shared by genotoxic PAHs, the pathways can be markedly different and complex for potentially non-genotoxic carcinogenic PAHs, or complex PAH mixtures. DBC is the most potent carcinogenic PAH studied (*in vivo* rodent skin tumor assay), with an RPF estimated 30-100 (30-100 times the potency of BAP, RPF of 1) [12]. While RPF correlates well with DNA adduct formation, it does not correlate well with tumor incidence for DBC, indicating non-genotoxic mechanisms may contribute to carcinogenesis [13]. There is substantial transcriptomics evidence that BAP and DBC can act through unique mechanisms leading to tumor development in mouse skin *in vivo* [13]. Previous work in an *in vivo* rodent model determined that key mechanisms and pathways able to discriminate between low, medium, and high tumorigenicity in rodent *in vivo* utilized genes belonging to inflammation signaling, oxidative stress, and cell adhesion and barrier integrity processes.

Toxicity testing in animal models is often resource-intensive, time-consuming, and inconsistently predictive of human responses. While humans and rodents share common cytochrome P450 enzymes for detoxification and elimination of toxicants, the rates of phase I reactions and preferred pathways of phase II reactions vary significantly [14]. There is evidence that the CYP450

activities of model organisms used for toxicity (mouse, rat, rabbit, dog, micropig, monkey) do not resemble human CYP450 activity profiles well [15, 16]. Focusing research efforts towards advancing human cell cultures allows evaluation of human-specific xenobiotic metabolism and responses, and the capacity for high throughput screening and bioassays. Increasingly, 3D cell cultures and organoid culture models are used for toxicological and pharmacological studies for their ability to better recapitulate *in vivo*-like cellular heterogeneity and physiological response. Their multicellularity, cell-cell interactions and cell-matrix interactions support establishment and maintenance of a cellular microenvironment homeostasis, which may be why cells cultured in 3D tend to exhibit greater resistance to cytotoxic injury [17]. Cells cultured in 3D with multiple cell types are found to better withstand oxidative stress rather than monoculture, and the cell-cell interactions and crosstalk allow further toxicological evaluation of processes such as disruptions in cellular adherence, cell migration, differentiation, and healing [18, 19].

Organotypic culture of human bronchial epithelial cells (HBEC) offer a physiologically relevant, sensitive model to study the effects of air pollutant chemicals and mixtures *in vitro*. The human airway epithelium is a major target zone of toxicity for inhaled air pollutants, and the expression of CYP metabolizing enzymes in HBECs make them ideal for studying PAH toxicity *in vitro*. In the present study, we employed the EpiAirway™ bronchial epithelium model, in which cells are differentiated at the air-liquid interface (ALI), to assess toxicity profiles of BAP and DBC, two potent carcinogens commonly found in air pollutant mixtures, in comparison to a PAH mixture. The 3D culture of primary bronchial epithelial cells was shown to be more toxicologically resistant than the 3D culture of immortalized bronchial epithelial cells in tobacco smoke toxicity evaluations [17]. In response to environmental toxicants, HBEC differentiated at the ALI exhibit degradation of tight junctions, decreased cell viability, and compensatory or protective responses at sub-toxic concentrations, including increased mucus secretion, and goblet cell hyperplasia and hypertrophy similar to

clinically documented changes in the bronchial epithelium of smokers [20, 21]. Transcriptional signatures were profiled short-term after treatment with BAP and DBC using a systems biology approach in a differentiated primary 3D HBEC model. Functional epithelial barrier integrity and cytotoxicity were also evaluated and compared to transcriptional data. Next-generation sequencing techniques provided a rapid, effective method to uniformly detect thousands of changes in the HBEC model after short-term PAH treatment.

2. Materials and Methods

2.1 Chemicals and Reagents

Cell culture media and phosphate buffered saline (PBS) were provided by MatTek Corporation (Ashland, MA). Benzo[*a*]pyrene (BAP; CAS# 50-32-8) and dibenzo[*def,p*]chrysene (DBC; CAS# 189-64-0) were purchased from MRIGlobal (Kansas City, MO). Coal Tar Extract,SRM 1597a,(CTE) was purchased form the National Institute of Standards & Technology (Gaithersburg, MD.) DNase I, TRIzol® reagent, Superscript® III First Strand Synthesis System, qPCR primers, and Pierce™ LDH Cytotoxicity Assay Kit were from Thermo Fisher Scientific (Waltham, MA). 2X SsoAdvanced™ Universal SYBER®Green Supermix was purchased from BioRad Laboratories, Inc. (Hercules, CA.)

2.2. Tissue Culture and Treatments

Primary HBEC differentiated on transwell inserts at the ALI (EpiAirway™ 100, MatTek, Ashland, MA) were transferred to 6-well plates each well containing 1 ml of assay medium and equilibrated for 24 hours at 37°C, 5% CO_2 followed by a change of fresh medium before treatment. Inserts were washed with phosphate buffered saline (PBS, pH 7.4) and then treated with PAHs in

acetone vehicle (n=4 per treatment) on apical surface for up to 48 hrs, BAP (1-500 µg/ml), DBC (1-50 µg/ml) and CTE (250 -1500 µg/ml). Dosing was chosen based on relative potency in BAP equivalents (BAP_{eq}) for DBC (~50 BAP_{eq}) and CTE (0.4 BAP_{eq}) as previously reported [12, 22]. At the end of each exposure regimen, the matrix and tissue from each well insert was carefully peeled away with forceps, placed in cryovials containing 0.5 ml TRIzol® reagent and snap frozen in liquid nitrogen. Frozen tissues were stored at -80°C until further analysis. Basal media was transferred to clean, sterile tubes and stored at -80°C for evaluation of cytotoxicity.

2.3 Histology

HBEC cultures were washed briefly with phosphate-buffered saline (PBS, pH 7.4) and fixed in 10% neutral buffered formalin for 48 h. The membranes were excised from the culture inserts with a surgical blade, fixed in 10% formalin, processed and embedded in paraffin. For staining and immunohistochemistry, 4 to 5-µm-thick sections were cut, mounted on slides, and deparaffinized by processing through a series of xylene and ethanol solutions. Sections were stained with hematoxylin and eosin (H&E) and analyzed by light microscopy using a Nikon Eclipse E400. Deparaffinized sections of cell culture membranes also were stained for tumor protein 63 (p63), proliferation marker protein Ki-67 (Ki67), and mucus-producing goblet cells identified by periodic acid Schiff's (PAS) staining. For Ki67 staining, paraffin sections were high-temperature antigen retrieved with BDTM Retrieval A solution (Dako). For Ki67 and p63 staining, endogenous peroxidase activity was blocked by immersing slides in methanol containing 3% hydrogen peroxide for 10 minutes. The following primary anti-human antibodies were applied for 30 minutes at room temperature: rabbit polyclonal antiserum against human p63 (1:100; PA5-36069; ThermoFisher, Rockford, IL) and Ki-67 (1:20; PA5-16785; ThermoFisher, Rockford, IL). MaxPoly-One Polymer HRP Rabbit Detection solution (MaxVision Biosciences, Bothell, WA) was applied for

7 minutes at room temperature and Nova Red (SK-4800; Vector Labs, Burlingame, CA) as chromagen was used with Dako hematoxylin (S3302) as counterstain. Serial sections of formalin-fixed paraffin-embedded cell culture membranes incubated with Dako Universal negative serum served as negative controls. Mucus-producing goblet cells were identified by periodic acid Schiff's (PAS) staining. Slides were mounted and examined by light microscopy. For immunofluorescence, membranes were fixed in ice-cold MeOH + acetone and incubated with primary antibody (monoclonal anti-human gastric Mucin-5B (MUC5B), sigma M5293, 1:250; monoclonal anti- β- tubulin, Sigma T7941, 1:500) overnight at 4^0 C, following with second antibody (1:200; anti-mouse IgG (H+L), F(ab')2 fragment (Alexa Fluor® 647 Conjugate, Cell Signaling Technology). The inserts were removed and mounted on slides using a Prolong Gold Antifade Reagent® (Thermos Fisher) for imaging with a Zeiss LSM 780 confocal microscope.

2.4. Transepithelial Electrical Resistance (TEER)

Transepithelial electrical resistance (TEER) measurements were made using an epithelial volt-ohmmeter (EVOM2, World Precision Instruments, Sarasota, FL). The EVOM2 was calibrated using a test electrode prior to the measurements. At time zero and 48 hrs (n=4) after treatment with BAP (1-500 µg/ml), DBC (1-50 µg/ml), CTE (250-1500 µg/ml), PBS, pH 7.4, was added to both apical and basal chambers and resistance was measured (ohms) for each insert. An empty culture insert was used to correct for the background resistance. Four cultures were used for each treatment concentration and time point. Percent TEER of control were calculated by subtracting background from TEER, then calculating the difference between 48 hr TEER minus background and 0 hr TEER minus background. Treatment effects on TEER were evaluated for significance ($p<0.05$) by one-way ANOVA with Dunnett's multiple testing correction.

2.5. Cell Viability

Lactate dehydrogenase (LDH) leakage was measured in media after treatment with PAHs (n=4) for 48 hrs using Pierce LDH Cytotoxicity Assay Kit (Thermo Scientific) following manufacturer instructions. The 48 hr timepoint was the longest PAH exposure period tested in HBEC, during which media is not changed. Briefly, basal medium samples (40 µl) were aliquoted into the wells of a 96-well plate. LDH reaction reagent (40 µl) was added to each sample and incubated at room temperature for 30 minutes while protected from light. Finally, 40µl of stop solution was added to each well and mixed. LDH activity was determined by subtracting absorbance at 680nm (background) from absorbance at 490nm (Synergy HTX plate reader, BioTek, Winooski, VT). A negative control of fresh cell culture medium, a positive control of medium from lysed cells, and vehicle only controls were included. Cytotoxicity was evaluated by one-way ANOVA with Dunnett's multiple testing correction ($p<0.05$).

2.6. RNA Isolation and Quality Control

Total RNA was isolated from HBEC (n=4) using TRizol® reagent and was quantified on a Synergy HTX plate reader equipped with a Take3 module (BioTek). RNA quality was evaluated based on 260/280 ratio (acceptable range 2.0-2.1) and by examining 18S and 28S peaks (Bioanalyzer 2100, Agilent, Santa Clara, CA). Acceptable RNA quality was based on RIN $\geq$ 8.5.

2.7. mRNA-Sequencing and Analysis

Total RNA from HBEC treated with BAP (500 µg/ml; 19.8 nmol), DBC (10 µg/ml, 0.35 nmol) and vehicle control (n=4 per treatment) for 48 hr were sent to the Oregon State University Center for Genome Research and Biocomputing Core facilities for library preparation and sequencing. mRNA was poly-A

selected, and libraries were prepared with the PrepXTM mRNA and Illumina sequencing workflow (Wafergen Biosystems, Fremont, CA). Paired-end sequencing (150 bp) was conducted with an Illumina HiSeq 3000 sequencer, which yielded ~30 million reads per sample. Sequenced reads were first put through Cutadapt (version 1.8.1) to trim adapter sequences from the paired-end reads. The human genome assembly GRCh38.84 was indexed using bowtie2-build (version 2.2.3) while the transcriptome was indexed using TopHat (version 2.1.1.) [23]. TopHat was used again to align the trimmed reads to indexed transcriptome and genome [24]. Differential expression was determined in CuffDiff (version 2.2.1) compared to vehicle control [25]. The differentially expressed gene lists ($q<0.05$) for oppositely regulated, commonly regulated, and uniquely regulated genes between BAP and DBC were used for pathway enrichment analysis in MetaCore (Clarivate Analytics, Philadelphia, PA). Statistical significance of over-connected interactions was calculated using a hypergeometric distribution, where the p value represents the probability of a particular mapping arising by chance for experimental data compared to the background [26]. Heatmaps were generated in MultiExperiment Viewer TM4 [27]. Network visualizations were generated in Cytoscape (v3.5.1) [28].

2.8. Quantitative PCR (qPCR)

cDNA was synthesized using a Superscript® III First Strand Synthesis Supermix kit per manufacturer's instructions. Reactions were diluted 1:5 with nuclease –free water and stored at -80°C until used for qPCR. A BioRad Laboratories, Inc. (Hercules, CA.) CFX96 Touch™ Real-Time PCR Detection System was used for running 20 µl qPCR reactions to survey key gene targets. Each reaction contained 2 µl cDNA template (10 ng RNA), 150 nM of each primer, 10 µl 2X SsoAdvanced™ Universal SYBER®Green Supermix, and nuclease–free water. A list of primer sequences is reported in Supplemental Table 1. The thermocycler was programmed for 1 cycle 95°C for 1 minute initial

denaturing, 40 cycles 95°C for 15 sec denaturing, 60°C for 30 sec annealing/elongation, and a melt curve 65-95°C/0.5° per 5 sec for validating single product amplification. The relative expression differences among treatments were calculated using the ΔΔCt comparative method and normalized to housekeeping genes *beta-actin* (*ACTB*) and *peptidylprolyl isomerase A* (*PPIA*). Genes significantly regulated by PAH treatment ($p<0.05$), including BAP (100-500 µg/ml), DBC (5-10 µg/ml) and CTE (500-1500 µg/ml) for 6-48 hr (48 hr only for CTE), were identified by one-way ANOVA with Tukey's multiple testing correction.

3. Results

3.1. Evaluation of differentiated HBEC cultured at ALI

The morphology of differentiated HBEC cultures was evaluated by histological methods prior to treatments. H&E staining of tissue sections indicated that cultures were fully differentiated into a pseudostratified mucociliary epithelium showing goblet cells and ciliated cells along the apical side (Fig. 1A). Epithelial cells were distinguished by cell-specific markers. Immunohistochemistry was used to visualize Ki67, which is a marker of actively proliferating cells identified exclusively on the basal side, (Fig 1B) and p63, which is a marker of basal epithelial cells (Fig 1C). Mucus producing goblet cells were visualized on the apical side with PAS stain (Fig. 1D). MUC5B (marker of glandular mucous cells) and B-tubulin (ciliated respiratory cells) were visualized by immunofluorescence (Fig. 1E). Cells treated with BAP, DBC and CTE at concentrations ranging 1-1500 µg/ml applied to the apical surface for 48 hours resulted in no increase in toxicity as measured by release of LDH into media (Fig. 2).

3.2. Global gene expression analysis

We investigated the effects of BAP and DBC treatment on 3D HBEC on the molecular level by analyzing global gene expression patterns using RNAseq. Raw and normalized sequencing files are available online at NCBI Gene Expression Omnibus (GSE128471). Of the more than 60,000 transcripts mapped, there were 3486 statistically significant ($q<0.05$). A heatmap of 3486 differentially expressed genes (DEG) was generated using an unsupervised hierarchical clustering analysis (Fig. 3A). BAP treatment resulted in 2244 DEG and DBC treatment resulted in 2126 DEG compared to vehicle control. The dendrogram shows that biological replicates for each treatment cluster together indicating the variance between treatments is greater than the variance measured within replicates for each treatment. Among the total DEG, about three-quarters of genes were unique to each treatment, and not differentially regulated by the other treatment (1360 DEG were unique to BAP, and 1242 DEG were unique to DBC). About a quarter of the DEG (884) were common between BAP and DBC as shown by the Venn diagram in Fig. 3B. Gene expression analysis supports the hypothesis that while BAP and DBC function through a subset of commonly regulated genes and pathways, each also have chemical-specific profiles that contribute to toxicity in human bronchial epithelial cells.

3.3. Barrier function toxicity as a common mechanism of toxicity in HBEC by BAP and DBC

To further analyze the treatment responses between BAP and DBC for mechanistic similarities and differences, the DEG were analyzed for significantly enriched pathways. Genes regulated in common by BAP and DBC, which means they were significantly different from control ($q<0.05$) for both treatments, were split into upregulated and downregulated subsets for analysis (Fig. 3C). Overall, pathways associated with cell cycle and nuclear receptor signaling were significantly enriched for genes increased by both BAP and DBC, while many pathways related to cell adhesion and barrier function were significantly enriched

for decreased gene sets. In fact, pathways related to barrier integrity were some of the most significantly enriched pathways affected by BAP and DBC treatment compared to control and broadly include pathways associated with cell adhesion, epithelial-to-mesenchymal transition, TGF-beta signaling and cytoskeleton. Genes specifically associated with three cell adhesion pathways (Cell adhesion_Cell junctions, Cell adhesion_Cadherins, and Cell adhesion_Integrin-mediated cell-matrix adhesion) were compiled into a gene list related to barrier function and visualized in a heatmap (Fig. 4A). Most genes associated with these pathways were significantly decreased ($q<0.05$) in common by BAP and DBC treatment compared to control and support functional measurements of barrier integrity in HBEC (Fig. 4B). One pathway (nuclear receptor transcriptional regulation) was significant for both the increased and decreased gene sets (compared to control) indicating this pathway, which broadly includes a number of nuclear signaling pathways, was significantly enriched by both datasets.

TEER in HBEC was measured as a functional indicator of barrier integrity 48 hours after chemical treatment and results are normalized to vehicle control (Fig. 4B). A significant decrease in TEER ($p<0.05$) was observed at the highest concentrations tested for BAP and DBC (500 µg/ml and 50 µg/ml, respectively) indicating a loss of cell barrier integrity. The effects of BAP and DBC on barrier integrity were compared to CTE as a mixture of PAHs that includes both BAP and DBC [12]. The dose-response range for BAP, DBC and CTE were broadly overlapping based on reported relative potency with DBC ranging 30-100 BAPeq and CTE 0.4 BAPeq [12, 22]. HBEC were more sensitive to barrier function toxicity by CTE, which resulted in significant decreases in TEER (66-73%) at concentrations as low as 500 µg/ml. While the reduction in TEER from BAP and DBC treatment correlate with a decrease in gene expression for barrier function as measured by RNASeq, specific gene expression biomarkers of tight junction and gap junction integrity were significantly decreased at concentrations lower than those that significantly reduced TEER suggesting that gene expression may be a more sensitive endpoint or there may be a threshold associated with gene level

changes that contribute to functional integrity measures. (Figs. 4C and 4D). Specifically, *tight junction protein 2* (*TJP2*) and *gap junction 1* (*GJA1*) were decreased following 48 hour exposure to BAP and DBC at concentrations lower than those required for functional impairment of barrier integrity as measured by TEER (Fig. 4C). Coal tar extract treatments also significantly ($p<0.05$) downregulated a number of barrier genes by qPCR, including *TJP2*, tight junction protein 1 (*TJP1)*, *GJA1*, and claudin 1 (*CLDN1)*. These genes were chosen based on relevance to tight junction and gap junction structures and BAP/DBC RNASeq results. Overall, these data show that the BAP, DBC and CTE all inhibit barrier integrity mediated by down regulation of gap junction and tight junction processes.

3.4. BAP and DBC uniquely regulate transcriptional targets of AHR and NRF2 in HBEC

Significantly enriched pathways ($p<0.05$) were also analyzed for DEG uniquely up and down regulated by BAP and DBC (Fig. 5). These data highlight a number of important biological processes that are regulated in a chemical-specific manner in HBEC. For example, BAP uniquely upregulates pathways related to cell cycle, hypoxia and oxidative stress while processes upregulated by DBC were related to inflammation and DNA damage signaling. DBC uniquely down-regulated genes from mitochondrial apoptosis pathways and the initiation and elongation processes of translation. BAP uniquely downregulated several pathways that DBC did not, notably the inflammation, IL-10, IL-2 signaling pathways and cell cycle G1-S regulation. BAP also downregulated several pathways related to barrier integrity that were observed to also be important for DBC (Fig. 3C).

Given the importance of oxidative stress as a mechanism of PAH toxicity, we focused on this pathway, which was only enriched in BAP, for confirmation by qPCR. Further, we noticed a subset of genes significantly regulated in

opposite directions by BAP and DBC that were associated with oxidative stress and antioxidant signaling processes. In general, these genes were upregulated by BAP and down regulated by DBC and included phase I and II metabolizing enzymes and known transcriptional targets of the *arylhydrocarbon receptor* (*AHR*) and *nuclear factor erythroid 2–related factor 2* (*NRF2*). Dose-dependent *CYP1A1* and *CYP1B1* induction were observed in HBEC after treatment by BAP and CTE for time points ranging 6-48 hr (Fig. 6A). However, during the same time range, DBC significantly decreased *CYP1A1* and *CYP1B1* in a dose-dependent manner (Fig. 6A). This unique pattern of response for CYP1A1 AND CYP1B1 by BAP and DBC, which is consistent with that previously published in mouse epithelium [12], was confirmed using overlapping concentrations for BAP and DBC in a subsequent experiment (Supplemental Figure 1). Similar results were observed for NAD(P)H quinone dehydrogenase (*NQO1)*, aldehyde dehydrogenase 3 family member A1 (*ALDH3A1)*, and glutathione S-transferase alpha (*GSTA)* in which dose-dependent increases were measured 48 hr after BAP and CTE treatment (by RNAseq and qPCR), while genes were either downregulated or not significantly changed (by qPCR or RNAseq) after treatment with DBC (Fig. 6B). One notable exception is the downregulation of *GSTA* by CTE, while BAP increased expression of this gene supporting that PAHs and PAH mixtures result in exposure-specific gene expression profiles in lung cells.

The extent of the differences in AHR and NRF2 signaling by BAP and DBC in HBEC is represented in the transcription factor signaling network in Fig. 6C. The 3486 DEG were filtered for genes significantly regulated in opposite directions by BAP and DBC. These genes were uploaded into Metacore for network building, and we found that *NRF2* and *AHR* are major hubs connecting genes that are oppositely regulated by BAP and DBC treatment. Using MetaCore's Interactome tool, an Interactions by Protein function analysis returned the following results for overconnected objects in the active dataset: the top 5 overconnected genes for BAP unique DEG list (up/down) were CAMP responsive element binding protein 1 (*CREB1*), androgen receptor (*AR*), MYC proto-

oncogene (*MYC*), RELA proto-oncogene (*RELA*), and estrogen receptor 1 (*ESR1*). The top 5 overconnected genes for the DBC unique DEG list (up/down) were *MYC*, *CREB1*, YY1 transcription factor (*YY1*), tumor protein 53 (*TP53*), *ESR1*. While they differ slightly in top interconnected genes, it is evident that many of the uniquely regulated genes are interconnected with common hub genes, or transcription factors (*MYC*, *CREB1*, *RELA*.) After filtering the DEG list to include only genes significantly regulated ($q<0.05$) by either BAP or DBC opposite to the other treatment, the Interactome Interactions by Protein analysis was rerun and returned the following top 5 overconnected genes: *NRF2*, kruppel like factor 4 (*KLF4*), *RELA*, cystatin B (*CSTB*), *TP53*. These genes, along with *AHR*, were added to build a network (Fig 6C) of oppositely regulated genes. Based on the top 5 overconnected gene networks, the opposite regulation suggests that *NRF2* and *KLF4* may play a role in modulating BAP and DBC response in a way that is unique between the two PAH treatments.

4. Discussion

This study employed a toxicogenomics approach for comparison of transcriptional differences between BAP and DBC in a 3D HBEC model to evaluate chemical biosignatures after exposure and inform known differences in toxicity to human airway epithelium. We have previously identified PAH-specific biosignatures in mouse skin epithelium *in vivo* linked to carcinogenic risk for PAHs and mixtures [13]. The EpiAirway™ bronchial epithelial model was chosen for its ability to recapitulate *in vivo* phenotypes of tissue structures, cellular responses, signaling, and functional barriers. The complexity of this model makes it an ideal tool to study perturbations in the complex and dynamic processes involved in the mechanisms of PAH toxicity. Global gene signatures for BAP and DBC were further compared to transcriptional biomarkers in HBEC cells after treatment with CTE, a complex mixture of PAHs, and biological and functional changes in cells. BAP and DBC treatment in the bronchial epithelium resulted in

over three thousand genes significantly altered between these two treatments. While a quarter of the genes were regulated in common between these two PAHs, the majority of genes are uniquely regulated by one PAH and not the other. A key strength of this study design is the ability to compare the response of thousands of genes in the human bronchial epithelial model to identify chemical-specific mechanisms and pathways.

4.1 PAH-related barrier integrity alteration

While transcriptional profiling highlighted major differences in regulated pathways and processes between BAP and DBC, the results also supported a degree of similarities between the PAHs. A quarter of the genes significantly regulated were regulated in common between BAP and DBC, and these genes were present in translation, inflammation, cell adhesion, and regulation of cell proliferation processes (Fig 3C). These shared pathways have been reported in studies assessing PAH transcriptional profiles in other models including the zebrafish and Mutamouse, notably processes pertaining to cell adhesion, inflammation, and translation [29, 30]. These commonly enriched pathways by different single PAHs across models and tissues supports the hypothesis that PAHs can share subsets of commonly regulated genes and pathways, yet ultimately function through chemical-specific bioactivity signatures that can contribute to their different toxicities in the target tissues.

In the present study, functional and gene expression assays were used in order to evaluate barrier function integrity after exposing HBECs to various PAH treatments. In pathway enrichment analysis, the pathways related to barrier integrity were some of the most significantly enriched pathways affected by BAP and DBC treatment compared to control. The majority of genes in the barrier integrity gene heatmap were downregulated by BAP and DBC treatment, supporting barrier integrity dysregulation as a shared mechanism of action between BAP and DBC, including epithelial to mesenchymal transition and cell

adhesion. Key genes involved in cell adhesion and epithelial mesenchymal transition have also been reported in PAH-treated HepG2 cells as well, indicating that short-term PAH treatment can result in hundreds of different genes expressed, between PAHs also of varying potencies, yet can share the traits of dysregulating cell junctions and promoting cellular migration [31].

PAHs have been found to decrease barrier function integrity, which in turn can lead to dysregulated inflammation and oxidative stress [32, 33]. Regulation of tight junction and gap junction proteins is essential in maintaining homeostasis in the lungs. Tight junction structures comprised of transmembrane proteins and plaques maintain tissue permeability and intercellular adhesion [33, 34]. Some of these structural proteins, particularly the occludins, have been found to be redox-sensitive in their assembly and breakdown [35]. Elevated oxidative stress and pro-inflammatory cytokines can also disrupt tight junction function, leading to increased airway inflammation [36]. Because dysregulation of tight junctions are associated with asthma and lung cancer, barrier integrity is evaluated as a target of PAH treatment and potential predictor of toxicity [34]. Tight junction downregulation tends to be correlated with TEER reductions, as well as reductions in cingulin, claudins, and other barrier proteins [34].

Trans-epithelial electrical resistance (TEER) measurements were taken to indirectly measure tight junction functional integrity and assess epithelial layer disruption. We found significantly reduced TEER measurements ($p<0.05$) by treatments of BAP, DBC, and CTE. The tight junction and gap junction markers *TJP2* and *GJA1* were also found to be downregulated by treatment to BAP and DBC, and correlated with reductions in TEER at those doses. Similarly, CTE treatment resulted in the significant downregulation of *TJP1*, *TJP2*, *GJA1*, and *CLN1*. The resulting epithelial barrier dysfunction from BAP, DBC, and CTE exposure, measured through TEER and qPCR, further support this as a mechanism of action likely to be shared by PAHs.

4.2 Uniquely regulated hub genes and pathways between BAP and DBC treatment may be the key to understanding DBC's heightened carcinogenic potential

Through global gene expression analysis, a total of 2602 transcripts/genes were identified to be uniquely regulated between BAP and DBC. Approximately half of these genes were uniquely regulated by BAP, while the other half was uniquely regulated only by DBC. Because BAP and DBC exhibit such large differences in their tumorigenic potency *in vivo* [12] and RPF estimate [4], we further investigated the specific roles of the uniquely regulated genes to gain insight on potential contributors to DBC's mechanism of action.

Through the pathway enrichment analysis, we found that BAP and DBC each uniquely regulated subsets of pathways, further indicating that these chemicals may act through dissimilar mechanisms of action. There is mounting evidence that PAHs can have individual chemical signatures that can be used to discriminate chemicals by their properties, including genotoxicity and bioactivity [13, 30, 37]. To date, there are a small but valuable number of studies analyzing the transcriptional profiles of PAH exposures on a number of models. These studies have found that across the developing zebrafish, mouse lung, mouse spleen, mouse skin, and currently the human airway epithelium, PAHs continue to exhibit unique transcriptional profiles with subsets of common, but often unique, enriched pathways and transcription factors [13, 30, 38, 39]. In the present study using a human bronchial epithelial model, we found that while BAP uniquely upregulates pathways related to hypoxia and oxidative stress, and DBC uniquely upregulated pathways related to inflammation and DNA damage signaling (Fig. 3C). These enriched pathways are a result of the over 1200 genes that are uniquely regulated by one PAH treatment, but not the other.

Through hub gene network building, we found shared and unique top over-connected genes (hub genes) for the BAP and DBC unique and oppositely regulated gene lists (Fig6C, 6D). The shared hub genes were *CREB1*, *RELA*, and

MYC, while BAP notably had *AR* as a unique hub gene and DBC had *TP53* as a unique hub gene. After filtering for significance, the top over-connected genes included *NRF2*, *KLF4*, and *TP53*. The network visualizations built relate two key points: BAP and DBC are regulated by a number of similar transcription factors that are known regulators of cell cycle, proliferation, and oxidative stress responses. All these processes related to cancer; however they are not regulated the same way. The genes are oppositely regulated by the same transcription factors, indicating chemical-specific processes occurring at the transcriptional level that are unable to be explained by what is currently known about classic PAH mechanisms of action. These data are consistent with unique differences for BAP and DBC reported in mouse skin epithelium *in vivo* and include processes previously identified as predictive of PAH carcinogenic risk suggesting that PAH-specific gene regulation linked to cancer outcome are maintained in human bronchial epithelial cells *in vitro* [12, 13, 40].

4.3 DBC dysregulates NRF2-mediated oxidative stress detoxification mechanisms

The mechanisms of action of BAP have been researched extensively, resulting in a wealth of knowledge on its effects in *in vitro* and *in vivo* systems [41-43]. BAP toxicity requires a series of CYP-dependent metabolic activation steps to become toxic metabolites, which then damage cellular constituents, including proteins and DNA through adduct formation and redox cycling [6, 42]. The findings of this study support the hypothesis that DBC may act through dysregulation of oxidative stress detoxification mechanisms, particularly by downregulating NRF2 targets. The nuclear factor-erythroid 2-related factor-2 (NRF2) is a transcription factor plays major roles in cellular antioxidant defense by regulating Phase II detoxification genes and activating protective antioxidant responses in the cell. Targets of NRF2 include NQO1, heme oxygenase (HMOX1), superoxide dismutase (SOD1), sulfiredoxin (SRX1), thioredoxin

(TXN), and glutathione peroxidases (GPXs), all of which are enzymes crucial for protective detoxification of oxidative burden. These genes were all downregulated in the DBC-treated HBEC, yet up-regulated in the BAP-treated HBEC. Particularly, the DBC-downregulated enzymes involved in redox reactions (oxidoreductases and redoxins, including multiple glutaredoxins, peroxiredoxins, thioredoxin, sulfiredoxin) typically catalyze reductions of intracellular biomolecules and reactive oxygen species to confer oxidative stress resistance. A loss in antioxidant activity is likely to increase cellular damage, since a key compensatory mechanism for chemical insult is hindered.

NRF2-deficient zebrafish morphants were found to have greater levels of cadmium-related oxidative injury, and NRF2 deficient mice are also more sensitive to chemical-induced toxicity, inflammatory stressors, and carcinogenesis, particularly in the lung [44]. Therefore, it is unsurprising that BAP and cigarette smoke exposures have been reported to cause more toxicity in NRF2 deficient mice [45]. Finally, NRF2 is thought to be protective against airway disorders as it is associated with loss of function mutations in patient cohorts with acute respiratory distress syndromes or lung cancers [46]. Overall, NRF2 is an important transcription factor in regulating a protective antioxidant response, and the observed downregulation of NRF2-regulated antioxidant genes by DBC but not by BAP suggests that suppressing this antioxidant gene network may be a potential major difference in mechanism of toxicity between BAP and DBC. It is possible that the inhibition of protective cellular mechanisms acts as a contributor to DBC's heightened carcinogenic potential, likely by compounding DBC toxicity from reactive metabolites.

We also found and confirmed, through qPCR, that a number of genes encoding enzymes involved in AHR-mediated PAH metabolism were oppositely regulated by BAP and DBC. Phase I enzymes *CYP1A1*, *CYP1B1*, *ALDH3A1*, and *NQO1* were dissimilarly regulated by BAP and DBC treatment. While BAP and CTE treatment significantly increased *CYP1A1* and *ALDH3A1*, DBC treatment significantly downregulated *CYP1A1* and *CYP1B1* expression. Because these

genes are inducible by AhR activation in response to environmental contaminant exposure, the effects of these genes in response to PAH treatment may be a contributing difference in how different environmental carcinogens exert their toxicity. It is very likely that parent PAHs and their various metabolites induce unique expression patterns of Phase I and Phase II enzymes that regulate further metabolism into either reactive, toxic compounds, or less toxic metabolites. This pattern of response is consistent with that previously reported in mouse skin epithelium in a limited dosing study [12, 40] and was confirmed in airway epithelium *in vitro* across dose and time. Further, studies investigating the role of inflammation on BAP pulmonary toxicity found that co-exposure of mice with BAP and lipopolysaccharide led to elevation of inflammatory pathways, inhibition of Phase I and II enzymes and decreased cell adhesion that correlated with increased genotoxicity compared to BAP treatment alone. [47-49]. These studies highlight the importance of inflammation on PAH-mediated lung disease and suggest that unique processes regulated by DBC related to inflammation, metabolism and cell-cell communication may mediate the enhanced carcinogenicity of DBC compared to BAP.

4.4 Advantages of profiling short-term bioactivity signatures of chemicals in 3D human airway epithelium

The results from this study support the use of systems approaches in broadly assessing and comparing mechanisms of chemical toxicity. This approach is particularly useful in comparing mechanisms of PAH exposure in a human *in vitro* model, both between chemicals and across model species. The RPF approach uses mouse *in vivo* data to derive cancer risk values to assess human cancer risk, effectively if mouse skin *in vivo* studies are representative of human PAH toxicity. While there is evidence of similar, short-term transcriptional responses observed across human airway epithelium and mouse skin, more

research is necessary to investigate the mechanisms of PAHs in humans, and whether these mechanisms are reflected in the mouse models used to derive RPFs.

The wealth of data generated from assessing short-term gene signatures can also be useful for comparing between specific chemical treatments and longer-term patient-derived gene signatures. From our study, the short-term gene signatures observed in BAP-treated human bronchial epithelium are consistent with specific transcriptional changes observed in the bronchial epithelium of smokers. Transcriptomic profiles in the lung epithelium of cigarette smokers share similarities with the BAP-treated human bronchial epithelium, particularly with similarly regulated Phase I and Phase II genes [50-53].

5. Conclusion

This work supported the utility of transcriptomic approaches in evaluating chemical-specific profiles of PAHs. Despite treatment for only 48 hours, the chemical signatures were markedly unique between BAP and DBC, and were consistent with differences between the chemicals across species (*in vivo* rodent). This work supports and demonstrates that efforts using short-term, systems biology data to inform mechanism of action profiling can be applied towards in-depth mechanistic assessments of PAH mixtures.

While prior research has focused on the liver and skin response to PAHs, we demonstrated that the human *in vitro* pulmonary epithelium cultured at the air-liquid interface is a toxicologically sensitive model to PAH transcriptional perturbation. The knowledge gained from studying additional mechanisms of toxicity, such as inflammation, oxidative stress response, and barrier integrity dysregulation, are valuable contributors to the growing field of predictive toxicology, as researchers can utilize knowledge of unique mechanisms to evaluate mechanistic contributors to cancer risk. In the current study, short-term transcriptional responses of PAH treatment provided evidence supporting barrier integrity dysregulation as a shared mechanism of action by PAHs, and *AHR* and

NRF2-related gene networks as potentially responsible for differences in Phase I, Phase II, and antioxidant responses to PAHs. These findings support research scrutinizing the applicability of the RPF, where the assumption of similar mode of action is necessary for quantitative PAH cancer risk assessment.

Conflict of Interest

The authors declare that there are no conflicts of interest.

Acknowledgements

This study was funded by Public Health Service grants P42ES016465 and T32ES07060.

References

1. Abdel-Shafy, H.I. and M.S.M. Mansour, *A review on polycyclic aromatic hydrocarbons: Source, environmental impact, effect on human health and remediation.* Egyptian Journal of Petroleum, 2016. **25**(1): p. 107-123.
2. Ravindra, K., R. Sokhi, and R. Van Grieken, *Atmospheric polycyclic aromatic hydrocarbons: Source attribution, emission factors and regulation.* Atmospheric Environment, 2008. **42**(13): p. 2895-2921.
3. Benbrahim-Tallaa, L., et al., *Carcinogenicity of diesel-engine and gasoline-engine exhausts and some nitroarenes.* The Lancet Oncology, 2012. **13**(7): p. 663-664.
4. IARC, *Some non-heterocyclic polycyclic aromatic hydrocarbons and some related exposures. Monographs on the evaluation of carcinogenic risks to humans.* IARC MONOGRAPHS ON THE EVALUATION OF CARCINOGENIC RISKS TO HUMANS, 2010. **92**.
5. IARC, *Diesel and gasoline engine exhausts and some nitrarenes.* IARC MONOGRAPHS ON THE EVALUATION OF CARCINOGENIC RISKS TO HUMANS, 2014. **105**.
6. Rengarajan, T., et al., *Exposure to polycyclic aromatic hydrocarbons with special focus on cancer.* Asian Pacific Journal of Tropical Biomedicine, 2015. **5**(3): p. 182-189.
7. Boffetta, P., N. Jourenkova, and P. Gustavsson, *Cancer risk from occupational and environmental exposure to polycyclic aromatic hydrocarbons.* Cancer Causes & Control, 1997. **8**(3): p. 444-472.
8. EPA, U.S., *Development of a Relative Potency Factor (Rpf) Approach for Polycyclic Aromatic Hydrocarbon (PAH) Mixtures (External Review Draft)*, U.S. Environmental Protection Agency, Editor. 2010: Washington, DC
9. Jarvis, I.W., et al., *Interactions between polycyclic aromatic hydrocarbons in complex mixtures and implications for cancer risk assessment.* Toxicology, 2014. **321**: p. 27-39.
10. Baird, W.M., L.A. Hooven, and B. Mahadevan, *Carcinogenic polycyclic aromatic hydrocarbon-DNA adducts and mechanism of action.* Environ Mol Mutagen, 2005. **45**(2-3): p. 106-14.
11. Moorthy, B., C. Chu, and D.J. Carlin, *Polycyclic aromatic hydrocarbons: from metabolism to lung cancer.* Toxicol Sci, 2015. **145**(1): p. 5-15.
12. Siddens, L.K., et al., *Polycyclic aromatic hydrocarbons as skin carcinogens: Comparison of benzo[a]pyrene, dibenzo[def,p]chrysene and three environmental mixtures in the FVB/N mouse.* Toxicology and applied pharmacology, 2012. **264**(3): p. 377-386.
13. Tilton, S.C., et al., *Mechanism-Based Classification of PAH Mixtures to Predict Carcinogenic Potential.* Toxicol Sci, 2015. **146**(1): p. 135-45.
14. Smith, D.A., *Species Differences in Metabolism and Pharmacokinetics: Are We Close to an Understanding?* Drug Metabolism Reviews, 1991. **23**(3-4): p. 355-373.

15. Bogaards, J.J.P., et al., *Determining the best animal model for human cytochrome P450 activities: a comparison of mouse, rat, rabbit, dog, micropig, monkey and man.* Xenobiotica, 2000. **30**(12): p. 1131-1152.
16. Turpeinen, M., et al., *Predictive value of animal models for human cytochrome P450 (CYP)-mediated metabolism: A comparative study in vitro.* Xenobiotica, 2007. **37**(12): p. 1367-1377.
17. Zavala, J., et al., *Assessment of Biological Responses of EpiAirway(™) 3-D Cell Constructs vs. A549 Cells for Determining Toxicity of Ambient Air Pollution.* Inhalation toxicology, 2016. **28**(6): p. 251-259.
18. Astashkina, A., B. Mann, and D.W. Grainger, *A critical evaluation of in vitro cell culture models for high-throughput drug screening and toxicity.* Pharmacology & Therapeutics, 2012. **134**(1): p. 82-106.
19. Sun, T., et al., *Culture of skin cells in 3D rather than 2D improves their ability to survive exposure to cytotoxic agents.* Journal of Biotechnology, 2006. **122**(3): p. 372-381.
20. Innes, A.L., et al., *Epithelial Mucin Stores Are Increased in the Large Airways of Smokers With Airflow Obstruction.* Chest, 2006. **130**(4): p. 1102-1108.
21. Balharry, D., K. Sexton, and K.A. BeruBe, *An in vitro approach to assess the toxicity of inhaled tobacco smoke components: nicotine, cadmium, formaldehyde and urethane.* Toxicology, 2008. **244**(1): p. 66-76.
22. Siddens, L.K., et al., *Cytochrome P450 1b1 in polycyclic aromatic hydrocarbon (PAH)-induced skin carcinogenesis: Tumorigenicity of individual PAHs and coal-tar extract, DNA adduction and expression of select genes in the Cyp1b1 knockout mouse.* Toxicology and Applied Pharmacology, 2015. **287**(2): p. 149-160.
23. Trapnell, C., L. Pachter, and S.L. Salzberg, *TopHat: discovering splice junctions with RNA-Seq.* Bioinformatics, 2009. **25**(9): p. 1105-11.
24. Trapnell, C., et al., *Transcript assembly and quantification by RNA-Seq reveals unannotated transcripts and isoform switching during cell differentiation.* Nat Biotechnol, 2010. **28**(5): p. 511-5.
25. Nookaew, I., et al., *A comprehensive comparison of RNA-Seq-based transcriptome analysis from reads to differential gene expression and cross-comparison with microarrays: a case study in Saccharomyces cerevisiae.* Nucleic Acids Res, 2012. **40**(20): p. 10084-97.
26. Nikolsky, Y., et al., *Functional analysis of OMICs data and small molecule compounds in an integrated "knowledge-based" platform.* Methods Mol Biol, 2009. **563**: p. 177-96.
27. Saeed, A.I., et al., *TM4: a free, open-source system for microarray data management and analysis.* Biotechniques, 2003. **34**(2): p. 374-8.
28. Shannon, P., et al., *Cytoscape: a software environment for integrated models of biomolecular interaction networks.* Genome Res, 2003. **13**.
29. Labib, S., et al., *Comparative transcriptomic analyses to scrutinize the assumption that genotoxic PAHs exert effects via a common mode of action.* Arch Toxicol, 2016. **90**(10): p. 2461-80.

30. Goodale, B.C., et al., *Structurally distinct polycyclic aromatic hydrocarbons induce differential transcriptional responses in developing zebrafish.* Toxicology and applied pharmacology, 2013. **272**(3): p. 656-670.
31. Song, M.K., et al., *Polycyclic aromatic hydrocarbons induce migration in human hepatocellular carcinoma cells (HepG2) through reactive oxygen species-mediated p38 MAPK signal transduction.* Cancer Sci, 2011. **102**(9): p. 1636-44.
32. Devalia, J.L., et al., *Mechanisms of pollution-induced airway disease: in vitro studies in the upper and lower airways.* Allergy, 1997. **52**(38 Suppl): p. 45-51; discussion 57-8.
33. Schamberger, A.C., et al., *Cigarette Smoke–Induced Disruption of Bronchial Epithelial Tight Junctions Is Prevented by Transforming Growth Factor-β.* American Journal of Respiratory Cell and Molecular Biology, 2014. **50**(6): p. 1040-1052.
34. Cao, X., et al., *Tight junction disruption by cadmium in an in vitro human airway tissue model.* Respir Res, 2015. **16**: p. 30.
35. Blasig, I.E., et al., *Occludin Protein Family: Oxidative Stress and Reducing Conditions.* Antioxidants & Redox Signaling, 2011. **15**(5): p. 1195-1219.
36. Coyne, C.B., et al., *Regulation of Airway Tight Junctions by Proinflammatory Cytokines.* Molecular Biology of the Cell, 2002. **13**(9): p. 3218-3234.
37. van Delft, J.H.M., et al., *Discrimination of genotoxic from non-genotoxic carcinogens by gene expression profiling.* Carcinogenesis, 2004. **25**(7): p. 1265-1276.
38. White, P.A., *The genotoxicity of priority polycyclic aromatic hydrocarbons in complex mixtures.* Mutation Research/Genetic Toxicology and Environmental Mutagenesis, 2002. **515**(1): p. 85-98.
39. Chepelev, N.L., et al., *Transcriptional Profiling of Dibenzo[def,p]chrysene-induced Spleen Atrophy Provides Mechanistic Insights into its Immunotoxicity in MutaMouse.* Toxicological Sciences, 2016. **149**(1): p. 251-268.
40. Larkin, A., et al., *Application of a fuzzy neural network model in predicting polycyclic aromatic hydrocarbon-mediated perturbations of the Cyp1b1 transcriptional regulatory network in mouse skin.* Toxicol Appl Pharmacol, 2013. **267**(2): p. 192-9.
41. Baird, W.M. and B. Mahadevan, *The uses of carcinogen-DNA adduct measurement in establishing mechanisms of mutagenesis and in chemoprevention.* Mutation Research/Fundamental and Molecular Mechanisms of Mutagenesis, 2004. **547**(1): p. 1-4.
42. Tung, E.W., et al., *Benzo[a]pyrene increases DNA double strand break repair in vitro and in vivo: a possible mechanism for benzo[a]pyrene-induced toxicity.* Mutat Res Genet Toxicol Environ Mutagen, 2014. **760**: p. 64-9.

43. Phillips, D.H., et al., *Metabolic activation of benzo[a]pyrene in vitro by hepatic cytochrome P450 contrasts with detoxification in vivo : experiments with hepatic cytochrome P450 reductase null mice.* Carcinogenesis, 2008. **29**(3): p. 656-665.
44. Chorley, B.N., et al., *Identification of novel NRF2-regulated genes by ChIP-Seq: influence on retinoid X receptor alpha.* Nucleic acids research, 2012. **40**(15): p. 7416-7429.
45. Kensler, T.W., N. Wakabayashi, and S. Biswal, *Cell survival responses to environmental stresses via the Keap1-Nrf2-ARE pathway.* Annu Rev Pharmacol Toxicol, 2007. **47**: p. 89-116.
46. Cho, H.Y. and S.R. Kleeberger, *Nrf2 protects against airway disorders.* Toxicol Appl Pharmacol, 2010. **244**(1): p. 43-56.
47. Shi, Q., et al., *Altered gene expression profiles in the lungs of benzo[a]pyrene-exposed mice in the presence of lipopolysaccharide-induced pulmonary inflammation.* Toxicol Appl Pharmacol, 2017. **336**: p. 8-19.
48. Shi, Q., R.W.L. Godschalk, and F.J. van Schooten, *Inflammation and the chemical carcinogen benzo[a]pyrene: Partners in crime.* Mutat Res, 2017. **774**: p. 12-24.
49. Arlt, V.M., et al., *Pulmonary Inflammation Impacts on CYP1A1-Mediated Respiratory Tract DNA Damage Induced by the Carcinogenic Air Pollutant Benzo[a]pyrene.* Toxicol Sci, 2015. **146**(2): p. 213-25.
50. Boyle, J.O., et al., *Effects of cigarette smoke on the human oral mucosal transcriptome.* Cancer Prev Res (Phila), 2010. **3**(3): p. 266-78.
51. Sridhar, S., et al., *Smoking-induced gene expression changes in the bronchial airway are reflected in nasal and buccal epithelium.* BMC Genomics, 2008. **9**: p. 259.
52. Chari, R., et al., *Effect of active smoking on the human bronchial epithelium transcriptome.* BMC Genomics, 2007. **8**(1): p. 297.
53. Team, A.S., *Shared Gene Expression Alterations in Nasal and Bronchial Epithelium for Lung Cancer Detection.* J Natl Cancer Inst, 2017. **109**(7).

Figure 2- 1.

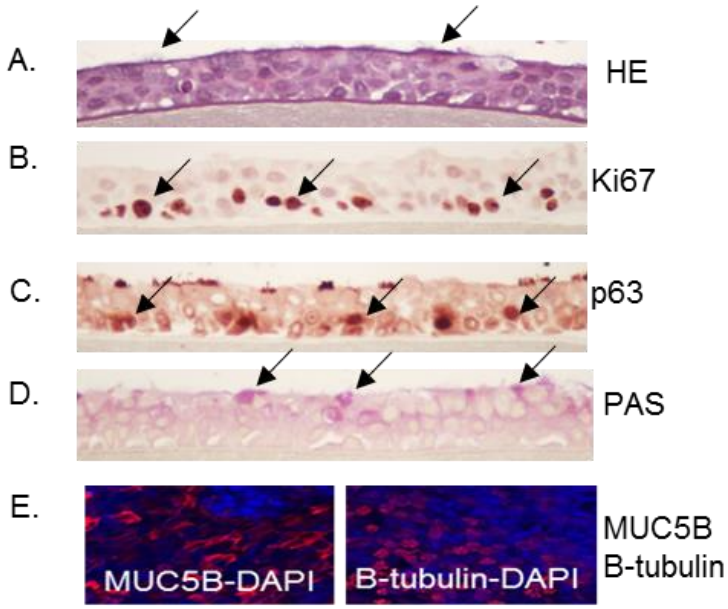

Figure 2- 1. Morphological characterization of primary 3D human bronchial epithelial cells (HBEC) in culture (MaTtek**).** HBEC cultures were fixed in 10% formalin 5 weeks after seeding onto membrane support. Tissue sections were stained with H&E (A) to observe ciliated cells, Ki67 (B) for actively proliferating cells, p63 (C) for basal cells, PAS (D) for goblet cells, and (E) MUC5B and β-tubulin (red with DAPI counterstain in blue) as markers of glandular mucous cells and ciliated respiratory cells, respectively. Examples of positively stained cells are indicated by arrows.

Figure 2-2.

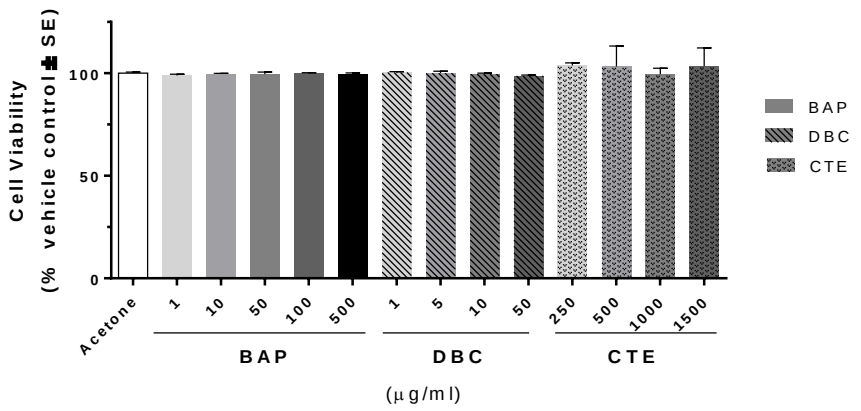

Figure 2-2. Cell viability measured by lactate dehydrogenase (LDH) leakage in cell media 48 hrs after exposure to PAHs. Values are presented as LDH leakage in media for treated cells compared to acetone vehicle control (% vehicle control ± standard error). LDH leakage from HBEC treated with benzo[*a*]pyrene (BAP), dibenzo[*def,p*]chrysene (DBC) and coal tar extract (CTE) were not significantly different ($p>0.05$) from vehicle control at any concentration (ANOVA).

Figure 2-3.

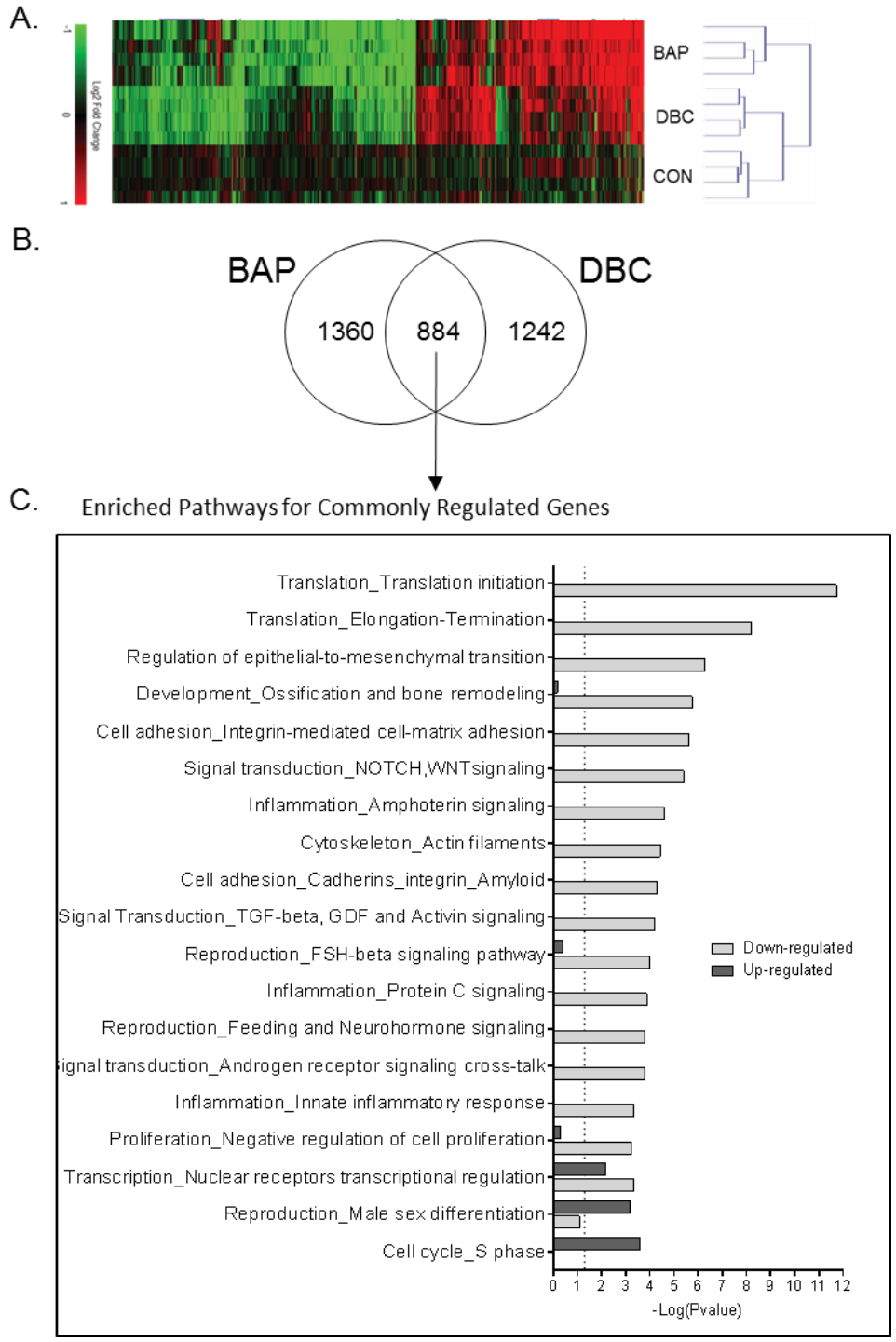

Figure 2-3. HBEC transcriptional response to BAP and DBC. Global gene expression was measured in HBEC 48 hrs after treatment with 500 ug/ml (19.8 nmol) benzo[a]pyrene (BAP) and 10 µg/ml (0.35 nmol) dibenzo[def,p]chrysene (DBC) by RNA sequencing. **(A)** Bidirectional hierarchical clustering by

Euclidean distance of genes differentially expressed ($q<0.05$) by BAP and DBC compared to vehicle control. Values are log2 fold change for all treatments compared with control; red, green, and black represent up-regulated, down-regulated and unchanged genes, respectively. **(B)** Venn diagram showing overlap of significantly regulated ($q <0.05$) genes by BAP and DBC in HBEC. **(C)** Functional enrichment of gene processes in HBEC using MetaCore network processes (GeneGo) for genes commonly regulated by BAP and DBC ($q<0.05$). Black bars represent functions for genes up-regulated and gray bars represent functions for genes down-regulated in common by BAP and DBC ($q<0.05$). The dashed line indicates the threshold for significance ($p<0.05$).

Figure 2-4.

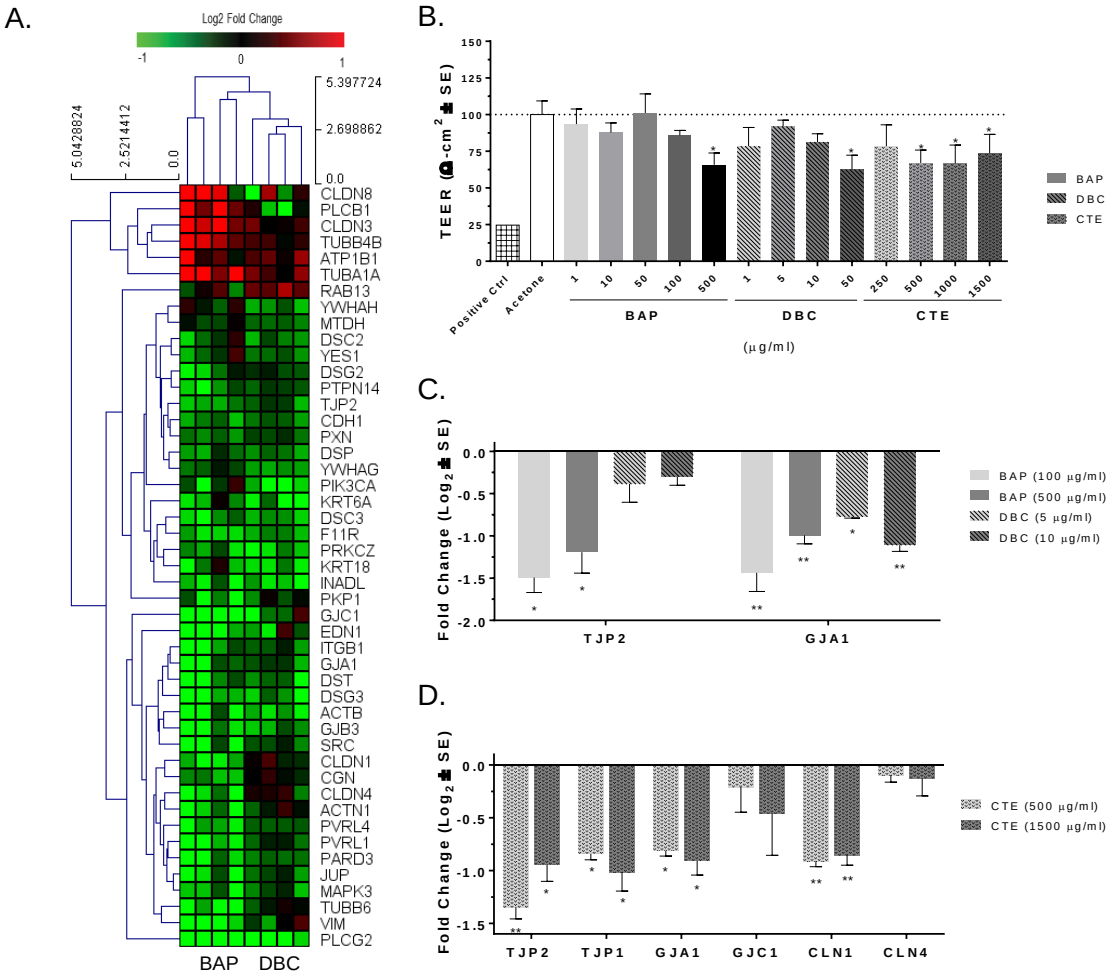

Figure 2-4. Decrease in barrier integrity of HBEC after treatment with BAP and DBC. (A) Bidirectional hierarchical clustering by Euclidean distance of differentially expressed genes associated with gap junction and tight junction signaling (q<0.05) after 48 hr treatment with benzo[*a*]pyrene (BAP) and dibenzo[*def*,*p*]chrysene (DBC) compared to vehicle control. Values are log2 fold change for all treatments compared with control; red, green, and black represent up-regulated, down-regulated and unchanged genes, respectively. **(B)** Transepithelial electrical resistance (TEER) measured in HBEC 48 hr after treatment with BAP, DBC and coal tar extract (CTE). Values are TEER (Ω-cm2) normalized to vehicle control (scaled to 100%). *Indicates significant reduction in TEER (p<0.05; ANOVA with Tukey's pairwise comparison). Expression of genes associated with barrier integrity were measured by quantitative PCR in HBEC after 48 hr treatment with BAP and DBC **(C)** and CTE **(D)**, respectively. Values are expressed as fold change (Log2; mean ± SE) compared to vehicle control. Asterisks indicate significance compared to vehicle control (*p<0.05; **p<0.001; ANOVA with Tukey's pairwise comparison).

Figure 2-5.

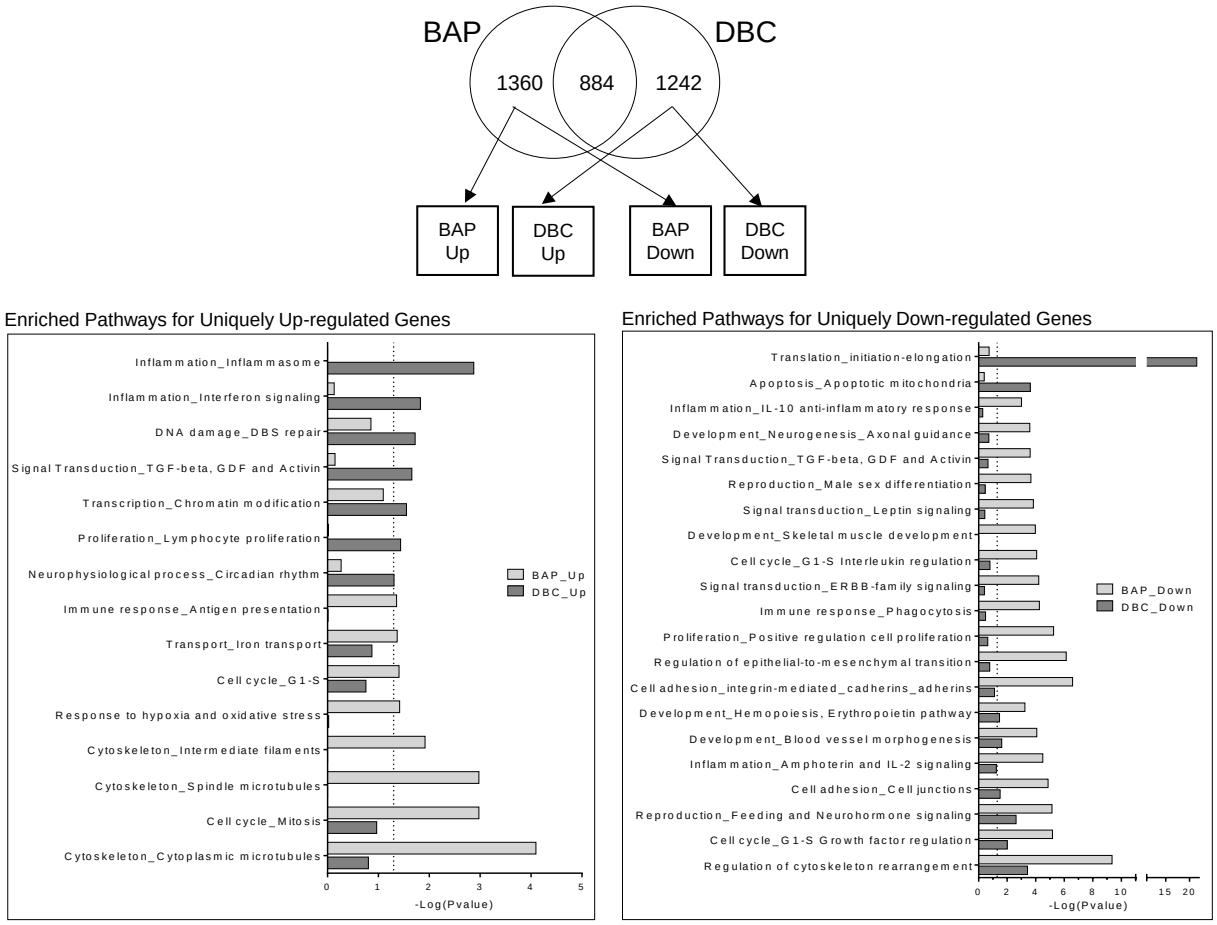

Figure 2-5. Genes uniquely regulated by BAP and DBC in HBEC. Global gene expression was measured in HBEC 48 hrs after treatment with 500 µg/ml (19.8 nmol) benzo[a]pyrene (BAP) and 10 µg/ml (0.35 nmol) dibenzo[def,p]chrysene (DBC) by RNA sequencing. Venn diagram shows genes uniquely regulated ($q < 0.05$) by BAP and DBC in HBEC. Statistical enrichment of biological network processes (MetaCore) is shown for genes uniquely up-regulated (left-panel) and down-regulated (right-panel) by BAP (light gray bars) and DBC (dark gray bars). The dashed line indicates the threshold for significance ($p<0.05$).

Figure 2-6.

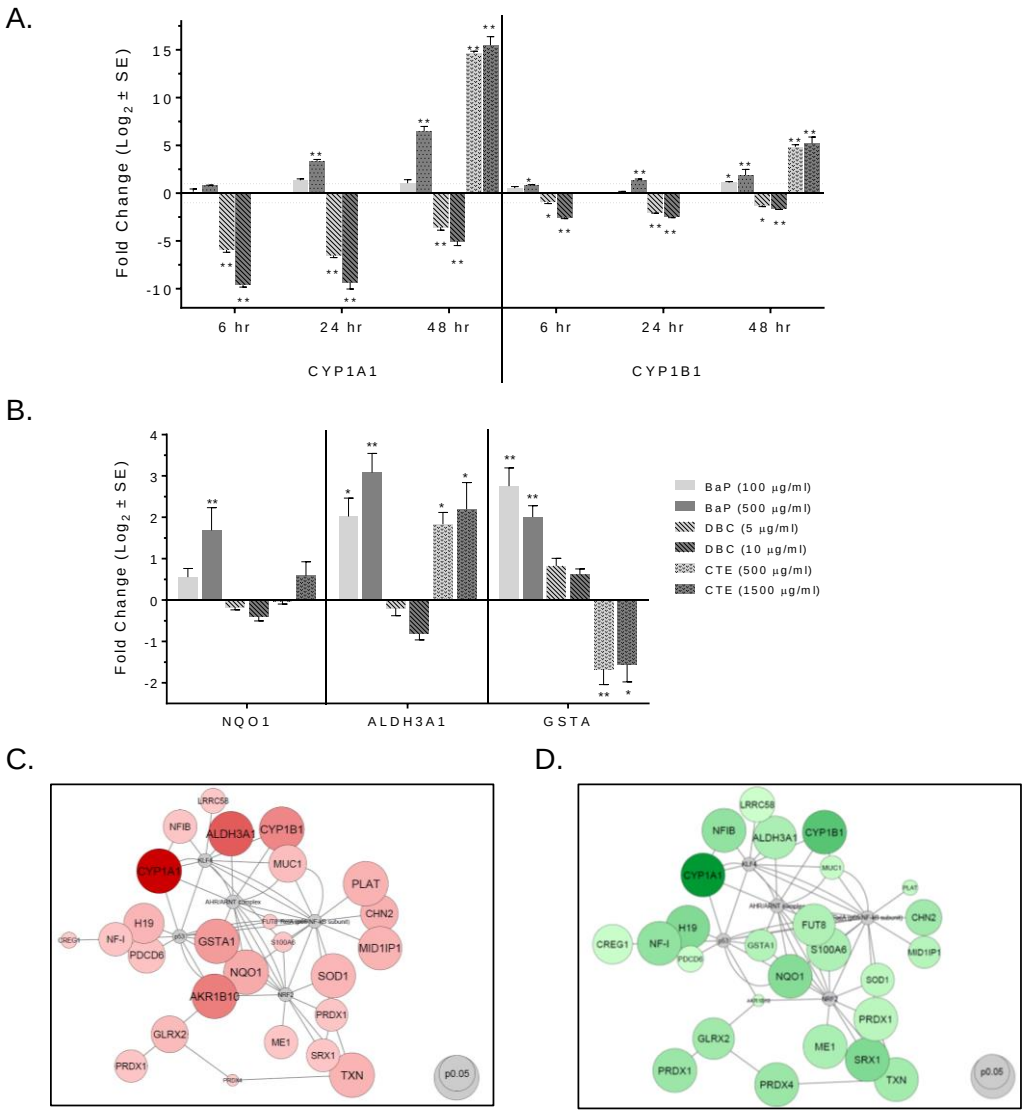

Figure 2-6. Unique regulation of AHR- and NRF2-mediated genes by BAP and DBC in HBEC. (A) Expression of CYP1A1 and CYP1B1 was measured by quantitative PCR in HBEC 6-48 hrs after treatment with BAP, DBC and CTE (48 hr only). **(B)** Expression of NQO1, ALDH3A1 and GSTA was measured by quantitative PCR in HBEC 48 hrs after treatment with BAP, DBC and CTE. **(C)** Transcription factor signaling networks for AHR and NRF2 in HBEC after treatment with 500 µg/ml (19.8 nmol) BAP (left, red) and **(D)** 10 µg/ml (0.35 nmol) DBC(right, green). Target nodes are up-regulated by BAP (red) and down-regulated by DBC (green). For panesl A and B, values are expressed as fold change (Log2; mean ± SE) compared to vehicle control. Asterisks indicate significance compared to vehicle control (*p<0.05; **p<0.001; ANOVA with Tukey's pairwise comparison). For panel C, as indicated in the legends, the size of nodes is associated with significance (larger is more significant) and the color

intensity represents magnitude of response (darker is larger response) for BAP and DBC compared to vehicle control.

CHAPTER 3 - Classifying polycyclic aromatic hydrocarbons by carcinogenic potency using *in vitro* biosignatures

Yvonne Chang[a], Celine Thanh Thu Huynh[a], Kelley M. Bastin[a], Brianna N. Rivera[a], Lisbeth K. Siddens[a,b], Susan C. Tilton[a,c,*]

[a]Environmental and Molecular Toxicology Department, Oregon State University, Corvallis, OR, USA
[b]Linus Pauling Institute, Oregon State University, Corvallis, OR, USA
[c]Superfund Research Program, Oregon State University, Corvallis, OR, USA
*Corresponding author at: Environmental and Molecular Toxicology Department, Oregon State University, Corvallis, OR 97330. *E-mail address*: susan.tilton@oregonstate.edu

Abstract

One of the most difficult challenges for risk assessment is evaluation of chemicals that predominately co-occur in mixtures like polycyclic aromatic hydrocarbons (PAHs). We previously developed a classification model in which systems biology data collected from mice shortly after chemical exposure accurately predict tumor outcome. The present study demonstrates translation of this approach into a human *in vitro* model in which chemical-specific bioactivity profiles from 3D human bronchial epithelial cells (HBEC) classify PAHs by carcinogenic potency. Gene expression profiles were analyzed from HBEC exposed to carcinogenic and non-carcinogenic PAHs and classification accuracies were identified for individual pathway-based gene sets. Posterior probabilities of best performing gene sets were combined via Bayesian integration resulting in a classifier with four gene sets, including aryl hydrocarbon receptor signaling, regulation of epithelial mesenchymal transition, regulation of angiogenesis, and cell cycle G2-M. In addition, transcriptional benchmark dose modeling of benzo[a]pyrene (BAP) showed that the most sensitive gene sets to BAP regulation were largely dissimilar from those that best classified PAH carcinogenicity challenging current assumptions that BAP carcinogenicity (and subsequent mode of action) is reflective of overall PAH carcinogenicity. These results illustrate utility of using systems toxicology approaches to analyze global gene expression towards carcinogenic hazard assessment.

1.0. Introduction

The environmental health science community recognizes PAHs as a re-emerging class of environmental pollutants due to their persistence and prominence in mixtures of concern [1-5]. PAHs are ubiquitous contaminants in the environment commonly generated by petrogenic and pyrogenic processes, including aluminum and coal-tar pitch production, and incomplete combustion of tobacco, wood, , and fossil fuels [6]. They account for 3 of the top 10 chemicals of concern at priority pollutant sites and are considered among the most important carcinogens in air pollution [5, 7]. The World Health Organization's International Agency for Research on Cancer (IARC) has designated several PAHs and mixtures, such as diesel exhaust, air pollution, coal and coke mixtures, as either Class 1 known or Class 2A/B probable/possible carcinogens to humans [2, 8-10]. Despite the fact that PAHs were the first class of chemicals identified as chemical carcinogens, little is known about the carcinogenic potential of many of the over 1500 polycyclic aromatic compounds or about potential mechanisms of carcinogenic action for this diverse class.

Current assessment of cancer risk for PAHs involves testing compounds in the 2-year rodent bioassay. These studies are time and resource-intensive, and often lack reproducibility or concordance. Furthermore, they require extrapolation of effects to humans, leading to further uncertainties regarding species-specific biology and chemical mode of action (MOA) [11]. Carcinogenic potential of PAHs has been historically evaluated for individual chemicals through intraperitoneal or dermal routes. However, PAH exposures occur as complex environmental mixtures through inhalation, oral, and dermal routes, which are difficult and cost-prohibitive to assess using traditional carcinogenicity assays. The primary method for estimating cancer risk of PAH mixtures is the relative potency factor (RPF) approach in which mixtures are evaluated based on a subset of individual component PAHs compared to benzo[*a*]pyrene (BAP) as a surrogate or reference [12]. However, we and others have found this approach inadequate

for predicting carcinogenicity of mixtures and also for certain individual PAHs, particularly those that function through alternate pathways or exhibit greater promotional capacity compared to BaP [13-16].

Previously we reported an approach for predicting potency of PAH chemicals and environmental PAH mixtures based on bioactivity profiles derived from global transcriptional analysis short-term post-exposure in a mouse skin cancer model [15]. This classification approach overcomes limitations of using RPFs for complex mixtures since it does not require knowledge about individual components of mixtures nor does it assume a common mechanism of action for all PAHs. Instead, we found that chemical-specific signaling after exposure provides a unique signature or bioactivity profile for each PAH/mixture that is reflective of its MOA and can be used to discriminate carcinogenic potency. Similar genomic-based models have successfully been applied to individual chemicals after short-term exposure to identify modes of action for distinguishing carcinogens from non-carcinogens in rodent *in vivo* and human *in vitro* [17, 18]. Other studies that have modeled non-additive effects of polycyclic aromatic compounds in mixtures on hepatotoxicity with gene expression data report the strong correlation of gene response with other toxicity endpoints *in vivo*, including histopathology and gross physiology, showing the benefits of using gene expression to evaluate quantitative differences in toxicity [19, 20].

In this study, we evaluated whether systems biology data collected from a human *in vitro* airway epithelial model can be used for accurate classification of carcinogenic potency of PAHs and PAH mixtures. Advanced cell culture and tissue engineering are increasingly recognized for their potential in mechanistic studies because the three-dimensional structure, metabolic and mitotic activity, multi-cellular communication and cell signaling better recapitulate *in vivo* response compared to cells grown in monolayer culture [21-23] Human bronchial epithelial cells cultured at the air-liquid interface were previously found to produce chemical-specific gene signatures after treatment with two carcinogenic PAHs, BAP and dibenzo[*def,p*]chrysene (DBC), that were consistent with gene

changes observed in mouse and showed chemical-specific signaling related to oxidative stress and inflammation may drive different MOAs for these PAHs [16]. These differences in gene signaling and regulation may thus contribute to subsequent differences in carcinogenic potency observed *in vivo* [15]. For this study, employing organotypic *in vitro* models allows for rapid generation of transcriptional biosignatures for analysis and comparison of PAH MOAs linked to adverse health outcomes.

2.0. Methods

2.1. Chemicals and reagents

Cell culture media and phosphate buffered saline (PBS) were provided by MatTek Corporation (Ashland, MA). Benzo[a]pyrene (BAP) CAS# 50-32-8 and dibenzo[def,p]chrysene (DBC) CAS# 189-64-0 were purchased from MRIGlobal (Kansas City, MO). Benz[a]anthracene (BAN) CAS# 56-55-3, phenanthrene (PHE) CAS# 85-01-8, and pyrene (PYR) CAS# 19-00-0 were acquired from Sigma-Aldrich dba. Millipore Sigma (St. Louis, MO.). Coal Tar Extract (CTE) (SRM 1597a) was purchased form the National Institute of Standards & Technology (Gaithersburg, MD.) DNase I, TRIzol® reagent, Superscript® III First Strand Synthesis System, qPCR primers, and Pierce™ LDH Cytotoxicity Assay Kit were from Thermo Fisher Scientific (Waltham, MA). 2X SsoAdvanced™ Universal SYBER®Green Supermix was purchased from BioRad Laboratories, Inc. (Hercules, CA.).

2.2. Tissue Culture and Chemical Exposures

For the 2D cell culture experiments, primary normal HBEC at passage 5 from Lonza Group (Basel, Switzerland) were expanded in PneumaCult^{TM}-Ex Plus Medium from Stemcell Technologies (Vancouver, Canada) and further

subcultured onto black-walled, clear-bottom 96-well plates until confluent, then exposed to chemical treatments for 24 hours using 2% dimethyl sulfoxide (DMSO) in Dulbecco's phosphate-buffered saline (DPBS) from Thermo Fisher Scientific (Waltham, MA).

For the differentiated 3D cell culture experiments, primary HBEC cultured on transwell inserts (EpiAirway™ 100, Mattek, Ashland, MA) were shipped overnight and received chilled on ice packs. Tissues were immediately transferred to 6-well plates each well containing 1 ml of assay medium and equilibrated for 24 hours at 37°C, 5% CO 2 followed by a change of fresh medium before any treatment regimens commenced. Tissues were prepared for treatment as follows. PBS (0.50 ml) was pipetted onto the apical surface of the inserts and the PBS was carefully removed along with mucus from the surface of the tissues to wash the cells prior to chemical exposure. The medium was replaced with 1 ml of fresh medium in the plate wells (basal side of the membrane). Single PAHs and coal tar were solubilized in acetone and applied (0.01 ml/insert) to the apical surface of tissues (n=4 per treatment) for up to 48 hrs, BAP (1-500 µg/ml), DBC (1-50 µg/ml), BAN (10-500 µg/ml), PYR (10-250 µg/ml), PHE (10-250 µg/ml) and CTE (250 -1500 µg/ml). Dosing was chosen based on relative potency in BAP equivalents as previously reported [13, 16, 24]. Basal media was transferred to clean, sterile tubes and stored at -80°C. At the end of each exposure regimen, lysis buffer was added to each insert, collected, and stored at -80°C until extraction using RNeasy extraction kit.

2.3. RNA Isolation and mRNA-Seq

Total RNA was isolated from HBEC (n=4) using RNeasy Mini Kit (Qiagen, Venlo, Netherlands) and was quantitated on a SYNERGY/HTX plate reader equipped with a Take3 module, then evaluated for quality with a Bioanalyzer 2100, Agilent (Santa Clara, CA). PAH dosing for sequencing was chosen based on BAP equivalents at concentrations similar to those used in prior

animal studies (applied to mouse skin) [13, 16, 24]. Acceptable RNA quality was based on RIN ≥ 8.5. Isolated mRNA were sequenced on Illumina HiSeq 3000, which yielded >350 million reads per lane. Sequenced reads were first put through Cutadapt (version 1.8.1) to trim adapter sequences from the paired-end reads. The human genome assembly GRCh38.84 was indexed using Bowtie2-build (version 2.2.3) while the transcriptome was indexed using TopHat (version 2.1.1) [25-27]. TopHat was used again to align the trimmed reads to indexed transcriptome and genome [27]. Featurecounts (from the Rsubread package v1.22.2) was used to summarize reads into count tables [28]. Differential expression was determined in DESeq2 (version 1.26.0) compared to vehicle control [29]. The differentially expressed gene lists ($q<0.05$) for each treatment were used for pathway enrichment analysis in MetaCore (GeneGO, Thomson Reuters). Statistical significance of over-connected interactions was calculated using a hypergeometric distribution, where the p value represents the probability of a particular mapping arising by chance for experimental data compared to the background [30]. Heatmaps were generated in MultiExperiment Viewer TM4 [31].

2.4. Posterior Probability Integration for Chemical Classification

Once significantly enriched pathways ($p<0.05$) were identified, they were further prioritized by differential significance across chemical exposure groups by calculating the standard deviations of the negative logarithm of the p values. The top 30 pathways with the greatest standard deviations were selected for chemical classification testing. PAH treatments were grouped based on RPF and BAP equivalence into four chemical classes (non-carcinogenic, low, moderate, and high). Non-carcinogenic PAHs were binned into Class 1, containing PYR and PHE. Lower potency carcinogenic treatments were assigned to Class 2, and the exposure groups were BAP10, BAP100, CTE, and BAN. Moderate-level carcinogenic potency was assigned to Class 3, with the highest dose of BAP

(BAP500). High-level carcinogenic potency was assigned to Class 4, for DBC-exposed samples, which has been demonstrated *in vivo* to have up to 100-fold greater carcinogenic potency than BAP [13]. Individual pathway gene sets were tested for classification performance in Visual Integration for Bayesian Evaluation (VIBE) v2.0 [32, 33], where probability matrices for significantly enriched pathways were calculated using Naïve Bayes statistical learning algorithm with 4-fold cross validation. Pathway gene sets with high-performing classification accuracies (0.70 and above) were prioritized for further testing in a Bayesian integration framework as described previously [15].

2.5. Transcriptional Benchmark Dose Modeling and Functional Classification

BMDExpress 2.0 (version 2.3) was used to perform benchmark dose (BMD) modeling analysis on transcriptomic data from 3D HBEC exposed to 10, 100, and 500 µg/uL BAP for 48 hours [34, 35]. The imported RNAseq data set was analyzed using the EPA BMDS Models (parametric), and multiple models were used to fit gene expression dose-response data, including hill, power, linear, and polynomial. For each gene, the best fitting model was selected based on best fit and nested Chi-square test (cutoff of 0.05), as previously described [35, 36]. A benchmark response (BMR) factor of 1.021 was selected to model a 5% response over background. Only genes with BMD values lower than the highest dose were included for the downstream Functional Classification Analysis using pre-defined biological process networks (Metacore). The median BMD of the selected process networks was used as the primary metric to evaluate overall pathway and process sensitivity to determine the most BAP-dose responsive and sensitive process networks.

2.6. Quantitative PCR

cDNA was synthesized using a Superscript® III First Strand Synthesis Supermix kit per manufacturer's instructions. Reactions were diluted 1:5 with nuclease–free water and stored at -80°C until used for qPCR. A BioRad Laboratories, Inc. (Hercules, CA.) CFX96 Touch™ Real-Time PCR Detection System was used for running 20 µl qPCR reactions to survey key gene targets. Each reaction contained 2 µl cDNA template (10 ng RNA), 150 nM of each primer, 10 µl 2X SsoAdvanced™ Universal SYBER®Green Supermix, and nuclease–free water. Primer sequences are as described in Chang et al. (2019) [16]. The thermocycler was programmed for 1 cycle 95°C for 1 minute initial denaturing, 40 cycles 95°C for 15 sec denaturing, 60°C for 30 sec annealing/elongation, and a melt curve 65-95°C/0.5° per 5 sec for validating single product amplification. The relative expression differences among treatments were calculated using the ΔΔCt comparative method and normalized to the housekeeping gene *peptidylprolyl isomerase A* (PPIA). Genes significantly regulated by PAH treatment ($p<0.05$) were identified by one-way ANOVA with Tukey's multiple testing correction.

2.7. Cell Viability

Lactate dehydrogenase (LDH) leakage was measured in media after treatment with PAHs (n = 4) for 48 hrs using Pierce LDH Cytotoxicity Assay Kit (Thermo Scientific) following manufacturer instructions as previously described [16]. Briefly, basal medium samples (40 µl) were aliquoted into the wells of a 96-well plate. LDH reaction reagent (40 µl) was added to each sample and incubated at room temperature for 30 minutes while protected from light. Finally, 40 µl of stop solution was added to each well and mixed. LDH activity was determined by subtracting absorbance at 680nm (background) from absorbance at 490nm (Synergy HTX plate reader, BioTek, Winooski, VT). A negative control of fresh cell culture medium, a positive control of medium from lysed cells, and vehicle

only controls were included. Cytotoxicity was evaluated by one-way ANOVA with Dunnett's multiple testing correction ($p<0.05$).

2.7. Oxidative Stress

For the reactive oxygen species detection assays, a 2',7'–dichlorofluorescin diacetate (DCFDA) solution (from Sigma-Aldrich, St. Louis, MO) was prepared at 2% DMSO in HBSS, and pipetted onto the cells. Immediately, the plate was read by a SYNERGY/HTX plate reader (BioTek Instruments Inc., Winooski, VT) at 485/20 and 528/20 nm excitation and emission. A positive control of menadione and vehicle only controls were included. Chemical-induced fluorescence was expressed as relative fluorescence (RFU) normalized to vehicle control (RFU/vehicle), and the data were fit to a nonlinear regression with variable slope to model dose-response curves and calculate EC50s.

3.0 Results

3.1. Global gene expression analysis

In this study, PAH gene signatures were measured in 3D HBEC after 48 hour treatment using RNAseq. Raw and normalized sequencing files are available at NCBI Gene Expression Omnibus (GSE128471). Of over 60,000 transcripts mapped and evaluated, there were 9,538 statistically significant transcripts ($q < 0.05$) identified as differentially regulated compared to vehicle control across all treatments. PAH treatment concentrations chosen for sequencing, which included a BAP dose-response and additional PAHs based on calculated BAP equivalents, did not result in any observed cytotoxicity (Supplemental File 1). Overall, BAP 10 µg/mL, 100 µg/mL, and 500 µg/mL exposure resulted in 1222, 41, 6309 differentially regulated genes (DEGs), respectively, ($q < 0.05$); BAN 500 µg/mL exposure resulted in 898 DEGs; CTE 1.5 mg/mL exposure resulted in 1505

DEGs; DBC 10 µg/mL exposure resulted in 3122 DEGs. Finally, the non-carcinogenic PAHs, PHE 100 µg/mL and PYR 500 µg/mL resulted in 1530 and 3 DEGs, respectively. There were no shared DEGs between all 8 treatment groups.

PAH treatments resulted in chemical-specific gene signatures as visualized by principal component analysis (PCA) (Fig 1A). Approximately 50% of the gene and sample variance across x and y axes are described in the first two components. Principal components 1 and 2 are shown in a 2D plot, with component 1 visualized across the x-axis (37.99% variance) and component 2 visualized across the y-axis (10.81%). In general, we observe marked separation between different PAH treatments, with the most separation observed in BAP 500 µg/mL and DBC. There is slight overlap between BAN and CTE, and between BAP 100 µg/mL and PHE. Overall, treatment-specific response is observed, with PAH exposure groups clustering more closely with samples of the same chemical and dose, suggesting chemical-specific and dose-specific gene signatures.

To compare PAH bioactivity at the gene level, subsets of genes associated with xenobiotic metabolism, aryl hydrocarbon receptor signaling, oxidative stress, and cell cycle regulation were highlighted in a heatmap (Fig 1B). Unsupervised hierarchical clustering was performed by Euclidean distance with average linkage clustering to generate gene and sample-level dendrograms. The heatmap illustrates unique patterns of expression across PAHs for some xenobiotic metabolism genes. CYP1A1 and CYP1B1 were upregulated by the two higher doses of BAP (100 µg/mL and 500 µg/mL), CTE, and BAN. However, DBC and PYR exposure resulted in decreased levels of these gene transcripts (Supplemental File 2). A similar pattern was observed for NQO1, SOD1, TXN, PRDX1, ALDH3A1, AKR1B1, and UGT1A1. For this subset of genes, DBC and the lowest sequenced dose of BAP (10 µg/mL) clustered more closely with non-carcinogenic PAHs than the low and moderate potency carcinogens (BAN, CTE, BAP 100 µg/mL, BAP 500 µg/mL) suggesting that PAHs function through unique mechanisms and that typical PAH biomarkers (e.g. CYP1A1) are not predictive of carcinogenic potency.

3.2. PAH-related Reactive Oxygen Species Generation

Due to PAH-associated transcriptional differences in redox genes, the chemicals were further investigated for PAH-induced ROS generation using a high throughput DCFDA fluorescence assay. PAH-induced ROS were detected by fluorescent DCFDA signal in 2D cultured HBEC, and chemical-induced ROS were expressed as relative fluorescence units (RFUs) normalized to vehicle control (Fig. 1C). Based off of maximal responses, BAN exposure was the most effective at inducing intracellular ROS, followed by CTE, DBC, and BAP. PHE and PYR did not elicit ROS generation in 2D HBEC. The median effective concentration (EC50) values of these concentration-response curves were 2.04 µg/mL (9µM) for benz[a]anthracene, 8.70µg/mL (29 µM) for DBC, 13.18 µg/mL (78 µM) for CTE, and 50.69 µg/mL (225 µM) for BAP. When comparing EC50s between PAHs, the EC50 of BAP is notably higher than the EC50s of BAN and CTE, indicating that BAP may be a less potent intracellular ROS generator than BAN and CTE. In this assay, we observe that all chemical treatments with known carcinogenic activity (BAP, BAN, CTE, DBC) had some level of ROS generation, while the non-carcinogenic PAHs (PYR, PHE) did not have any detectable ROS-generating activity. However, ROS generation potential in the 2D HBEC did not reflect chemical carcinogenic potency or RPF. For example, BAN is estimated to be five times less carcinogenic as BAP with an RPF of 0.2, yet demonstrates much greater potency in producing intracellular ROS, resulting in a much lower EC50 of 2.04 µg/mL (9 µM). BAN surpassed all other PAHs tested in its ability to generate ROS, including the high molecular weight carcinogen DBC, which has a RPF estimate of 30-100.

3.3. Pathway-based classification of PAHs in 3D HBEC

Pathway selection for classification accuracy testing in Bayesian framework. A primary goal of this study was to develop a predictive model using chemical-gene signatures following short-term exposure of a human organotypic

culture model to non-carcinogenic and carcinogenic PAHs. With a limited dataset, we utilized an expert knowledge-driven approach to 1. Designate chemical classes based on carcinogenic potency informed by calculated RPFs and prior mouse *in vivo* studies [13, 24], and 2. Develop a classification approach using *in vitro* data by testing and integrating prioritized pathway gene sets with high ability to correctly assign a sample into its designated class.

A pathway enrichment analysis was conducted to identify biological function associated with the 9,555 genes significantly regulated ($q < 0.05$) by the PAH exposure groups. Overall, the PAH exposure groups' individual DEGs significantly enriched a total of 125 pathways. Overall, 92 pathways were significantly enriched by at least 2 treatments, indicating a wide range of biological coverage associated with PAH exposure. Pyrene did not significantly enrich any pathways. A key goal of this study is to identify pathways better suited for chemical carcinogenicity predictive classification, so statistical filtering was used to prioritize pathway gene sets to be tested for classification performance. Significantly enriched pathways were prioritized for classification testing based on differential significance (standard deviation of negative log p-value) to identify pathways that were most dissimilar among PAH exposure groups. The top 30 most differentially significant pathways were selected for further testing and visualized in a heatmap showing significance in yellow and white, and lack of significance in blue (Fig. 2). In addition, aryl hydrocarbon receptor signaling was included since it had previously been identified to be differentially regulated by PAHs (Fig. 1B, Supplemental File 2).

Each gene set was tested individually for classification ability and quantified by a classification accuracy (CA). The resulting CAs for tested gene sets ranged 0.50 – 0.88. An example of a perfect classifier is shown in Fig. 3A1 in which the predicted (X-axis) and true class (y-axis) are identical resulting in 100% classification accuracy. Representative well-performing, poor performing and randomly generated gene sets are provided for comparison (Figs. 3A2-4). To generate the random gene set, 138 genes, which represents the average size of

annotated gene sets, were randomly selected from the overall 9,555 DEG in the study. While a perfect classifier returns a 1.00 or 100% CA, a random classifier returns a 0.50, or 50% CA.

Some processes, for example the translation elongation-termination gene set, did not classify chemicals any better than genes identified at random (Fig. 3A3). Gene sets for other pathways yielded higher classification scores, showing they were able to successfully discriminate samples into relevant chemical classes (Fig. 3A2).

Integration of multiple pathways for improved classification accuracy. Based on prior data showing that integration across multiple pathways results in improved classification accuracy, candidate gene sets were identified and selected for Bayesian integration to identify a combination that improved CA performance [15]. This integration approach was driven by knowledge that individual carcinogenic PAHs can act through multiple modes of action within cells and PAHs have diverse modes of actions. As with *in vitro* assay endpoints, there is unlikely to be one single pathway gene set that is predictive of different PAHs due to their many genotoxic and nongenotoxic MOAs. By testing combinations of pathway gene sets having 70% CA and higher, a four pathway set was discovered to produce an improved CA (Fig. 3B). The combination of four gene sets (aryl hydrocarbon receptor signaling, regulation of epithelial mesenchymal transition, regulation of angiogenesis, and cell cycle G2-M) resulted in the best CA score of 0.91, or 91% CA. Here, the CA performance of the integrated gene sets exceeded the CA performance of any of the individual gene sets (0.78-0.88). Overall, these results demonstrate that chemical biosignatures from *in vitro* studies can be used to inform classification based on *in vivo* outcomes and that integration across pathway-derived gene sets can improve overall accuracy.

3.4. Transcriptomic Dose-Response Modeling of BAP in 3D HBEC

To understand which genes and pathways are most sensitive to dose after treatment with BAP, transcriptomic dose-response modeling was performed with

a three-point dose response of BAP-exposed HBEC. BMD analyses determines a chemical exposure concentration (μg/mL) at which a defined level of response occurs (5% standard deviation). The primary goal of conducting this analysis was to identify the biological functions most sensitive to BAP dose-response in the airway epithelium. In addition, we were interested in whether the gene sets that provided the highest CA across a group of PAHs overlapped with those that were highly sensitive to dose-response treatment by BAP. Pathway level BMD modeling was applied to the prioritized gene sets (Section 3.3) and the most sensitive gene set to BAP dose-response regulation in 3D HBEC was Protein folding in the endoplasmic reticulum (ER) and cytoplasm, which modelled 27 genes with the lowest BMD median (Fig. 4A). The top ten most sensitive pathways with lowest BMD medians are highlighted (Fig. 4B) and include processes associated with cell cycle (mitosis, S phase, and G1-S growth factor regulation); cytoskeleton (cytoplasmic microtubules and actin filaments), ubiquitin related proteolysis, and DNA damage double-strand repair. Notably, the top ten most sensitive gene sets to BAP dose-response regulation did not overlap with the pathways that performed best for PAH classification of carcinogenic potential. Overall, these data show that the bioactivity profiles most associated with PAH carcinogenesis are not consistent with those that are most sensitive to BAP suggesting that PAHs, as a class, can function through unique mechanisms when compared to BAP alone.

Due to the lack of overlap between the methods, the pathway-level BMD modeling for BAP was expanded to include all process network categories as described in Metacore (Thomson Reuters) beyond just those prioritized for classification. This grouping of process networks into broad biological categories allows for BMD to be calculated for each biological category ranking them in order of sensitivity to BAP dose-response. The top 3 most significantly enriched (lowest minimum p-value out of all 8 exposure groups) pathways per process network category were selected for custom upload into the BMD analysis and the resulting BMD medians were averaged (Supplemental File 3). Overall, the

biological categories most sensitive to BAP dose-response gene regulation in HBEC were protein folding (avg BMD median = 4.74 µg/mL), DNA damage (avg BMD median = 6.58 µg/mL), cytoskeleton (8.92 µg/mL), cell adhesion (10.74 µg/mL), and cell cycle (11.06 µg/mL). Comparatively, the least sensitive pathway categories to BAP gene regulation were proliferation (121.78 µg/mL) and autophagy (134.75 µg/mL).

4.0. Discussion

Previously, we developed an approach to use gene signatures generated from mouse skin short-term after chemical treatment to accurately predict cancer outcome [15]. The present study demonstrates the successful translation of this approach into a human *in vitro* tissue model. We observed that gene biosignatures collected from 3D human bronchial epithelium exposed to a range of carcinogenic and non-carcinogenic PAHs can be used to accurately classify chemicals by potency. Gene expression profiles were analyzed to identify chemical-gene signatures at the pathway level. Gene sets related to several biological pathways were integrated and evaluated for classification performance to differentiate PAHs by carcinogenic class. Individual endpoints and biomarkers, such as intracellular ROS generation and CYP450 gene regulation, were insufficient predictors of carcinogenicity in this study. Benchmark dose modeling of BAP showed that the most sensitive pathway gene sets to BAP regulation were largely dissimilar from the pathways that best classified PAH carcinogenicity. These results illustrate the utility of using systems toxicology approaches to analyze global gene expression information towards carcinogenic hazard/risk assessment of PAHs. In addition to identification of gene sets, we also find evidence to challenge current assumptions that BAP carcinogenicity (and subsequent MOA) is reflective of overall PAH carcinogenicity.

4.1. Predicting carcinogenicity with individual biomarkers

Chemical carcinogenesis is a complex process that involves numerous biological processes and molecular targets during initiation, promotion, and progression. Thus, the complexity in mechanisms of carcinogenicity contributes to difficulty identifying singular endpoints or *in vitro* assays to predict carcinogenic hazard of chemicals [15, 16, 37]. While many carcinogenic PAHs have genotoxic modes of action and induce DNA damage through adduct formation [38-40], some carcinogenic PAHs also exhibit non-genotoxic modes of action that include estrogenic/antiestrogenic activity[41, 42], dysregulation of cell proliferation [43, 44], inhibition of gap-junctional intercellular communication [45, 46], and generation of ROS and oxidative stress [47-50].

Overall, we found that specific gene targets and endpoints in HBEC, such as CYP1A1 induction and ROS generation, were limited in their ability to predict degree of carcinogenic hazard. The diversity in MOAs for PAH toxicity may contribute to the difficulty in identifying single biomarkers and *in vitro* endpoints to evaluate carcinogenic hazard of chemicals with complex mechanisms. Other commonly reported biomarkers for carcinogenicity, such as DNA adduct formation, have also been observed to lack correlation with carcinogenesis [15]. While specific biomarkers and endpoints may not adequately assess carcinogenic hazard, a growing body of research suggests utility in toxicogenomic biomarkers and gene sets in evaluating carcinogenic hazard and carcinogenic MOA. mRNA and miRNA gene expression profiles have been used successfully to discriminate among carcinogens in various experimental model systems [17, 18]. In this study, we did not observe a clear pattern of carcinogenicity driving the clustering and grouping of samples in PCA and hierarchical clustering from global gene expression data. For this reason, we focused our study towards identifying subsets of genes that are high-performing classifiers to degree of carcinogenic hazard.

4.2. Utilization of in vitro biosignatures to classify chemicals based on health outcomes

Toxicogenomics usage in carcinogenic hazard assessment has progressed considerably in the past two decades; numerous methods have been developed to successfully identify genes linked to specific carcinogenic mechanisms and to develop approaches to predict and classify chemicals. In earlier toxicogenomic studies, correlational analyses and hierarchical clustering were commonly employed methods to identify subsets of genes to describe mechanisms of chemical toxicity [51]. Similar approaches have been applied to identify patterns of gene expression that discriminate between genotoxic and non-genotoxic carcinogens [52-55] or identify specific pathways that respond differently between genotoxic and non-genotoxic chemicals [56, 57]. Over the years, studies have advanced towards modeling approaches in which gene expression profiling can robustly discriminate carcinogens based on clearly different MOAs [54, 58, 59]

In our present study, we noted that PAH-specific signatures from global gene expression did not correlate with carcinogenic potency nor could be used to easily discriminate carcinogenic from non-carcinogenic PAHs. However, we hypothesized that global gene expression data could be organized into pathways or gene sets that may accurately classify treatments by potency. To address this challenge, we utilized a Bayesian posterior integration approach to assess classification accuracies for an integrated set of biological functions. These approaches have previously been applied to identify predictive biomarkers for chronic obstructive pulmonary disorder (COPD) [60] and type I diabetes through integration of disparate data streams, including proteins, metabolites, and lipids [32]. We have also previously described application of a pathway-based classification model for predicting carcinogenic risk of PAHs in mouse skin *in vivo* in which integration across multiple gene sets improved overall accuracy compared to each gene set independently [15]. A goal of the current study is to apply this approach to an organotypic human airway epithelial model to analyze, prioritize, and identify gene sets as classifiers and demonstrate feasibility of the classification framework *in vitro*. The resulting integrated CA of 91% indicates

that when the gene sets for AhR signaling, regulation of epithelial-mesenchymal transition, regulation of angiogenesis, and cell cycle G2-M are combined in an integrated classification, the overall accuracy performance can improve (Fig. 3). Further, the best classifiers identified from human airway epithelium *in vitro*, while overlapping, are distinct from those previously identified in mouse skin epithelium *in vivo*, which may be due to the expanded number of gene sets or PAHs tested or due to model-specific responses. Similar genomic-based models have been applied to individual chemicals after short-term exposure in rats to identify modes of action for distinguishing carcinogens from non-carcinogens in multiple tissues showing that the prediction of carcinogenicity was tissue-dependent and was most effective with tissue-specific gene classifier identification [17].

These studies demonstrate the importance of diversifying toxicogenomics analysis approaches beyond traditional methods of global gene expression analyses and adopting specialized analysis approaches to appropriately filter and query data. As toxicogenomics continues to be adopted in predictive toxicology, the opportunities for novel analyses and data integration continue to expand. We and others have found success using prediction models and classification approaches towards transcriptomic approaches to discriminate chemicals by carcinogenic hazards [15, 52, 60]. Beyond carcinogenic hazard assessment, these approaches have potential in further applications including disease prediction, biomarker development, drug safety, and mechanistic studies.

4.3. Dose-response modeling of BAP in human airway epithelium

Dose-response modeling of toxicogenomic data allows for quantitative assessment to estimate point of departure or threshold response for application to human health risk assessments [61-64]. In addition, it provides a better understanding of chemical MOA in different model systems. Through dose-response assessment of BAP in 3D HBEC, we observed that the most sensitive processes impacted by BAP in human airway epithelium included cell adhesion,

cytoskeleton, DNA damage and protein folding/stress response. These data support prior studies that have reported these DNA damage and repair mechanisms and cytoskeleton processes as targets for PAH toxicity to the lung and airway epithelium *in vivo* [13, 14, 65-67]. In particular, processes associated with barrier integrity were disrupted by exposure to BAP and PAHs *in vitro* in HepG2 and bronchial epithelium [16, 68-70]. PAH-induced disruption of the epithelial barrier and cell adhesion processes can lead to dysregulated inflammation and oxidative stress [71, 72]. Elevated oxidative stress and pro-inflammatory cytokines, in turn, disrupt tight junction function leading to increased airway inflammation [73]. Our BMD modelling results support *in vitro* and *in vivo* assay findings that cell adhesion, cytoskeleton, DNA damage, and stress response genes likely contributing modes of BAP toxicity and are among the most sensitive gene pathways to BAP-induced gene expression changes.

In addition, transcriptomic dose-response modeling allows for the direct comparison of gene sets most sensitive to BAP regulation to those identified as most predictive of PAH carcinogenicity in HBEC. Current EPA guidelines for PAH mixture carcinogenic risk assessment rely on comparing PAHs to BAP as a reference. A key assumption of this approach is that mechanisms of BAP carcinogenesis are representative of other carcinogenic PAHs However, there exist a wide range of known and proposed MOAs for PAHs suggesting that not all PAHs function through common mechanisms compared to BAP [15, 16, 74, 75]. Our BMD modeling data support the hypothesis that PAHs can function through different mechanisms than BAP to contribute to carcinogenicity. In this study, the pathway gene sets most sensitive to BAP dose-response regulation were overall dissimilar to the high-performing gene set classifiers for PAH carcinogenicity. While the cell cycle category commonly found between the high-performing gene-set classifiers (cell cycle G2-M), and BAP (cell cycle S phase and G1-S regulation), the exact gene sets that performed best in classification did not rank among the top ten BAP-sensitive gene sets. In addition, BMD analysis identified stress response (protein folding and ubiquitin proteolysis) and DNA damage

among the most sensitive pathways for BAP regulation. The transcriptional BMD median threshold values are well within range of *in vivo* derived points of departure for inhalation-specific cancer development [76]. While the goal of this study was not to derive points of departure for BAP, these results serve as an example of how toxicogenomics data can be modeled to support human health risk assessment.

5.0. Conclusion

Accurate carcinogenic assessment of PAHs and PAH mixtures has remained a challenge in toxicology and risk assessment. These studies show that chemical-gene biosignatures can be utilized to classify PAHs by carcinogenic hazard using *in vitro* models and inform potential mechanisms of action for PAHs in human bronchial epithelium. In addition, transcriptional BMD analysis show that processes most sensitive to BAP dose-response regulation are not necessarily the same as those that are most predictive of carcinogenic potential. These studies support the use of systems biology data collected from *in vitro* models for human health risk assessment. These studies support the use of systems biology data for use in human health risk assessments and to improve understanding of mechanisms associated with chemical toxicity and adverse health outcomes. Although the utilization of toxicogenomics in chemical carcinogenic hazard evaluation has developed significantly in the past decade, there have remained gaps in our understanding of PAH chemical and mixture effects in human systems. Overall, our findings support usage of organotypic human tissue cultures, implementation of toxicogenomics in cancer hazard evaluation, and a need for further studies to compare the applicability of BAP as a reference carcinogen for PAH mixture cancer risk assessment.

Author Contributions

All authors read and approved the final version of this manuscript. Y. Chang performed the experimental studies, data analysis and wrote the paper; C. Huynh and K. Bastin performed the BMD modeling; B. Rivera performed the oxidative stress and cell viability assays; L. Siddens performed the chemical treatments; S. Tilton supervised research and edited the manuscript.

Declaration of Competing Interests

The authors declare that there are no conflicts of interest.

Acknowledgements

This study was funded by Public Health Service grants P42ES016465 and T32ES07060 and a grant from the Center for Alternatives to Animal Testing, Johns Hopkins University.

References

1. Jarvis, I.W., et al., *Interactions between polycyclic aromatic hydrocarbons in complex mixtures and implications for cancer risk assessment.* Toxicology, 2014. **321**: p. 27-39.
2. IARC, *Some non-heterocyclic polycyclic aromatic hydrocarbons and some related exposures.* IARC Monographs and the Evaluation of Carcinogenic Risks to Humans, 2010. **92**.
3. IARC, *Diesel and Gasoline Engine Exhausts and Some Nitroarenes.* IARC Monographs and the Evaluation of Carcinogenic Risks to Humans, 2013. **105**.
4. IARC, *Outdoor Air Pollution.* IARC Monographs and the Evaluation of Carcinogenic Risks to Humans, 2015. **109**.
5. ATSDR. *ATSDR. ATSDR's Substance Priority List: Agency for Toxic Substances and Disease Registry*. 2017 11/18/2018]; Available from: https://www.atsdr.cdc.gov/spl/#2017spl.
6. Abdel-Shafy, H.I. and M.S.M. Mansour, *A review on polycyclic aromatic hydrocarbons: Source, environmental impact, effect on human health and remediation.* Egyptian Journal of Petroleum, 2016. **25**(1): p. 107-123.
7. Ramesh, A., et al., *Global environmental distribution and human health effects of polycyclic aromatic hydrocarbons*. 2011, Boca Raton, FL: CRC Press.
8. Benbrahim-Tallaa, L., et al., *Carcinogenicity of diesel-engine and gasoline-engine exhausts and some nitroarenes.* The Lancet Oncology, 2012. **13**(7): p. 663-664.
9. IARC, *Diesel and gasoline engine exhausts and some nitrarenes.* IARC MONOGRAPHS ON THE EVALUATION OF CARCINOGENIC RISKS TO HUMANS, 2014. **105**.
10. Rengarajan, T., et al., *Exposure to polycyclic aromatic hydrocarbons with special focus on cancer.* Asian Pacific Journal of Tropical Biomedicine, 2015. **5**(3): p. 182-189.
11. Gottmann, E., et al., *Data quality in predictive toxicology: reproducibility of rodent carcinogenicity experiments.* Environmental health perspectives, 2001. **109**(5): p. 509-514.
12. EPA, U.S. *Development of a relative potency factor (RPF) approach for polycyclic aromatic hydrocarbon (PAH) mixtures*. 2010 [cited EPA/635/R-08/012A; Available from: http://cfpub.epa.gov/ncea/cfm/recordisplay.cfm?deid=194584.
13. Siddens, L.K., et al., *Polycyclic aromatic hydrocarbons as skin carcinogens: comparison of benzo[a]pyrene, dibenzo[def,p]chrysene and three environmental mixtures in the FVB/N mouse.* Toxicol Appl Pharmacol, 2012. **264**(3): p. 377-86.
14. Courter, L.A., et al., *The influence of diesel exhaust on polycyclic aromatic hydrocarbon-induced DNA damage, gene expression, and tumor initiation in Sencar mice in vivo.* Cancer Lett, 2008. **265**(1): p. 135-47.

15. Tilton, S.C., et al., *Mechanism-Based Classification of PAH Mixtures to Predict Carcinogenic Potential*. Toxicol Sci, 2015. **146**(1): p. 135-45.
16. Chang, Y., et al., *Comparative mechanisms of PAH toxicity by benzo[a]pyrene and dibenzo[def,p]chrysene in primary human bronchial epithelial cells cultured at air-liquid interface*. Toxicology and Applied Pharmacology, 2019. **379**: p. 114644.
17. Gusenleitner, D., et al., *Genomic models of short-term exposure accurately predict long-term chemical carcinogenicity and identify putative mechanisms of action*. PLoS One, 2014. **9**(7): p. e102579.
18. Song, M.K., et al., *Identification of molecular signatures predicting the carcinogenicity of polycyclic aromatic hydrocarbons (PAHs)*. Toxicol Lett, 2012. **212**(1): p. 18-28.
19. Kopec, A.K., et al., *Automated dose-response analysis and comparative toxicogenomic evaluation of the hepatic effects elicited by TCDD, TCDF, and PCB126 in C57BL/6 mice*. Toxicol Sci, 2010. **118**(1): p. 286-97.
20. Kopec, A.K., et al., *Non-additive hepatic gene expression elicited by 2,3,7,8-tetrachlorodibenzo-p-dioxin (TCDD) and 2,2',4,4',5,5'-hexachlorobiphenyl (PCB153) co-treatment in C57BL/6 mice*. Toxicol Appl Pharmacol, 2011. **256**(2): p. 154-67.
21. Birgersdotter, A., R. Sandberg, and I. Ernberg, *Gene expression perturbation in vitro--a growing case for three-dimensional (3D) culture systems*. Semin Cancer Biol, 2005. **15**(5): p. 405-12.
22. Kimlin, L., J. Kassis, and V. Virador, *3D in vitro tissue models and their potential for drug screening*. Expert Opin Drug Discov, 2013. **8**(12): p. 1455-66.
23. McKim, J.M., Jr., *Building a tiered approach to in vitro predictive toxicity screening: a focus on assays with in vivo relevance*. Comb Chem High Throughput Screen, 2010. **13**(2): p. 188-206.
24. Siddens, L.K., et al., *Cytochrome P450 1b1 in polycyclic aromatic hydrocarbon (PAH)-induced skin carcinogenesis: Tumorigenicity of individual PAHs and coal-tar extract, DNA adduction and expression of select genes in the Cyp1b1 knockout mouse*. Toxicol Appl Pharmacol, 2015. **287**(2): p. 149-60.
25. Trapnell, C., L. Pachter, and S.L. Salzberg, *TopHat: discovering splice junctions with RNA-Seq*. Bioinformatics, 2009. **25**(9): p. 1105-11.
26. Trapnell, C., et al., *Transcript assembly and quantification by RNA-Seq reveals unannotated transcripts and isoform switching during cell differentiation*. Nat Biotechnol, 2010. **28**(5): p. 511-5.
27. Trapnell, C., et al., *Differential gene and transcript expression analysis of RNA-seq experiments with TopHat and Cufflinks*. Nat Protoc, 2012. **7**(3): p. 562-78.
28. Liao, Y., G.K. Smyth, and W. Shi, *featureCounts: an efficient general purpose program for assigning sequence reads to genomic features*. Bioinformatics, 2014. **30**(7): p. 923-30.

29. Love, M.I., W. Huber, and S. Anders, *Moderated estimation of fold change and dispersion for RNA-seq data with DESeq2.* Genome Biol, 2014. **15**(12): p. 550.
30. Nikolsky, Y., et al., *Functional analysis of OMICs data and small molecule compounds in an integrated "knowledge-based" platform.* Methods Mol Biol, 2009. **563**: p. 177-96.
31. Saeed, A.I., et al., *TM4: a free, open-source system for microarray data management and analysis.* Biotechniques, 2003. **34**(2): p. 374-8.
32. Webb-Robertson, B.-J.M., et al., *Bayesian Posterior Integration for Classification of Mass Spectrometry Data*, in *Statistical Analysis of Proteomics, Metabolomics, and Lipidomics Data Using Mass Spectrometry*, S. Datta and B.J.A. Mertens, Editors. 2017, Springer International Publishing: Cham. p. 203-211.
33. Beagley, N., K.G. Stratton, and B.J. Webb-Robertson, *VIBE 2.0: visual integration for bayesian evaluation.* Bioinformatics, 2010. **26**(2): p. 280-2.
34. Yang, L., B.C. Allen, and R.S. Thomas, *BMDExpress: a software tool for the benchmark dose analyses of genomic data.* BMC Genomics, 2007. **8**(1): p. 387.
35. Phillips, J.R., et al., *BMDExpress 2: enhanced transcriptomic dose-response analysis workflow.* Bioinformatics (Oxford, England), 2019. **35**(10): p. 1780-1782.
36. Labib, S., et al., *A framework for the use of single-chemical transcriptomics data in predicting the hazards associated with complex mixtures of polycyclic aromatic hydrocarbons.* Archives of toxicology, 2017. **91**(7): p. 2599-2616.
37. Labib, S., et al., *Comparative transcriptomic analyses to scrutinize the assumption that genotoxic PAHs exert effects via a common mode of action.* Arch Toxicol, 2016. **90**(10): p. 2461-80.
38. Topinka, J., et al., *DNA adduct formation in mammalian cell cultures by polycyclic aromatic hydrocarbons (PAH) and nitro-PAH in coke oven emission extract.* Mutation Research/Genetic Toxicology and Environmental Mutagenesis, 1998. **419**(1): p. 91-105.
39. Ross, J.A., et al., *Adenomas induced by polycyclic aromatic hydrocarbons in strain A/J mouse lung correlate with time-integrated DNA adduct levels.* Cancer Res, 1995. **55**(5): p. 1039-44.
40. Baird, W.M. and B. Mahadevan, *The uses of carcinogen-DNA adduct measurement in establishing mechanisms of mutagenesis and in chemoprevention.* Mutation Research/Fundamental and Molecular Mechanisms of Mutagenesis, 2004. **547**(1): p. 1-4.
41. Sievers, C.K., et al., *Differential action of monohydroxylated polycyclic aromatic hydrocarbons with estrogen receptors α and β.* Toxicological sciences : an official journal of the Society of Toxicology, 2013. **132**(2): p. 359-367.

42. Kummer, V., et al., *Estrogenic activity of environmental polycyclic aromatic hydrocarbons in uterus of immature Wistar rats.* Toxicol Lett, 2008. **180**(3): p. 212-21.
43. Plíšková, M., et al., *Deregulation of Cell Proliferation by Polycyclic Aromatic Hydrocarbons in Human Breast Carcinoma MCF-7 Cells Reflects Both Genotoxic and Nongenotoxic Events.* Toxicological Sciences, 2004. **83**(2): p. 246-256.
44. Vondráček, J., A. Kozubík, and M. Machala, *Modulation of Estrogen Receptor-Dependent Reporter Construct Activation and G0/G1–S-Phase Transition by Polycyclic Aromatic Hydrocarbons in Human Breast Carcinoma MCF-7 Cells.* Toxicological Sciences, 2002. **70**(2): p. 193-201.
45. Bláha, L., et al., *Inhibition of Gap-Junctional Intercellular Communication by Environmentally Occurring Polycyclic Aromatic Hydrocarbons.* Toxicological Sciences, 2002. **65**(1): p. 43-51.
46. Upham, B.L., et al., *Nongenotoxic effects of polycyclic aromatic hydrocarbons and their oxygenation by-products on the intercellular communication of rat liver epithelial cells.* Fundam Appl Toxicol, 1994. **23**(3): p. 470-5.
47. Penning, T.M., et al., *Dihydrodiol Dehydrogenases and Polycyclic Aromatic Hydrocarbon Activation: Generation of Reactive and Redox Active o-Quinones.* Chemical Research in Toxicology, 1999. **12**(1): p. 1-18.
48. Park, J.-H., et al., *Polycyclic Aromatic Hydrocarbon (PAH) o-Quinones Produced by the Aldo-Keto-Reductases (AKRs) Generate Abasic Sites, Oxidized Pyrimidines, and 8-Oxo-dGuo via Reactive Oxygen Species.* Chemical Research in Toxicology, 2006. **19**(5): p. 719-728.
49. An, J., et al., *The combined effects of BDE47 and BaP on oxidatively generated DNA damage in L02 cells and the possible molecular mechanism.* Mutat Res, 2011. **721**(2): p. 192-8.
50. Hanzalova, K., P. Rossner, and R.J. Sram, *Oxidative damage induced by carcinogenic polycyclic aromatic hydrocarbons and organic extracts from urban air particulate matter.* Mutation Research/Genetic Toxicology and Environmental Mutagenesis, 2010. **696**(2): p. 114-121.
51. Burczynski, M.E., et al., *Toxicogenomics-Based Discrimination of Toxic Mechanism in HepG2 Human Hepatoma Cells.* Toxicological Sciences, 2000. **58**(2): p. 399-415.
52. Magkoufopoulou, C., et al., *A transcriptomics-based in vitro assay for predicting chemical genotoxicity in vivo.* Carcinogenesis, 2012. **33**(7): p. 1421-1429.
53. van Delft, J.H.M., et al., *Comparison of supervised clustering methods to discriminate genotoxic from non-genotoxic carcinogens by gene expression profiling.* Mutation Research/Fundamental and Molecular Mechanisms of Mutagenesis, 2005. **575**(1): p. 17-33.

54. van Delft, J.H.M., et al., *Discrimination of genotoxic from non-genotoxic carcinogens by gene expression profiling.* Carcinogenesis, 2004. **25**(7): p. 1265-1276.
55. Lee, S.J., et al., *Distinguishing between genotoxic and non-genotoxic hepatocarcinogens by gene expression profiling and bioinformatic pathway analysis.* Scientific Reports, 2013. **3**(1): p. 2783.
56. Kim, J.-Y., et al., *Identification of potential biomarkers of genotoxicity and carcinogenicity in L5178Y mouse lymphoma cells by cDNA microarray analysis.* Environmental and Molecular Mutagenesis, 2005. **45**(1): p. 80-89.
57. Watanabe, T., et al., *Discrimination of genotoxic and non-genotoxic hepatocarcinogens by statistical analysis based on gene expression profiling in the mouse liver as determined by quantitative real-time PCR.* Mutation Research/Genetic Toxicology and Environmental Mutagenesis, 2012. **747**(2): p. 164-175.
58. Mathijs, K., et al., *Discrimination for Genotoxic and Nongenotoxic Carcinogens by Gene Expression Profiling in Primary Mouse Hepatocytes Improves with Exposure Time.* Toxicological Sciences, 2009. **112**(2): p. 374-384.
59. Williams, A., et al., *A predictive toxicogenomics signature to classify genotoxic versus non-genotoxic chemicals in human TK6 cells.* Data in Brief, 2015. **5**: p. 77-83.
60. Wang, J., et al., *A semiautomated framework for integrating expert knowledge into disease marker identification.* Dis Markers, 2013. **35**(5): p. 513-23.
61. Shao, K. and A.J. Shapiro, *A Web-Based System for Bayesian Benchmark Dose Estimation.* Environ Health Perspect, 2018. **126**(1): p. 017002.
62. Guo, X. and N. Mei, *Benchmark Dose Modeling of In Vitro Genotoxicity Data: a Reanalysis.* Toxicol Res, 2018. **34**(4): p. 303-310.
63. Mezencev, R. and S.S. Auerbach, *The sensitivity of transcriptomics BMD modeling to the methods used for microarray data normalization.* PLoS One, 2020. **15**(5): p. e0232955.
64. Farmahin, R., et al., *Recommended approaches in the application of toxicogenomics to derive points of departure for chemical risk assessment.* Arch Toxicol, 2017. **91**(5): p. 2045-2065.
65. Courter, L.A., et al., *Urban dust particulate matter alters PAH-induced carcinogenesis by inhibition of CYP1A1 and CYP1B1.* Toxicol Sci, 2007. **95**(1): p. 63-73.
66. Banni, M., et al., *Assessing the impact of Benzo[a]pyrene on Marine Mussels: Application of a novel targeted low density microarray complementing classical biomarker responses.* PLoS One, 2017. **12**(6): p. e0178460.
67. Marston, C.P., et al., *Effect of a complex environmental mixture from coal tar containing polycyclic aromatic hydrocarbons (PAH) on the tumor*

initiation, PAH-DNA binding and metabolic activation of carcinogenic PAH in mouse epidermis. Carcinogenesis, 2001. **22**(7): p. 1077-86.

68. Song, M.K., et al., *Polycyclic aromatic hydrocarbons induce migration in human hepatocellular carcinoma cells (HepG2) through reactive oxygen species-mediated p38 MAPK signal transduction.* Cancer Sci, 2011. **102**(9): p. 1636-44.
69. Oesterling, E., M. Toborek, and B. Hennig, *Benzo[a]pyrene induces intercellular adhesion molecule-1 through a caveolae and aryl hydrocarbon receptor mediated pathway.* Toxicol Appl Pharmacol, 2008. **232**(2): p. 309-16.
70. McGarry, M.A., et al., *Benzo(a)pyrene, but not 2,3,7,8-tetrachlorodibenzo-p-dioxin, alters cell adhesion proteins in human uterine RL95-2 cells.* Biochem Biophys Res Commun, 2002. **294**(1): p. 101-7.
71. Devalia, J.L., et al., *Mechanisms of pollution-induced airway disease: in vitro studies in the upper and lower airways.* Allergy, 1997. **52**(38 Suppl): p. 45-51; discussion 57-8.
72. Schamberger, A.C., et al., *Cigarette smoke-induced disruption of bronchial epithelial tight junctions is prevented by transforming growth factor-β.* Am J Respir Cell Mol Biol, 2014. **50**(6): p. 1040-52.
73. Coyne, C.B., et al., *Regulation of airway tight junctions by proinflammatory cytokines.* Mol Biol Cell, 2002. **13**(9): p. 3218-34.
74. Billiard, S.M., et al., *Nonadditive effects of PAHs on Early Vertebrate Development: mechanisms and implications for risk assessment.* Toxicological Sciences, 2007. **105**(1): p. 5-23.
75. Incardona, J.P., et al., *Developmental toxicity of 4-ring polycyclic aromatic hydrocarbons in zebrafish is differentially dependent on AH receptor isoforms and hepatic cytochrome P4501A metabolism.* Toxicol Appl Pharmacol, 2006. **217**(3): p. 308-21.
76. Thyssen, J., et al., *Inhalation studies with benzo[a]pyrene in Syrian golden hamsters.* J Natl Cancer Inst, 1981. **66**(3): p. 575-7.

Figure 3-1.

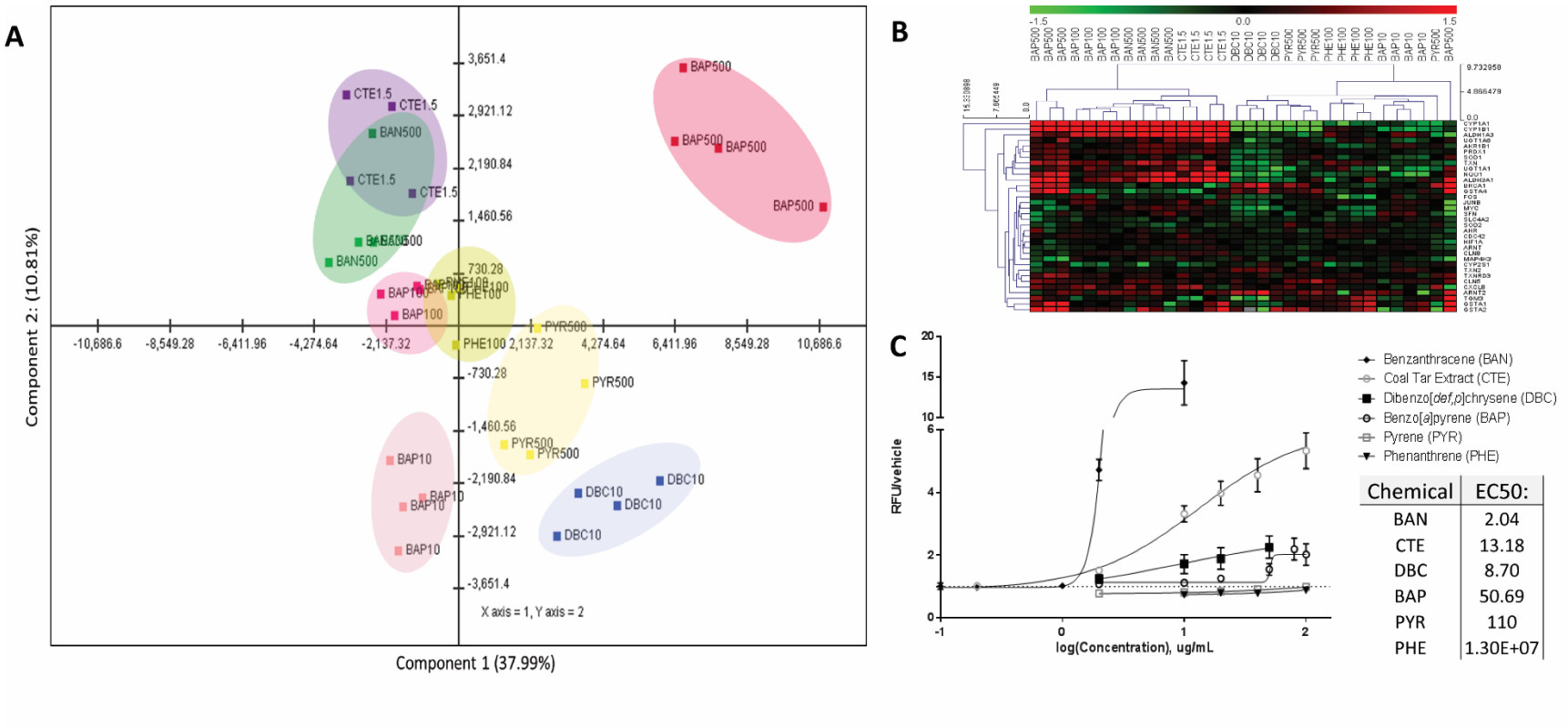

Figure 3-1. Differential effects of PAHs in human bronchial epithelial cells. (A) Principal components analysis (PCA) of global gene expression of HBEC exposed to PAHs. The horizontal axis represents PC 1 and the vertical axis represents PC 2. The captured variance of these first 2 components account for 47.22% of the total variance, and variance-correlation of gene expression resulted in variable clustering of PAHs. (B) Transcriptional regulation of genes by PAHs. Comparison of gene expression using RNASeq. Subsets of genes associated with xenobiotic metabolism, AhR signaling, oxidative stress, and cell cycle regulation were highlighted in a heatmap. Values are log2-fold change for all treatments compared with experimental control; red, green, and black represent upregulated, downregulated, and unchanged genes, respectively. (C) Intracellular ROS generation as measured by DCFDA. Chemical-induced fluorescence was expressed as relative fluorescence (RFU) normalized to vehicle control (RFU/vehicle), and the data were fit to a nonlinear regression with variable slope to model dose-response curves and calculate EC50s.

Figure 3-2.

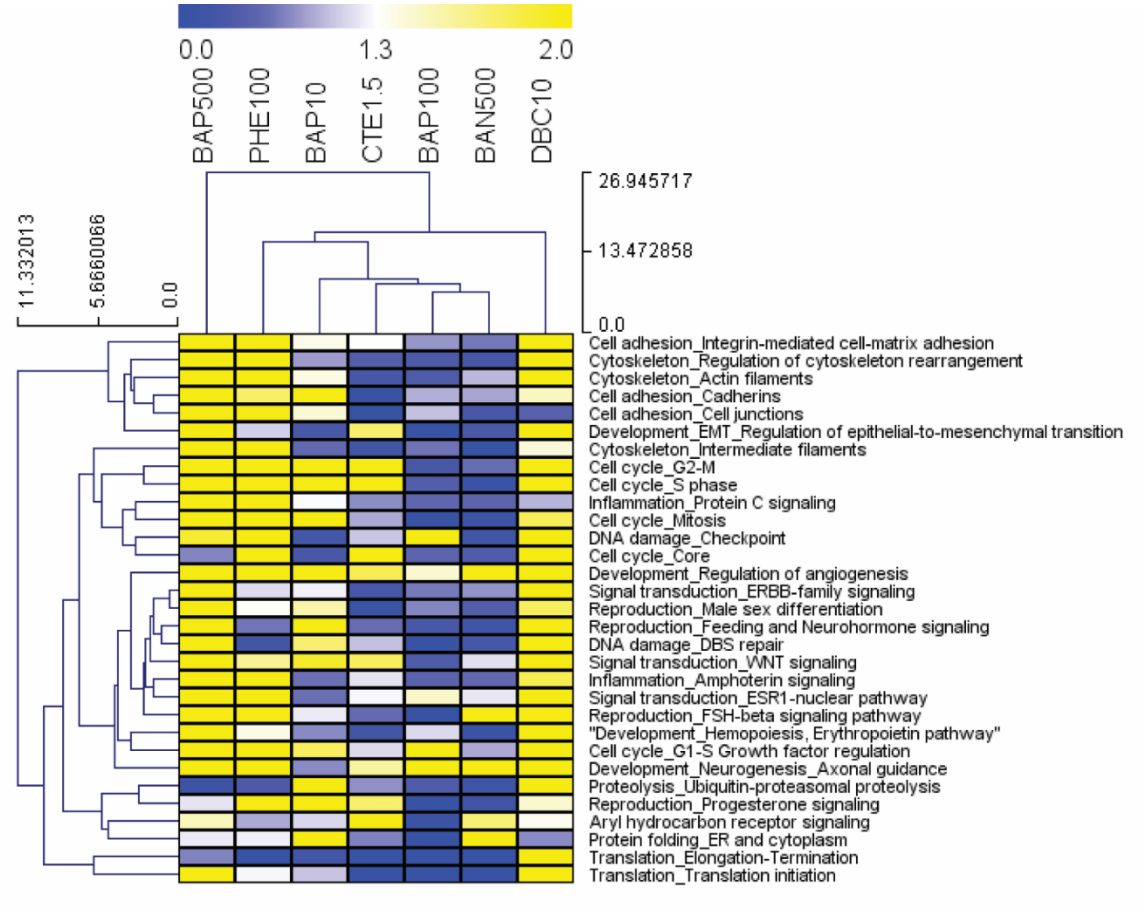

Figure 3-2. Pathway enrichment analysis of differentially regulated genes by PAH and PAH mixture exposure. Functional enrichment analysis was performed in MetaCore (GeneGO, Thomson Reuters) based on mapping of the significant ($p<0.05$) genes in each treatment group onto built-in functional network processes. Heatmap visualizing the top 30 most differentially significant process networks (greatest std(-logpval) regulated by 7 PAH treatments ($p<0.01$ for at least one PAH group). Values are pval that have been transformed (-logpvalue) for pathway enrichment of treatments, where blue, white, and yellow represent -logpvalue = 0, 1.3 ($p<0.05$), and 2.0 ($p<0.01$), respectively.

Figure 3-3.

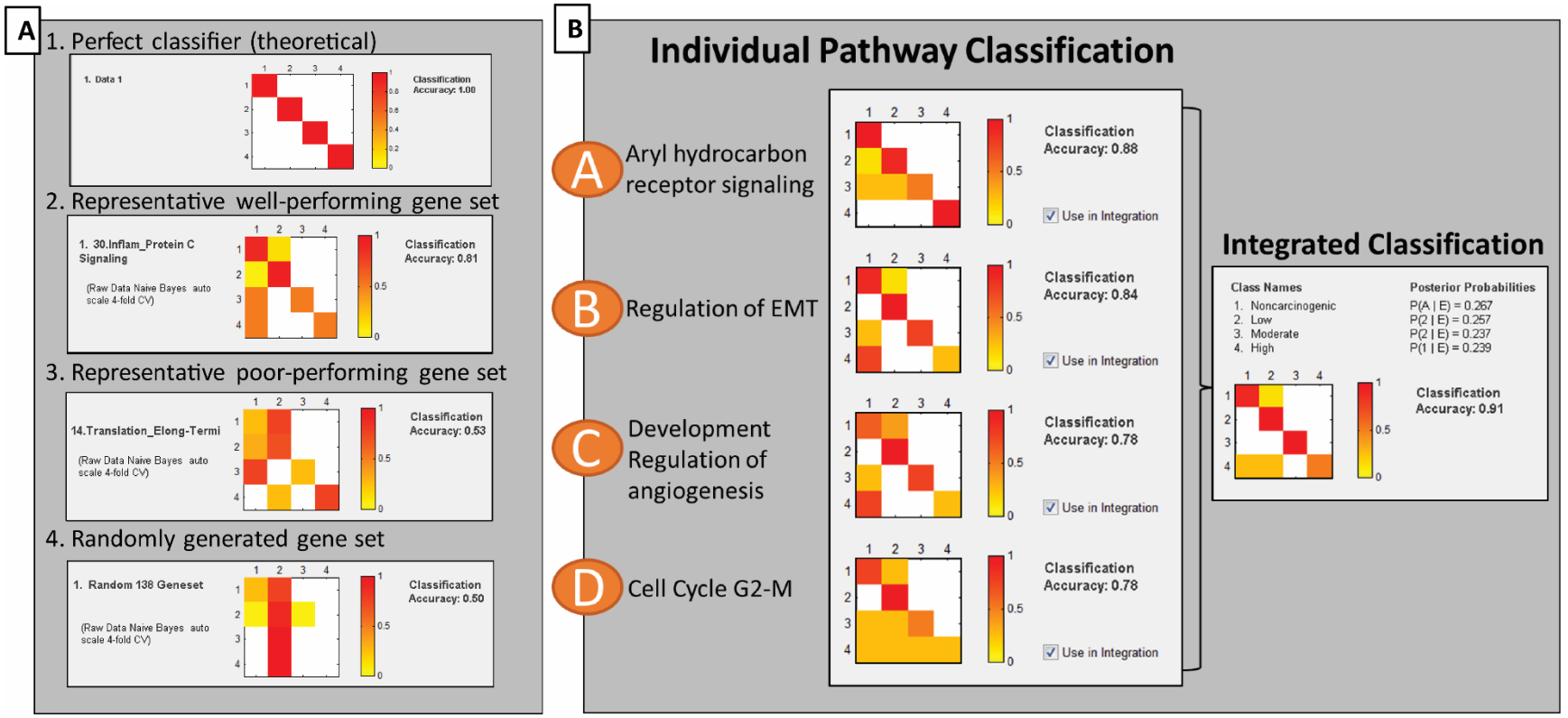

Figure 3-3. Classification of PAHs based gene sets. Classification accuracy (CA) heatmaps of gene-based classification performance, where classes 1-4 indicate carcinogenic potency (non-carcinogenic, low, moderate, high). Colors indicate proportion of samples classified into specific classes, where red represents most or all samples, and white represents zero samples. Therefore, a theoretical perfect classifier results in a diagonal line of red squares. (A) Probability matrices for gene sets were calculated using Naïve Bayes statistical learning algorithm with 4-fold cross validation. Here, the CA heatmaps demonstrate the possible range of classification performance, from theoretically perfect classifiers (1.00) to randomly generated gene sets that do not classify better than random (0.50). (B) Bayesian integration of top-performing pathway gene sets. Integrated CA (0.91) is indicated on the right, and exceeds the individual CA performance of individual pathway gene sets.

Figure 3-4.

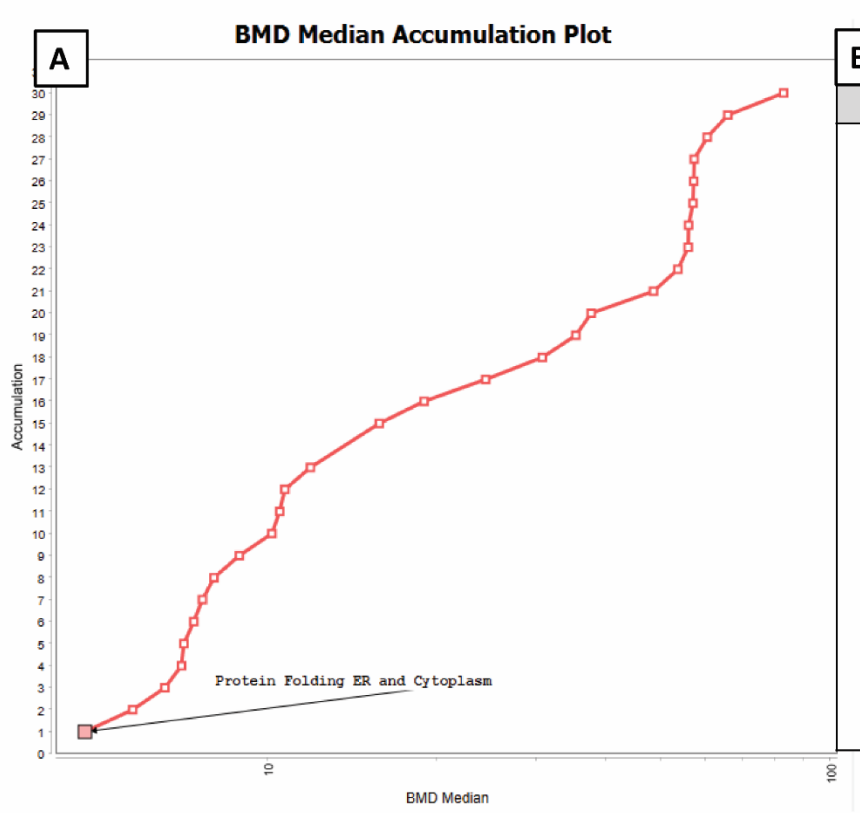

B

	Process Network/Gene Set	Genes	BMD Median
1	Protein Folding ER and Cytoplasm	27	4.74034
2	Proteolysis_Ubiquitin – proteasomal proteolysis	58	5.762835
3	Cell cycle Mitosis	71	6.57577
4	DNA damage_DBS repair	64	7.036435
5	Cytoskeleton Cytoplasmic microtubules	69	7.10826
6	Protein folding_Folding in normal condition	59	7.39789
7	Cell Adhesion_Cell Junctions	76	7.667215
8	Cell cycle_S phase	74	8.037845
9	Cytoskeleton Actin Filaments	81	8.91842
10	Cell Cycle G1-S Growth Factor Regulation	79	10.1861

Figure 3-4. Benchmark dose (BMD) analysis of transcriptomic data from 3D HBEC exposed to Benzo[a]pyrene (BAP). BMD values represent estimated median doses causing a 5% shift over the background rate of response associated with each gene set. (A) Distributions of modelled BMD estimates of BAP through a category analysis of the top 30 differentially significant pathway gene sets. The vertical axis represents the relative rank of the pathway gene sets, sorted by BMD median (ascending), while BMD median values are depicted across the horizontal axis. (B) Table of top ten most sensitive pathway gene sets to BAP gene regulation with number of genes modelled and BMD median. Genes from these pathways have the lowest BMD median values modelled, of the top 30 pathways.

CHAPTER 4 - Linking Co-regulated Gene Modules with Polycyclic Aromatic Hydrocarbon-related Cancer Risk in the 3D Human Bronchial Epithelium

Yvonne Chang[†], Julia E. Rager[‡*], Susan C. Tilton[†§]

Affiliations

[†]Environmental and Molecular Toxicology Department, Oregon State University, Corvallis, OR, United States
[‡]Department of Environmental Sciences and Engineering, Gillings School of Global Public Health, The University of North Carolina, Chapel Hill, NC, United States
*Institute for Environmental Health Solutions, and Curriculum in Toxicology, The University of North Carolina, Chapel Hill, NC, United States
[§] Superfund Research Program, Oregon State University, Corvallis, OR, United States

Corresponding Author
Susan C. Tilton, Environmental and Molecular Toxicology Department, Oregon State University, Corvallis, OR 97330, United States; email: susan.tilton@oregonstate.edu
Julia E. Rager, Department of Environmental Sciences and Engineering, Chapel Hill, NC 27599, United States; email: jrager@unc.edu

ABSTRACT

Exposure to polycyclic aromatic hydrocarbons (PAHs) often occur as complex chemical mixtures, which are linked to numerous adverse health outcomes in humans, with cancer as the greatest concern. The cancer risk associated with PAH exposures is commonly evaluated using the relative potency factor (RPF) approach, which estimates PAH mixture carcinogenic potential based on the sum of relative potency estimates of individual PAHs, compared to benzo[a]pyrene (BAP), a reference carcinogen. The present study evaluates molecular mechanisms related to PAH cancer risk through integration of transcriptomic and bioinformatic approaches in a 3D human bronchial epithelial cell (HBEC) model. Significantly regulated genes from human bronchial epithelium exposed to 7 PAHs and PAH mixtures were analyzed using a weighted gene coexpression network analysis (WGCNA) two-tiered approach, first to identify gene sets co-modulated to RPF, and then to link genes to a more comprehensive list of regulatory values, including inhalation-specific risk values. Over 3,000 genes associated with processes of cell cycle regulation, inflammation, DNA damage, and cell adhesion processes were found to be co-modulated with increasing RPF with pathways for cell cycle S phase and cytoskeleton actin identified as the most significantly enriched biological networks correlated to RPF. In addition, co-modulated genes were linked to additional cancer-relevant risk values, including inhalation unit risks, oral cancer slope factors, and cancer hazard classifications from the World Health Organization's International Agency for Research on Cancer. These gene sets represent potential biomarkers that could be used to evaluate cancer risk associated with PAH mixtures. Among the risk values and categorizations, RPF and IARC shared the most similar responses in positively and negatively correlated gene modules. Here, we demonstrated a novel manner of integrating gene sets with chemical toxicity equivalence estimates through WGCNA to understand potential mechanisms. Similar studies could further inform cancer risk evaluations and hazard assessments by incorporating organotypic human *in vitro* models with additional endpoints and risk values associated with chemical exposures.

INTRODUCTION

PAHs as global contaminants

Polycyclic aromatic hydrocarbons (PAHs) are a ubiquitous class of environmental contaminants that are found in ambient air, indoor air, water, and soil. Of hundreds of identified and studied PAHs, currently 16 PAHs are listed on the US Environmental Protection Agency (EPA) high priority pollutant list [1]. 16 priority PAHs were identified based on relative abundance in the environment and toxicity, but there are PAHs beyond the list of 16 that have higher toxicity in complex environmental mixtures [2]. Atmospheric PAHs can also participate in long range transport, and settle in soil and water leading to many possible routes of exposure, including ingestion, inhalation, and dermal contact [3-8]. The hazards and risks of PAH exposure may also depend on the mixture composition and exposure route.

Routes of exposure to PAHs in occupational and non-occupational settings include ingestion, inhalation, and dermal contact [8]. Adverse human health outcomes linked to exposure include skin irritation, immunosuppression, and skin, lung, and prostate cancer. With cancer as the health effect of greatest concern, numerous regulatory agencies including the US EPA and the European Chemicals Agency (ECHA) have developed restrictions to limit the exposure and sale of petroleum products containing at least eight of these PAHs. However, accurate human health risk assessment for PAHs remains a challenge.

Cancer risk assessment of PAHs

The current EPA framework for PAH regulation involves estimating cancer risk using a component-based relative potency factor (RPF) approach in which risk for PAH mixtures are estimated based on sum relative potency for component PAHs present in the mixture. In this approach, benzo[a]pyrene (BAP) is used as a reference carcinogen and cancer risk is reported in terms of BAP equivalents (BAPeq). At present, RPF estimates exist for only 27 PAHs. A major limitation of

this approach includes its heavy reliance on dose-response assessments of traditional, two-year *in vivo* rodent carcinogenicity bioassays that are lengthy and resource-intensive. Further, they often facilitate PAH exposure using intraperitoneal injection or dermal exposure. These may not adequately represent PAH routes of exposure in humans and could fail to capture the true risk of individuals PAHs, particularly with relation to tumorigenicity in lung tissue. There is an urgent need to develop alternative approaches for chemical hazard assessment and regulation.

Other regulatory values that incorporate additional routes of exposure include inhalation unit risk, cancer slope factor, reference concentration, reference dose, and cancer hazard categorizations through the International Agency for Research on Cancer (IARC) and assessments from the US EPA Integrated Risk Information System (IRIS). To adequately evaluate lung-specific PAH cancer hazards, additional risk and regulatory values such as inhalation unit risk, and reference concentrations (RfC) should be considered. In the present study, oral slope factor (OSF) and reference dose (RfD) were also included for the sake of completeness and to cover more chemical space than the limited number of chemicals for which there are RPF estimates for. Currently, there are limited investigations examining possible links between biological mechanisms and such increased cancer risks and toxicity values across different chemicals within a chemical class.

Utility of Transcriptional Signatures in Chemical Hazard Assessment

Transcriptomics has emerged as a mechanistically informative method for evaluating biological functions and pathways targeted by xenobiotics. Transcriptional profiling of gene signatures has been especially informative in identifying adverse drug reaction mechanisms [9] and hepatocarcinogen modes of action [10, 11]. There are a growing number of studies employing transcriptomics approaches to evaluate individual chemicals in an effort to predict mixture interactions such as concentration addition or independent action models [12, 13].

Transcriptomic data can also be used to provide critical MOA data to improve risk estimates. An example of such application is the transcriptomic profiling of benzo[a]pyrene, where multiple transcriptional analyses approaches have contributed to risk assessment. Gene expression profiling in multiple tissues in animal studies have contributed to MOA evaluations of BAP-sensitive genes and pathways affected in different organs of an animal study [14]. Transcriptomic information can also be modelled to derive benchmark dose values (BMD) for use as a point of departure value (PoD) for quantitative risk assessment [14, 15]. Additionally, transcriptional profiling in furan-exposed mouse liver tissue showed that benchmark dose values (BMD) derived from toxicogenomics data were consistent across multiple genomics platforms (RNAseq, microarray, and qPCR) and predictive of the two-year cancer bioassay-based PoD [16]. In cases of unknown, understudied, or complex toxicant mechanisms of action, there is a significant amount of opportunity present in employing bioinformatics applications to detect early effects from exposure and to discern responses from different chemical exposures at the transcriptomic-level [17].

Standard methods for global gene expression analyses, which typically filter by differential expression criteria for pathway enrichment, can restrict the number of possible toxicogenomic biomarkers identified. We previously analyzed transcriptional gene signatures from an *in vitro* bronchial epithelium exposed to a range of carcinogenic PAHs, and identified pathway gene sets towards the successful development of a classification model to accurately predict chemical carcinogenic potency (unpublished, Chang 2020). However, a limitation of this gene classifier identification was the reliance on pathway annotation. Novel bioinformatics approaches may help overcome these limitations. One such method, known as the weighted gene co-expression network analysis (WGCNA), provides a systems biology approach to explore genes regulated together [18, 19]. Researchers have noted the benefit of a co-expression approach where gene signature identification would not be independent of pathway annotations [20]. A co-expression network analysis approach simultaneously allows the identification

of genes associated with a specific parameter, rather than chemical-specific gene regulation. Groups of genes are identified as modules through an initial correlation analysis; then gene modules are related to traits or parameters, which can span dose, time, chemical traits, and biological phenotypes [18, 21]. This co-expression approach has been applied successfully in the field of toxicology to identify novel transcription factors associated with bisphenol A exposure [22] and genes and proteins linked to adverse health effects associated with increased inorganic arsenic exposure [23].

Study overview and goal

While the cancer-related health effects of PAHs and PAH mixtures have been evaluated in numerous cell-based and animal studies, there remains a lack of understanding of the genes and pathways affected by different carcinogenic PAHs in an inhalation-relevant model. There also exist data gaps in understanding genes and signaling events implicated in chemical carcinogenesis. WGCNA can be used to correlate transcriptional changes with increasing cancer risk (RPF), thereby allowing comparisons across chemicals and mixtures with different relative potencies. Therefore, co-expression analysis serves as a novel approach to investigate PAH-induced system-wide biological changes in an organotypic tissue model and may contribute MOA information to future cancer hazard and risk assessment. The goal of the present study was to identify gene sets co-modulated in relation to estimated human cancer risk and regulatory values and to better understand biological signaling important for chemically-induced disease. Network analysis of these co-modulated molecules was carried out to understand the biological functions and signaling networks of genes most significantly co-modulated in relation to cancer risk.

METHODS

Chemicals and Reagents

Cell culture media and phosphate buffered saline (PBS) were provided by MatTek Corporation (Ashland, MA). Benzo[a]pyrene (BAP) CAS# 50-32-8 and dibenzo[def,p]chrysene (DBC) CAS# 189-64-0 were purchased from MRIGlobal (Kansas City, MO). Benz[a]anthracene (BAN) CAS# 56-55-3, phenanthrene (PHE) CAS# 85-01-8, and pyrene (PYR) CAS# 19-00-0 were acquired from Sigma-Aldrich Chemical (St. Louis, MO.). PAHs used in the simulated air mixture (AM) were purchased from Sigma-Aldrich Chemical (St.Louis, MO.) Coal Tar Extract (CTE) standard reference material (SRM 1597a) was purchased from the National Institute of Standards & Technology (Gaithersburg, MD.) DNase I, TRIzol® reagent, Superscript® III First Strand Synthesis System, qPCR primers, and Pierce™ LDH Cytotoxicity Assay Kit were from Thermo Fisher Scientific (Waltham, MA). 2X SsoAdvanced™ Universal SYBER®Green Supermix was purchased from BioRad Laboratories, Inc. (Hercules, CA.) A simulated AM designed from published results of air samples collected in Beijing, China and analyzed for parent, nitrated, and oxygenated PAHs was produced as follows. Five parent PAHs were selected based on their abundance and biological relevance. Three additional methylated PAHs were selected for addition of non-carcinogenic components. Benzo[b]fluoranthene CAS# 205-99-2, benz[e]pyrene CAS# 192-97-2, benzo[g,h,i]perylene CAS# 191-24-2, benzo[a]pyrene, dibenzo[def,p]chrysene, 2-methylnaphthalene CAS# 91-57-6, 1-methylnaphthalene CAS# 90-12-0, and 1,3-dimethylnaphthalene CAS# 575-41-7 were added in the reported proportions relative to the sum of the eight chosen PAHs. The simulated mixture was solubilized in acetone vehicle.

Tissue Culture and Chemical Exposures

Tissue culture and chemical exposures were described previously (Chapter 3). Briefly, primary HBEC differentiated on transwell inserts (EpiAirway™ 100, Mattek, Ashland, MA) equilibrated for 24 hours at 37°C, 5% CO_2 followed by a change of fresh medium. Single PAHs and mixtures were solubilized in acetone and applied (0.01 ml/insert) to the apical surface of tissues (n=4 per treatment) for

up to 48 hrs, BAP (1-500 µg/ml), DBC (1-50 µg/ml), BAN (10-500 µg/ml), PYR (10-250 µg/ml), PHE (10-250 µg/ml), AM (125-2000 µg/ml) and CTE (250 -1500 µg/ml). Forty eight hours post treatment, PBS (0.20ml) was added to the apical surface of each insert and 48 hr TEER recorded. Apical washes and basal media were transferred to clean, sterile tubes and stored at -80°C. At the end of each exposure regimen, lysis buffer was added to each insert, collected, and stored at -80°C until extraction using RNeasy extraction kit.

Transcriptomic Analyses

Total RNA samples were isolated and sequenced by Illumina HiSeq3000 through the Oregon State University's Center for Genome Research and Biocomputing Core facilities as described previously (Chang et al., submitted). Sequenced reads were processed with Cutadapt (version 1.8.1) to trim adapter sequences from the paired-end reads. The human genome assembly GRCh38.84 was indexed using botwie2-build (version 2.2.3) while the transcriptome was indexed using Tophat (version 2.1.1.) [24]. TopHat was used to align the trimmed reads to indexed transcriptome and genome [25]. FeatureCounts, from the Subread package (version 1.6.0) was used to generate count tables.

Statistical Evaluation of Transcriptional Changes Associated with PAHs

Sequence count data were used to identify genes with expression levels associated with each PAH exposure. A comparative analysis of RNAseq data was determined in DESeq2 (version 1.26.0) [26]. The non-normalized count table output from FeatureCounts was input into DESeq2 to estimate differential gene expression as logarithmic fold change (log2FC) compared to vehicle control. Genes included for further analysis in WGCNA met the statistical criteria of $q<0.05$ for at least one chemical exposure group with no undetected values in the remaining exposure groups.

Organizing Cancer Risk Values across Databases

To relate human cancer risk to our PAH treatments, we first used relative potency factors (RPFs) from the U.S. Environmental Protection Agency Integrated Risk Information System's (IRIS) 2010 recommendation of an RPF approach for the carcinogenic risk assessment of PAH mixtures. The RPF approach assigns a numerical value to each chemical based on experimentally-derived carcinogenic potency, scaled as greater or less than BAP (RPF of 1). The dose-specific cancer risk of PAH mixtures were calculated by multiplying available RPFs to the proportions (mg/kg) of the individual PAH present in the mixtures. All treatments, including individual PAHs, had BAPeq calculated by multiplying dose with RPF.

Additional cancer-relevant regulatory values, such as oral slope factor (OSF) and inhalation unit risk (IUR) were downloaded from databases, prioritized in order of availability from EPA IRIS, then CTV. Other cancer-relevant risk and classification values, such as reference dose (RfD), reference concentration (RfC), IRIS, and IARC cancer hazard classifications were included for completeness. While many of these health risk values were predicted with variable confidence, the authors felt that it was important to consider inhalation risk values, to serve as comparisons against RPF and OSF, which are derived through oral and dermal routes of exposure. IRIS and IARC categories also were converted to a numerical scale, with 0 representing least and 4 representing greatest hazard, or group 1.

Identifying Genes with Co-Modulated Expression Patterns through WGCNA

To identify co-modulated gene sets within the transcriptomic dataset of PAH and PAH mixtures treated HBEC, weighted gene co-expression analysis (WGCNA) was employed to calculate integrated measures from co-modulated genes. WGCNA is a quantitative, systems biology approach that describes correlation patterns between groups of genes [18]. All genes that were identified as significantly regulated across at least one treatment (13644 genes in total) were analyzed collectively using the WGCNA R package [19]. WGCNA was used to identify clusters (modules) of highly interconnected genes across both experimentally and database-derived traits and regulatory values, all correlated

with each other, and thus considered co-modulated. The steps have been previously summarized [18-20, 22, 27]. Overall network and module statistics were performed following methods described by Langfelder et al. [18]. First, Pearson correlation coefficients were calculated for all pairwise comparisons of genes. The resulting Pearson correlation matrix was transformed into an adjacency matrix resulting in a weighted network describing connection strengths between genes. To allow genes with both negative and positive correlations to be grouped together, an unsigned network was used. A power of 16 and minimum gene module size of 50 was used to construct co-expression gene networks that were weighted to prioritize genes with high correlations. Modules were then identified as groups of interconnected genes in the weighted network analysis with high topological overlap, measured based on an average linkage hierarchical clustering. The resulting modules represent clusters of highly interconnected genes with high positive or negative correlations. With these defined modules, the first principal component of the modules were calculated and referred to as eigenmodules, then correlated with toxicity values where statistical significance was evaluated [18].

Network Analysis of Co-Modulated Genes associated with Cancer Risk Values

Network analysis was carried out to understand systems-level responses that occur within a co-modulated set of mRNAs identified through WGCNA. For the first tier of the analysis, RPF-associated genes from prioritized module eigengene were further analyzed for pathway enrichment analysis in Metacore (Clarivate Analytics, Philadelphia, PA). Statistical significance of over-connected interactions was calculated using a hypergeometric distribution, where the p value represents the probability of a particular mapping arising by chance for experimental data compared to the background [28]. Average FDRs for network categories were calculated for further analysis. Network visualizations were prepared in Cytoscape (v3.5.1) [29].

RESULTS

Identifying Regulatory Values Relevant to PAH Cancer Risk

This study evaluated the biological effects of HBEC exposure to PAHs and PAH mixtures as an effort to link cellular responses to cancer-relevant regulatory and hazard classification values. For tier one analysis, experiment-specific risk values were calculated. Cancer potency factors (BAPeq) were calculated using the RPF approach, for PAHs with RPF estimates available. Limitations of this approach included missing RPF estimates for as many as 57 RPFs out of the 73 PAHs in Coal tar extract mixture (78%), and 4 missing from the total of 8 PAHs in the air mixture sample (50%). Calculations by mass determined that 75% of the components in CTE were unaccounted for by RPF and BAPeq, while 58% of the PAHs by mass in AM were unaccounted for. Conditional Toxicity Value (CTV) was used to fill most missing values [30], and while this resulted in an experimentally calculated, weight of evidence derived (EPA IRIS) value or predicted (CTV) value, the applicability domain was high for almost all chemicals for CTV, indicating low confidence in those predictions. However for the sake of completeness, those values were included in the analysis to provide inhalation-relevant risk values to compare across.

Transcriptomic analysis

The effects of PAH and PAH mixture exposure in 3D HBEC were investigated using a transcriptomic profiling approach through RNAseq analysis. Raw and normalized sequencing files are available online at NCBI Gene Expression Omnibus (GSE128471). Over 60,000 mRNA transcripts were mapped and evaluated, and 13,644 genes were identified as statistically significant ($q < 0.05$), with at least one gene significantly regulated by a chemical exposure group. The number of genes that showed significant differential expression varied according to each exposure condition, with numbers ranging from 3 (pyrene) to over 9000 (air mixture). Because the number of significantly regulated genes varied so

highly between exposure groups, it was advantageous to employ an approach that evaluated co-modulated expression profiles regardless of significant differential expression.

Identifying Co-Modulated Genes associated with Cancer RPF

This first tier of the analysis identified and prioritized module eigengenes, or gene modules, linked to experimental-specific traits to the gene dataset. Twenty-three gene modules were identified through WGCNA (**Fig. 1A**), representing groups of genes that are co-modulated across PAH and PAH mixtures treatments. Of the experimental-specific sample traits, BAPeq-related module eigengenes were prioritized for further analysis as potential gene hubs of relevance to increased calculated cancer risk (**Table 1)**. Six module eigengenes were significantly correlated to BAPeq, or RPF cancer risk.We prioritized the top most significant positively and negatively correlated modules associated with BAPeq for further analysis to identify which genes and cellular networks and processes were most co-modulated and involved in the processes of cellular response to carcinogenic PAH treatment. One module eigengene ("MEturquoise") was identified as the most significantly positively correlated with BAPeq ($p=0.01$), while another module eigengene ("MEred") was identified as the most significantly negatively correlated with BAPeq ($p=0.0007$). Because BAPeq is calculated directly from RPF, significant gene clusters to this trait represents genes comodulated across BAPeq and therefore the RPF approach of cancer risk evaluation. The co-modulation of 2078 transcripts or genes were identified in the MEturquoise module eigengene of interest. Interestingly, the 9 PAH treatments were moderately well represented in this gene list, where PAH exposure groups with a lower number of significantly regulated genes ($p<0.05$) still had a majority of their genes present in MEturquoise. The MEturquoise module identified 2078 total co-modulated transcripts, and included 7 transcripts identified as miRNAs and 303 transcripts identified as lncRNAs. This module contained co-modulated genes such as *BRCA1*, *BRCA2*,

NR2F2, *TP53AIP1*, *JUNB*, and *HMOX1*, and many additional genes related to cell cycle and inflammation (**Fig. 1B)**.

In the MERed gene module, 1021 transcripts were found to be significantly negatively co-modulated. These transcripts included 2 miRNAs and 15 lncRNAs. Many of these genes are downregulated in response to BAPeq. However, within MEred module eigengene there are also genes negatively correlated to the overall trend of MEred (**Fig. 1C**). These include genes important for cell motility junction organization, including FMN1, DYNC2LI1, DNAL1, and CLDN8.

Network Analysis of Co-modulated Genes in Prioritized Module Eigengenes

To assess biological relevance of the genes identified in each prioritized module eigengene, a pathway enrichment analysis of MEturquoise and MEred was conducted (**Fig 2**). Network analysis of genes identified process networks that were significantly enriched (FDR<0.05) by both prioritized modules, as well as process networks unique enriched by one but not the other. These process networks were organized into "network categories", grouped by their broader biological categories (ex. Cell Cycle S Phase was grouped into the Cell Cycle network category). The positively correlated MEturquoise significantly enriched process networks related to cell cycle regulation, DNA damage, signal transduction, and cardiac development (**Fig 2**). These process network categories were uniquely enriched by the MEturquoise module, and MEred did not share any significant process network enrichment in these network categories. In contrast, MEred significantly enriched processes related to cell adhesion, cytoskeleton, protein folding, transcription, and translation, while MEturquoise did not. Both modules enriched heavily enriched process networks related to inflammation (9 specific process networks enriched by MEturquoise, and 15 specific process networks enriched by MEred).

To further study network regulation of the genes in each prioritized pathways, process networks were further profiled through a network analysis visualization comparing module membership of network genes. The Cell Cycle S phase process network was the most significantly enriched network (FDR=1.16E-

09) unique to METurquoise (**Fig 3A**), while the Cytoskeleton-Actin filaments network was the most significantly enriched network (FDR=4.24E-06) unique to MERed (**Fig 3B**). The networks were analyzed as undirected networks through Cytoscape (v3.8.0), and the size of the nodes in the network were mapped to calculated betweenness centrality for each gene, and edges mapped to annotated interactions (undirected) from Metacore. The betweenness centrality parameter represents the extent to which a vertex in the shortest paths between other vertices, and helps identify genes with maximum number of shortest paths crossing between other nodes, with the largest number of edges passing through. In the Cell Cycle S phase gene network, the top gene nodes with the highest centrality measures from MEturquoise were CDK1, MCM2, and PCNA. In the Cytoskeleton-Actin filaments network, the gene nodes with the highest centrality measures from MERed included ACTG1, c-SRC, ACTB, and Cortactin.

Identifying Co-Modulated Genes associated with Additional Cancer Regulatory Values

To evaluate relationships between co-modulated genes and regulatory values and hazard classifications, we included additional database-derived values, particularly inhalation-relevant values, such as IUR, RfC, OSF, RfD, and IRIS and IARC cancer hazard classifications (**Fig. 4)**. For this analysis, RPF was also included, and because these values are not related to specific chemical doses, the highest concentration of BAP was selected. The gene modules that correlated the most significantly with RPF were MEtwo, at $p = 0.02$ (positive correlation) and MEfourteen, at $p = 0.02$ (negative correlation) (Figure 4 and Table 2). Certain regulatory and hazard classifications' correlations were found to be more similar to RPF's module correlations than other regulatory values. Specifically, RPF and RfD did not share any significantly correlated module eigengenes; however RPF shared two significantly correlated modules with oral slope factor (OSF). When the regulatory value groups' overall correlations were evaluated through unsupervised hierarchical clustering, we found that RPF's correlations to the module eigengenes were the most similar to IARC hazard classifications, followed by IRIS, then OSF,

IUR, RfD, and RfC (**Fig. 4)**. Through this analysis, we observed that select module eigengenes were significantly correlated by RPF, yet different module eigengenes were significantly correlated by different risk value types. MEthirteen was highly significantly correlated (p=3E-4) by oral slope factor. Inhalation unit risk (IUR) was significantly linked to MEten. These uniquely correlated modules suggest that a combined approach of multiple regulatory values can be used to identify potential biomarkers that may have greater applications in chemical safety and hazard assessment.

DISCUSSION

As the toxicology community shifts towards *in vitro* testing and computational biology, novel approaches in transcriptional data analyses must be developed and refined to fill unmet needs in chemical hazard assessment [31]. The ultimate goal of toxicity testing is to generate and understand data to protect the public and environment from harmful chemicals. However, traditional *in vivo* toxicity testing is limited in its throughput and capacity to provide mechanistic information linking apical endpoints to the underlying processes involved in chemical toxicity [32]. Current "-omics" level approaches evaluating PAH carcinogenicity have focused on identifying chemical-specific mechanisms and been largely successful contributing towards development of predictive approaches of chemical MOA [33-37]. However, past studies have not focused on identifying broader patterns in affected biomolecules across different parameters of PAHs, such as cancer risk. Here, we evaluated the transcriptional signatures of a range of carcinogenic PAHs tested in a 3D *in vitro* airway epithelium, and utilized a WGCNA approach to identify gene modules significantly correlated to increasing cancer risk calculated through RPF. After exposing a 3D human bronchial epithelium to 9 PAH exposure groups including mixtures, early transcriptional changes associated with increasing cancer risk were identified and prioritized for further study.

Overall, we identified groups of genes with similar expression patterns that were significantly correlated in relation to PAH cancer RPF estimates. We also compiled additional risk values both specific and non-specific to inhalation. Through our co-expression analysis, we identified two significantly co-modulated gene clusters to prioritize for further study. Genes identified from these modules significantly enriched distinct subsets of process network categories, including processes from cell cycle regulation and cytoskeleton. Finally, our expanded co-expression analysis identified two shared gene modules between RPF, IARC classes, and cancer slope factor.

Carcinogenic PAH exposure is associated with alterations in cell cycle S phase gene regulation

This study was identifed cell cycle S phase genes as an important and highly enriched pathway associated with MEturquoise. METurquoise genes were significantly positively correlated with increased RPF estimates. Our results are consistent with other findings that PAH exposure is linked to alterations in cell cycle processes. Previous research has identified dysregulation of cell proliferation as a potential mechanism of BAP and BAN activity [38]. The P53 signaling pathway is also activated in response to stress, which includes DNA damage [39]. Several genes identified in METurquoise (**Fig 1B**) (i.e. *TP53BP2* and *MDM2*) are involved in p53 signaling [40-42]. Cyclin-dependent kinase (*CDK1*) was also identified as a gene of interest in MEturquoise, and normally functions in cell cycle progression via S phase initiation [43]. Dysregulation of these signaling pathways may be important in early cellular responses to PAH exposure. A well-understood mechanism of BAP carcinogenesis is its genotoxic activity forming diolepoxide DNA adducts [44-47]. Our findings support several reports that exposure to BAP can cause S phase arrest through DNA damage signaling [38, 48, 49].

Hub genes identified in the network (*CDK1*, *MCM2*, *PCNA*) have roles central to controlling cell cycle progression and responding to DNA damage (**Fig. 3A)**. However, their involvement with environmental carcinogens have not been clearly established. Our network analysis identified several highly connected hub

genes central to the network, which include the minichromosome maintenance protein 2 (*MCM2*), a regulator of DNA synthesis, and the cyclin dependent kinase (*CDK1*), which controls progression into S phase of the cell cycle and induces senescence in response to DNA damage [50-53]. Malfunction or dysregulation of these proteins have been linked to the development of cancers in multiple tissues, including lung and breast [53-57]. While BAP exposure has previously been linked to alterations in CDK1 and MDM2 activity, the findings of this network analysis support S phase gene regulation as a major cellular network perturbed by carcinogenic PAH exposure [48, 49, 58].

Carcinogenic PAH exposure dysregulates actin cytoskeleton gene networks

In our analysis of MEred module genes, we identified the cytoskeleton actin filament network as a top negatively correlated gene network to PAH cancer risk. Several hub genes (*ACTG1, ACTB, c-SRC)* were also identified as hub genes with high betweenness centrality measures (**Fig. 3B)**. These findings suggest that genes integral to actin cytoskeleton structure, maintenance, and regulation, are negatively associated with increased PAH cancer risk. Similar mechanistic studies also found that short-term exposure to PAHs or PAH-containing mixtures result in the down-regulation of several cell adhesion, motility, and cytoskeletal-involved processes, including epithelial-mesenchymal transition [59-63]. These processes can be indicators of cancer promotion and progression, and can co-regulate in complex signaling networks during cancer progression. Actin filament reorganization is directly responsible for driving cancer cell motility, morphological changes, and alterations in extracellular matrix and adhesion [64-66]. Additionally, actin-based adhesion protein complexes are integral in linking cells via cell-cell adhesion and to the extra extracellular matrices. Taken together, these findings support the role of actin cytoskeletal networks as early biomarkers and indicators of cellular changes affected by carcinogenic PAH exposure.

Comparisons of regulatory values and associated gene modules

PAH cancer risk assessment has traditionally relied on the use of RPF estimates available only for a subset of PAHs [67]. However, we adapted WGCNA in a novel manner in an effort to identify genes similarly associated to RPF and other risk values and hazard classifications. Notably, we identified overlap in significant gene module membership between RPF and at least one other risk value in two modules. We also found that RPF correlation patterns was the most similar to that of IARC cancer classes. These results suggest that the RPF approach currently has more similar hazard designations towards chemicals, compared to IARC classifications, which classifies chemicals as carcinogens based on weight of evidence [68-70]. Inversely, many chemicals, including heterocyclic PAHs, present in PAH mixtures evaluated did not have RPF estimates nor IARC classifications; yet had OSF and IUR values. These differences in missing values may have contributed to dissimilarities in correlation patterns with RPF, and thus prioritize the need the evaluate gene clusters where similarities have been identified. While direct comparisons between differing regulatory and risk values not feasible, this analysis focused on identifying shared gene clusters and exploring correlations across risk values.

Advantages of identifying co-modulated gene sets across cancer risk

Data generation from chemical transcriptional profiling has yielded a wealth of chemical-gene signatures; however researchers lack adequate measures to understand broader patterns across chemical groups. The results from this study demonstrate a novel and effective method to identify gene associations across multiple chemicals and parameters. There were several advantages to using RPF as the primary chemical risk value for identification of co-modulated gene associations. RPF estimates are derived through a weight of evidence approach, and so RPF values are substantiated by *in vivo* tumorigenic evidence [67]. Typically, multiple chronic rodent cancer bioassays are evaluated towards the development of an RPF estimate. We identified cellular networks positively and negative associated with cancer risk in the 3D HBEC model, and our findings supported several reports

in the literature, indicating that short-term gene signatures can be particularly useful in identifying genes linked to cancer. A major benefit of a co-expression approach is that subtle gene changes and biological interactions may be captured [20], allowing identification of similarly regulated gene networks. Previous research using WGCNA has found that gene modules identified in drug-induced hepatocyte transcriptional changes are correlated to adverse outcomes and toxicity [71]; however some of the top ranked gene modules identified had little biological annotation, indicating a unique capability of this approach [72]. Investigation of these poorly annotated genes and lesser understood signaling networks may prove useful in developing novel biomarkers to identify potential drivers of chemical toxicity. In this study, we identified 9 miRNAs and over 300 lncRNAs as significantly correlated with PAH cancer risk. Thus there is high potential for identifying novel or understudied biomarkers related to PAH-specific cancer risk through applications of WGCNA.

Study limitations

There were several disadvantages to using regulatory values to evaluate correlation to co-modulated gene sets in our analysis. Our limited dataset used for chemical biosignature profiling (9 chemical doses, with 2 mixtures) included only two non-carcinogenic PAHs. It is possible that expansion of this dataset to include more non-carcinogenic and extremely carcinogenic PAHs, in greater doses, could help strengthen increase specificity of gene associations. In addition, the RPF estimates available to calculate BAPeqs were derived from murine and rodent models, from studies where animals were exposed orally and through intraperitoneal injection, which do not represent typical routes of PAH exposures for human. Most importantly, inhalation was not considered in deriving RPF estimates. The IURs we included from CTV completed our trait table, however a majority of the chemical values sourced for chemical mixtures were predicted from CTV, rather than experimentally derived. CTV was a useful tool in supplementing data-poor chemicals with predicted health regulatory values.

However, this data was frequently low confidence, from CTV's high percent of applicability domain. Additionally, the second tier of our analysis did not allow taking chemical dose into consideration; only one dataset per chemical was able to be associated to database-derived regulatory and hazard values. Finally, a limitation of this toxicogenomics approach was the inability to distinguish between chemical-specific differences or cancer risk-related differences. This challenge could be partially resolved through addition of different chemicals at higher RPF or BAPeq, such that similarly comodulated genes between extreme carcinogens could be identified across a greater number of chemicals. As we continue to complete our evaluations of PAHs in the 3D HBEC, further gene expression information will be collected to expand our understanding of cancer risk-related biomarkers.

CONCLUSIONS

This study examined relationships between co-modulated gene sets and chemical risk values relevant to human cancer risk, with the goal of identifying key pathways, and gene hubs linked to cancer risk of PAH and PAH mixtures. For the first time, PAH-responsive genes were linked to relative potency factor via calculations of BAPeq through a quantitative systems biology approach. We prioritized positively and negatively associated modules for further study, and these genes significantly enriched distinct biological functions including cell cycle, cytoskeleton, and inflammation. This study also identified module eigengenes significantly associated with additional regulatory values and hazard classifications including IARC classifications, oral cancer slope factors, and inhalation unit risks. Some regulatory values (IARC, IRIS, OSF) shared greater numbers of commonly correlated modules with RPF than other regulatory values (IUR, RfC, RfD), suggesting potential value in using them when RPF is unavailable. This study utilized transcriptional signatures in response to short-term chemical exposures to identify potential biomarkers and associations between regulatory values and biological activity. Such an approach could be used to relate organotypic, human

in vitro-derived toxicogenomics information towards regulatory applications in the near future.

Funding Sources

This study was funded by Public Health Service grants P42ES016465 and T32ES07060.

Notes

The authors declare they have no competing financial interests.

Abbreviations

ME, module eigengene; miRNA, microRNA; NCBI, National Center for Biotechnology Information; qRT-PCR, real-time reverse transcriptase polymerase chain reaction; RfD, reference dose; U.S. EPA, United States Environmental Protection Agency; WHO, World Health Organization; WGCNA, weighted gene co-expression analysis

REFERENCES

1. Bojes, H.K. and P.G. Pope, *Characterization of EPA's 16 priority pollutant polycyclic aromatic hydrocarbons (PAHs) in tank bottom solids and associated contaminated soils at oil exploration and production sites in Texas*. Regulatory Toxicology and Pharmacology, 2007. **47**(3): p. 288-295.
2. Andersson, J.T. and C. Achten, *Time to Say Goodbye to the 16 EPA PAHs? Toward an Up-to-Date Use of PACs for Environmental Purposes*. Polycyclic Aromatic Compounds, 2015. **35**(2-4): p. 330-354.
3. Witt, G. and H. Siegel, *The Consequences of the Oder Flood in 1997 on the Distribution of Polycyclic Aromatic Hydrocarbons (PAHs) in the Oder River Estuary*. Marine Pollution Bulletin, 2000. **40**(12): p. 1124-1131.
4. Witter, B., M. Winkler, and K. Friese, *Depth Distribution of Chlorinated and Polycyclic Aromatic Hydrocarbons in Floodplain Soils of the River*. Acta hydrochimica et hydrobiologica, 2003. **31**(4-5): p. 411-422.
5. Genualdi, S.A., et al., *Trans-Pacific and Regional Atmospheric Transport of Polycyclic Aromatic Hydrocarbons and Pesticides in Biomass Burning Emissions to Western North America*. Environmental Science & Technology, 2009. **43**(4): p. 1061-1066.
6. Killin, R.K., et al., *Transpacific and regional atmospheric transport of anthropogenic semivolatile organic compounds to Cheeka Peak Observatory during the spring of 2002*. Journal of Geophysical Research: Atmospheres, 2004. **109**(D23).
7. Lafontaine, S., et al., *Relative Influence of Trans-Pacific and Regional Atmospheric Transport of PAHs in the Pacific Northwest, U.S.* Environmental Science & Technology, 2015. **49**(23): p. 13807-13816.
8. Abdel-Shafy, H.I. and M.S.M. Mansour, *A review on polycyclic aromatic hydrocarbons: Source, environmental impact, effect on human health and remediation*. Egyptian Journal of Petroleum, 2016. **25**(1): p. 107-123.
9. Cui, Y. and R.S. Paules, *Use of transcriptomics in understanding mechanisms of drug-induced toxicity*. Pharmacogenomics, 2010. **11**(4): p. 573-585.
10. Lee, S.J., et al., *Distinguishing between genotoxic and non-genotoxic hepatocarcinogens by gene expression profiling and bioinformatic pathway analysis*. Scientific Reports, 2013. **3**(1): p. 2783.
11. Watanabe, T., et al., *Discrimination of genotoxic and non-genotoxic hepatocarcinogens by statistical analysis based on gene expression profiling in the mouse liver as determined by quantitative real-time PCR*. Mutation Research/Genetic Toxicology and Environmental Mutagenesis, 2012. **747**(2): p. 164-175.
12. Xia, P., et al., *Pathway-based assessment of single chemicals and mixtures by a high-throughput transcriptomics approach*. Environment International, 2020. **136**: p. 105455.

13. Labib, S., et al., *A framework for the use of single-chemical transcriptomics data in predicting the hazards associated with complex mixtures of polycyclic aromatic hydrocarbons.* Archives of toxicology, 2017. **91**(7): p. 2599-2616.
14. Moffat, I., et al., *Comparison of toxicogenomics and traditional approaches to inform mode of action and points of departure in human health risk assessment of benzo[a]pyrene in drinking water.* 2015. **45**(1): p. 1-43.
15. Chepelev, N., et al., *Integrating toxicogenomics into human health risk assessment: Lessons learned from the benzo[a] pyrene case study.* Critical reviews in toxicology, 2015. **45**: p. 44-52.
16. Webster, A.F., et al., *Impact of Genomics Platform and Statistical Filtering on Transcriptional Benchmark Doses (BMD) and Multiple Approaches for Selection of Chemical Point of Departure (PoD).* PLoS One, 2015. **10**(8): p. e0136764.
17. Heijne, W.H.M., et al., *Systems toxicology: applications of toxicogenomics, transcriptomics, proteomics and metabolomics in toxicology.* Expert Review of Proteomics, 2005. **2**(5): p. 767-780.
18. Zhang, B. and S. Horvath, *A general framework for weighted gene co-expression network analysis.* Stat Appl Genet Mol Biol, 2005. **4**: p. Article17.
19. Langfelder, P. and S. Horvath, *WGCNA: an R package for weighted correlation network analysis.* BMC Bioinformatics, 2008. **9**: p. 559.
20. Maertens, A., et al., *MPTP's Pathway of Toxicity Indicates Central Role of Transcription Factor SP1.* Archives of Toxicology, 2015. **89**(5): p. 743-755.
21. Alexander-Dann, B., et al., *Developments in toxicogenomics: understanding and predicting compound-induced toxicity from gene expression data.* Molecular omics, 2018. **14**(4): p. 218-236.
22. Maertens, A., et al., *Weighted Gene Correlation Network Analysis (WGCNA) Reveals Novel Transcription Factors Associated With Bisphenol A Dose-Response.* Frontiers in Genetics, 2018. **9**(508).
23. Rager, J.E., et al., *Benchmark Dose Modeling Estimates of the Concentrations of Inorganic Arsenic That Induce Changes to the Neonatal Transcriptome, Proteome, and Epigenome in a Pregnancy Cohort.* Chemical Research in Toxicology, 2017. **30**(10): p. 1911-1920.
24. Trapnell, C., L. Pachter, and S.L. Salzberg, *TopHat: discovering splice junctions with RNA-Seq.* Bioinformatics, 2009. **25**(9): p. 1105-11.
25. Trapnell, C., et al., *Transcript assembly and quantification by RNA-Seq reveals unannotated transcripts and isoform switching during cell differentiation.* Nat Biotechnol, 2010. **28**(5): p. 511-5.
26. Love, M.I., W. Huber, and S. Anders, *Moderated estimation of fold change and dispersion for RNA-seq data with DESeq2.* Genome Biology, 2014. **15**(12): p. 550.

27. Smith, M.L., et al., *Time-Course Analysis of Brain Regional Expression Network Responses to Chronic Intermittent Ethanol and Withdrawal: Implications for Mechanisms Underlying Excessive Ethanol Consumption.* PLOS ONE, 2016. **11**(1): p. e0146257.
28. Nikolsky, Y., et al., *Functional analysis of OMICs data and small molecule compounds in an integrated "knowledge-based" platform.* Methods Mol Biol, 2009. **563**: p. 177-96.
29. Shannon, P., et al., *Cytoscape: a software environment for integrated models of biomolecular interaction networks.* Genome Res, 2003. **13**.
30. Wignall, J.A., et al., *Conditional Toxicity Value (CTV) Predictor: An In Silico Approach for Generating Quantitative Risk Estimates for Chemicals.* Environ Health Perspect, 2018. **126**(5): p. 057008.
31. Krewski, D., et al., *Toxicity Testing in the 21st Century: A Vision and a Strategy.* Journal of Toxicology and Environmental Health, Part B, 2010. **13**(2-4): p. 51-138.
32. Daston, G. and P. McNamee, *Alternatives to Toxicity Testing in Animals: Challenges and Opportunities.* Environmental Health Perspectives - ENVIRON HEALTH PERSPECT, 2005.
33. Webb-Robertson, B.-J.M., et al., *Bayesian Posterior Integration for Classification of Mass Spectrometry Data*, in *Statistical Analysis of Proteomics, Metabolomics, and Lipidomics Data Using Mass Spectrometry*, S. Datta and B.J.A. Mertens, Editors. 2017, Springer International Publishing: Cham. p. 203-211.
34. Tilton, S.C., et al., *Mechanism-Based Classification of PAH Mixtures to Predict Carcinogenic Potential.* Toxicol Sci, 2015. **146**(1): p. 135-45.
35. Williams, A., et al., *A predictive toxicogenomics signature to classify genotoxic versus non-genotoxic chemicals in human TK6 cells.* Data in Brief, 2015. **5**: p. 77-83.
36. Eun, J.W., et al., *Discriminating the molecular basis of hepatotoxicity using the large-scale characteristic molecular signatures of toxicants by expression profiling analysis.* Toxicology, 2008. **249**(2): p. 176-183.
37. Burczynski, M.E., et al., *Toxicogenomics-Based Discrimination of Toxic Mechanism in HepG2 Human Hepatoma Cells.* Toxicological Sciences, 2000. **58**(2): p. 399-415.
38. Plíšková, M., et al., *Deregulation of Cell Proliferation by Polycyclic Aromatic Hydrocarbons in Human Breast Carcinoma MCF-7 Cells Reflects Both Genotoxic and Nongenotoxic Events.* Toxicological Sciences, 2004. **83**(2): p. 246-256.
39. Sigal, A. and V. Rotter, *Oncogenic Mutations of the p53 Tumor Suppressor: The Demons of the Guardian of the Genome.* Cancer Research, 2000. **60**(24): p. 6788.
40. Samuels-Lev, Y., et al., *ASPP proteins specifically stimulate the apoptotic function of p53.* Molecular cell, 2001. **8**(4): p. 781-794.
41. Sullivan, A. and X. Lu, *ASPP: a new family of oncogenes and tumour suppressor genes.* British Journal of Cancer, 2007. **96**(2): p. 196-200.

42. Iwabuchi, K., et al., *Two cellular proteins that bind to wild-type but not mutant p53.* Proceedings of the National Academy of Sciences of the United States of America, 1994. **91**(13): p. 6098-6102.
43. Schwermer, M., et al., *Sensitivity to cdk1-inhibition is modulated by p53 status in preclinical models of embryonal tumors.* Oncotarget, 2015. **6**(17): p. 15425-15435.
44. Alexandrov, K., M. Rojas, and S. Satarug, *The critical DNA damage by benzo(a)pyrene in lung tissues of smokers and approaches to preventing its formation.* Toxicol Lett, 2010. **198**(1): p. 63-8.
45. Piberger, A.L., et al., *BPDE-induced genotoxicity: relationship between DNA adducts, mutagenicity in the in vitro PIG-A assay, and the transcriptional response to DNA damage in TK6 cells.* Archives of Toxicology, 2018. **92**(1): p. 541-551.
46. Tarantini, A., et al., *Polycyclic aromatic hydrocarbons in binary mixtures modulate the efficiency of benzo[a]pyrene to form DNA adducts in human cells.* Toxicology, 2011. **279**(1-3): p. 36-44.
47. Tung, E.W., et al., *Benzo[a]pyrene increases DNA double strand break repair in vitro and in vivo: a possible mechanism for benzo[a]pyrene-induced toxicity.* Mutat Res Genet Toxicol Environ Mutagen, 2014. **760**: p. 64-9.
48. Alam, S., et al., *Downregulation of Cdc2/CDK1 Kinase Activity Induces the Synthesis of Noninfectious Human Papillomavirus Type 31b Virions in Organotypic Tissues Exposed to Benzo[a]pyrene.* Journal of Virology, 2010. **84**(9): p. 4630.
49. Xiao, H. and S.V. Singh, *Cellular response to benzo[a]pyrene-7,8-diol-9,10-epoxide exposure in human lung cancer cells.* Cancer Research, 2005. **65**(9 Supplement): p. 275.
50. Chen, X., et al., *Enrichment of Cdk1-cyclins at DNA double-strand breaks stimulates Fun30 phosphorylation and DNA end resection.* Nucleic Acids Research, 2016. **44**(6): p. 2742-2753.
51. Fan, X. and J.J. Chen, *Role of Cdk1 in DNA damage-induced G1 checkpoint abrogation by the human papillomavirus E7 oncogene.* Cell Cycle, 2014. **13**(20): p. 3249-59.
52. Müllers, E., et al., *Residual Cdk1/2 activity after DNA damage promotes senescence.* Aging cell, 2017. **16**(3): p. 575-584.
53. Fei, L. and H. Xu, *Role of MCM2–7 protein phosphorylation in human cancer cells.* Cell & Bioscience, 2018. **8**(1): p. 43.
54. Huang, T.-H., et al., *Epidermal growth factor receptor potentiates MCM7-mediated DNA replication through tyrosine phosphorylation of Lyn kinase in human cancers.* Cancer cell, 2013. **23**(6): p. 796-810.
55. Fei, L., et al., *RACK1 promotes lung cancer cell growth via an MCM7/RACK1/ Akt signaling complex.* Oncotarget, 2017. **8**(25): p. 40501-40513.
56. Yu, C.H., et al., *A combination of mRNA expression profile and miRNA expression profile identifies detection biomarkers in different tumor stages*

of laryngeal squamous cell carcinoma. Eur Rev Med Pharmacol Sci, 2018. **22**(21): p. 7296-7304.
57. Yang, W.-X., Y.-Y. Pan, and C.-G. You, *CDK1, CCNB1, CDC20, BUB1, MAD2L1, MCM3, BUB1B, MCM2, and RFC4 May Be Potential Therapeutic Targets for Hepatocellular Carcinoma Using Integrated Bioinformatic Analysis.* BioMed Research International, 2019. **2019**: p. 1245072.
58. Hsing, A., D. Faller, and C. Vaziri, *DNA-damaging aryl hydrocarbons induce Mdm2 expression via p53-independent post-transcriptional mechanisms.* The Journal of biological chemistry, 2000. **275**: p. 26024-31.
59. Labib, S., et al., *Comparative transcriptomic analyses to scrutinize the assumption that genotoxic PAHs exert effects via a common mode of action.* Arch Toxicol, 2016. **90**(10): p. 2461-80.
60. Staal, Y.C.M., et al., *Modulation of gene expression and DNA adduct formation in HepG2 cells by polycyclic aromatic hydrocarbons with different carcinogenic potencies.* Carcinogenesis, 2006. **27**(3): p. 646-655.
61. Siddens, L.K., et al., *Polycyclic aromatic hydrocarbons as skin carcinogens: Comparison of benzo[a]pyrene, dibenzo[def,p]chrysene and three environmental mixtures in the FVB/N mouse.* Toxicology and applied pharmacology, 2012. **264**(3): p. 377-386.
62. Chang, Y., et al., *Comparative mechanisms of PAH toxicity by benzo[a]pyrene and dibenzo[def,p]chrysene in primary human bronchial epithelial cells cultured at air-liquid interface.* Toxicology and Applied Pharmacology, 2019. **379**: p. 114644.
63. Libalova, H., et al., *Transcriptional response to organic compounds from diverse gasoline and biogasoline fuel emissions in human lung cells.* Toxicology in Vitro, 2018. **48**: p. 329-341.
64. Xuan, B., et al., *Dysregulation in Actin Cytoskeletal Organization Drives Increased Stiffness and Migratory Persistence in Polyploidal Giant Cancer Cells.* Scientific Reports, 2018. **8**(1): p. 11935.
65. Olson, M.F. and E. Sahai, *The actin cytoskeleton in cancer cell motility.* Clin Exp Metastasis, 2009. **26**(4): p. 273-87.
66. Bachir, A.I., et al., *Actin-Based Adhesion Modules Mediate Cell Interactions with the Extracellular Matrix and Neighboring Cells.* Cold Spring Harbor perspectives in biology, 2017. **9**(7): p. a023234.
67. EPA, U.S., *Development of a Relative Potency Factor (Rpf) Approach for Polycyclic Aromatic Hydrocarbon (PAH) Mixtures (External Review Draft)*, U.S. Environmental Protection Agency, Editor. 2010: Washington, DC
68. IARC, *Some non-heterocyclic polycyclic aromatic hydrocarbons and some related exposures. Monographs on the evaluation of carcinogenic risks to humans.* IARC MONOGRAPHS ON THE EVALUATION OF CARCINOGENIC RISKS TO HUMANS, 2010. **92**.

69. IARC, *Diesel and gasoline engine exhausts and some nitrarenes*. IARC MONOGRAPHS ON THE EVALUATION OF CARCINOGENIC RISKS TO HUMANS, 2014. **105**.
70. IARC Working Group on the Evaluation of Carcinogenic Risks to Humans., World Health Organization., and International Agency for Research on Cancer., *Bitumens and bitumen emissions, and some N- and S-heterocyclic polycyclic aromatic hydrocarbons*. IARC monographs on the evaluation of carcinogenic risks to humans,. 2013, Lyon: IARC Press. v, 342 p.
71. Sutherland, J.J., et al., *Assessing Concordance of Drug-Induced Transcriptional Response in Rodent Liver and Cultured Hepatocytes*. PLOS Computational Biology, 2016. **12**(3): p. e1004847.
72. Sutherland, J.J., et al., *Toxicogenomic module associations with pathogenesis: a network-based approach to understanding drug toxicity*. The Pharmacogenomics Journal, 2018. **18**(3): p. 377-390.

TABLES

Table 4-1. Tier one: Gene modules significantly (p< .05) associated with RPF.

Module	Correlation	p-value
Turquoise	0.79	0.01
Magenta	0.73	0.03
Lightgreen	-0.65	0.05
Black	-0.68	0.05
Grey60	-0.69	0.04
Royalblue	-0.72	0.03
Red	-0.82	0.007

Table 4-2. Tier two: Gene modules significantly (p< .05) associated with RPF.

Module	Correlation (max)	p-value (min)	Risk value(s)
Two	0.82	0.02	RPF
Five	0.85	0.02	OSF, RPF
Fourteen	-0.84	0.02	OSF, RPF, IARC
Seventeen	-0.77	0.05	RPF

Figure 4-1.

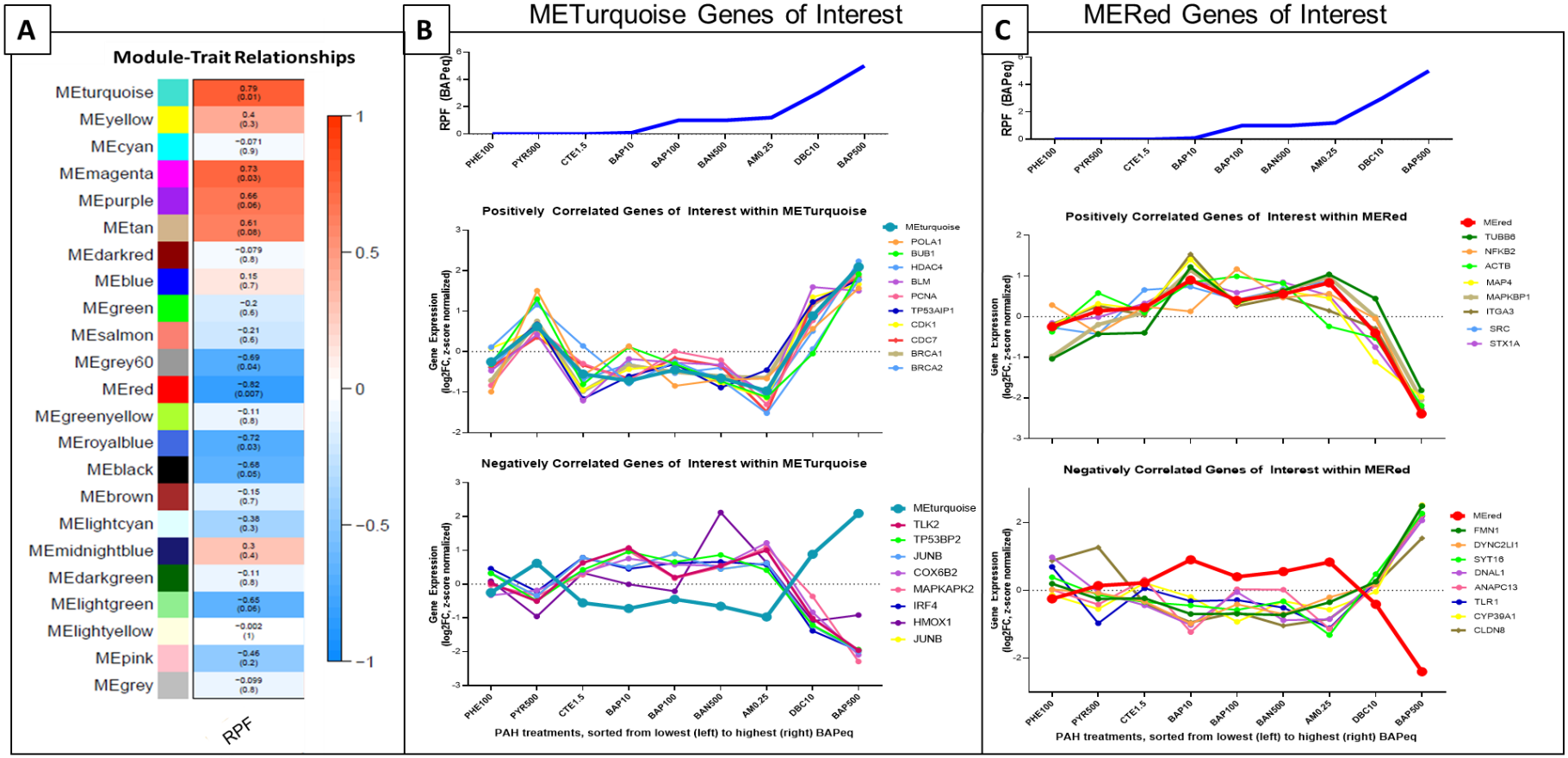

Figure 4-1. Module-Trait Relationships and Genes of Interest (A) Module-Trait Relationships matrix. Correlation matrix shows that several module eigengenes (MEs) were highly correlated with PAH cancer risk values (RPF). Degree of correlation is colored, with red as positive and blue as negative, and p-values in parentheses. **(B) METurquoise Genes of Interest.** The most positively correlated module eigengene ("MEturquoise") was prioritized for evaluation; genes of interest that had expression levels correlated to MEturquoise are shown. Expression levels are Z-score normalized. **(C) MERed Genes of Interest.** The most significantly negatively correlated module eigengene ("MERed") was priotized for evaluation; genes of interest shown, ranked by RPF, with expression levels Z-score normalized.

Figure 4-2.

	Meturquoise (+)		Mered (-)	
Network Category	**Number (ave FDR)**	**Pathways**	**Number (ave FDR)**	**Pathways**
Cell cycle	8 (0.01)	Core, G1-S, G1-S Growth factor regulation, G1-S Interleukin regulation, G2-M, Meiosis, Mitosis, S phase	NS	
DNA damage	3 (0.011)	Checkpoint, DBS repair	NS	
Signal transduction	3 (0.021)	Cholecystokinin signaling, ESR1-nuclear pathway, NOTCH signaling	NS	
Cardiac development	1 (0.009)	Wnt_beta-catenin, Notch, VEGF, IP3 and integrin signaling	NS	
Cell adhesion	NS		4 (0.011)	Cadherins, Cell junctions, Integrin-mediated cell-matrix adhesion, Integrin priming
Cytoskeleton	NS		3 (0.001)	Actin filaments, Regulation of cytoskeleton rearrangement, Intermediate filaments
Protein folding	NS		2 (0.023)	Response to unfolded proteins, ER and cytoplasm
Transcription	NS		1 (0.017)	mRNA processing
Translation	NS		1 (0.006)	Regulation of initiation
Development	2 (0.017)	Hemopoiesis, Erythropoietin pathway, Regulation of angiogenesis	2 (0.008)	Hemopoiesis, Erythropoietin pathway, Axonal guidance
Reproduction	1 (0.049)	FSH-beta signaling pathway	2 (0.026)	Feeding and Neurohormone signaling, FSH-beta signaling pathway
Apoptosis	2 (0.017)	Apoptosis stimulation by external signals, Apoptotic nucleus	2 (0.018)	Anti-Apoptosis mediated by external signals by Estrogen, Apoptotic mitochondria
Inflammation	9 (0.014)	Amphoterin signaling, IFN-gamma signaling, IL-10 anti-inflammatory response, Innate immune response to RNA viral infection, Innate inflammatory response, Neutrophil activation, NK cell cytotoxicity, Phagocytosis, TREM1 signaling	15 (0.011)	Phagosome in antigen presentation, Protein C signaling, Phagocytosis, TREM1 signaling, Neutrophil activation, IL-2 signaling, Amphoterin signaling, Innate inflammatory response, Kallikrein-kinin system, IL-10 anti-inflammatory response, Inflammasome, IL-6 signaling, BCR pathway, TCR signaling, Histamine signaling

Figure 4-2. Network Category table of prioritized module eigengenes MEturquoise and MEred. Pathway enrichment analysis was conducted, and a broader network category-level significant enrichment score was calculated. Numbers indicate number of pathways enriched under each network category, and ave FDR (average false discovery rate) shown in parentheses. Distinct biological networks were enriched by MEturquoise and MEred, as well as several network categories commonly enriched, notably Inflammation.

Figure 4-3.

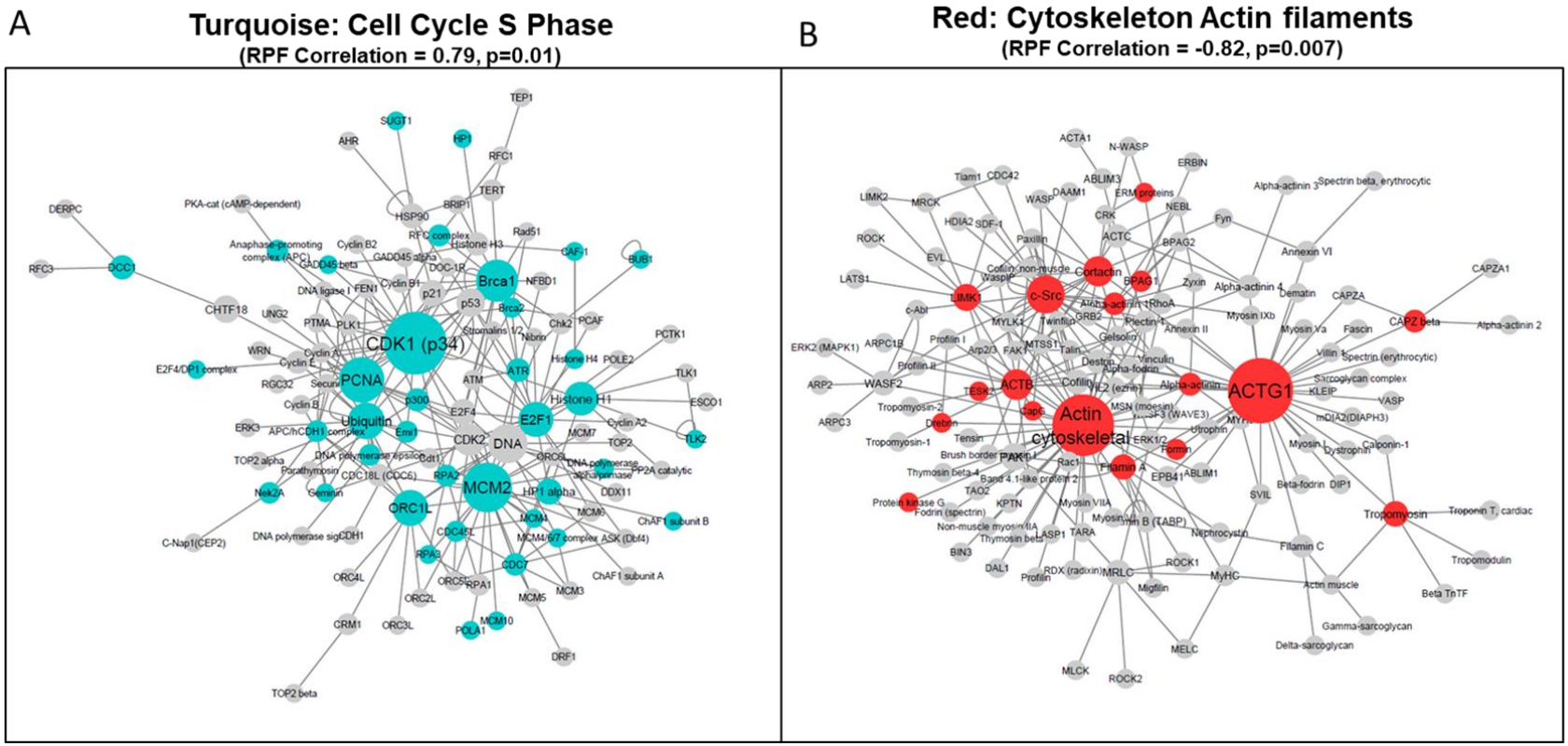

Figure 4-3. Networks showing most significantly enriched networks associated with prioritized gene modules. (A) METurquoise significant enrichment of the Cell cycle S phase gene network, and **(B) MEred significant enrichment of the Cytoskeleton actin filament gene network.** Node sizes denote betweennenss centrality measures calculated in each network. A larger node, or "hub gene" thus represents a gene or biomolecule that stands in between the shortest paths connecting the maximum number of neighboring nodes to each other.

Figure 4-4.

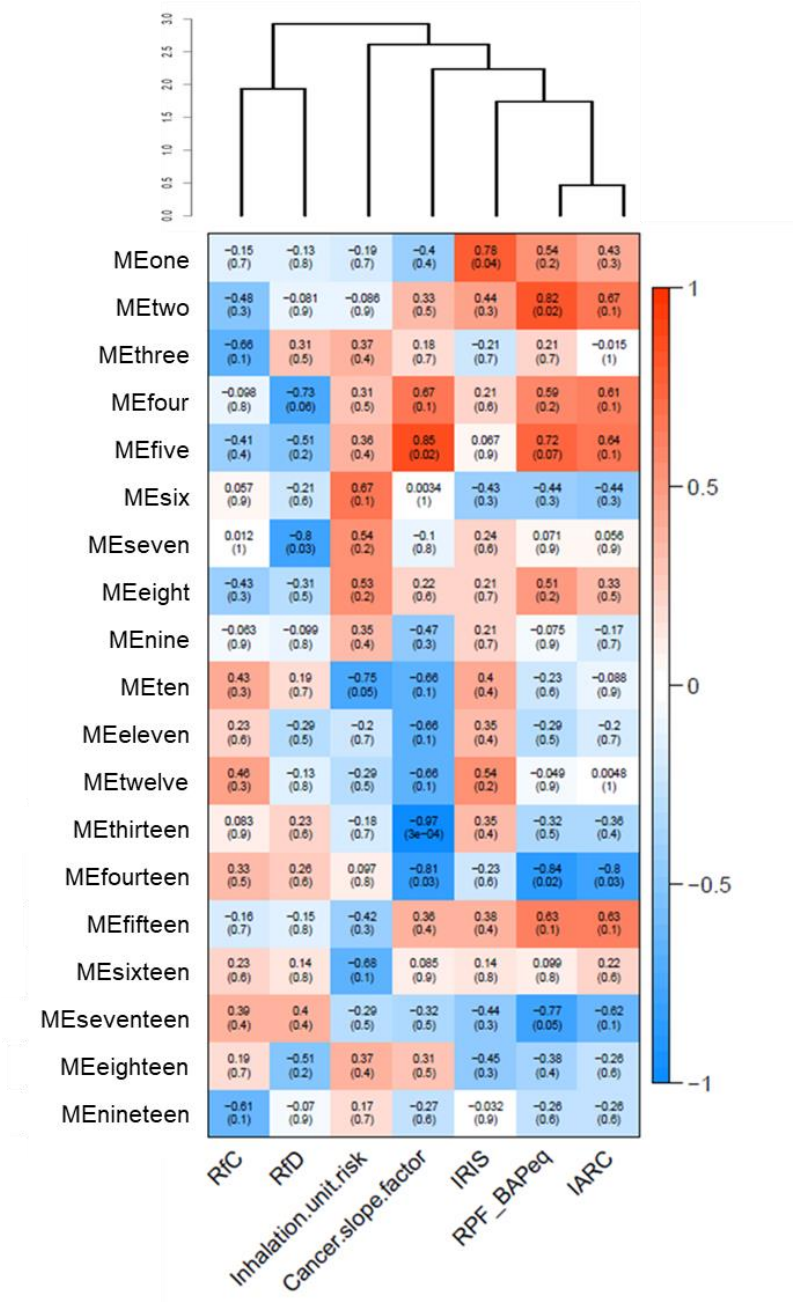

Figure 4-4. Module-Trait Relationship Correlation matrix Linking Module Eigengenes with Risk Values. Correlation matrix shows that several module eigengenes (MEs) were highly correlated with PAH cancer risk values (RPF), as well as correlated in common between RPF, OSF, and IARC classes. Unsupervised hierarchical clustering was performed on the correlation values and the dendrogram identifies RPF and IARC as having the most similar module correlation patterns. Degree of correlation is colored, with red as positive and blue as negative, and p-values in parentheses

Chapter 5 – Discussion

Exposure to environmental PAHs are nearly unavoidable, due to their prevalence in various forms of environmental media. Inhalation exposure to PAHs have been linked to an increased risk of acute lower respiratory infections, chronic obstructive pulmonary disease, and lung cancer [1, 2]. The primary method for estimating cancer risk of PAH mixtures is the relative potency factor (RPF) approach, which estimates mixture cancer risk based on a subset of individual component PAHs compared to benzo[a]pyrene (BAP) [3]. However, recent studies have found this approach inadequate for predicting carcinogenicity of mixtures and also for certain individual PAHs, particularly those that function through alternate pathways or exhibit greater promotional capacity compared to BAP [4-7]. Additionally, the RPF approach is limited by lack of information on PAH MOAs and adequate assessment approaches for mixtures, leading to the over or under-estimation of carcinogenic potency [6, 8-10]. A heavy reliance on *in vivo* rodent studies used to estimate RPF for individual PAHs also introduces additional uncertainty regarding species-specific biology and chemical mode of action (MOA) [11].

Through the studies described in this dissertation, we employed an organotypic HBEC model to advance our understanding of the early mechanisms involved in carcinogenicity and toxicity of PAHs. Through these studies, we developed and evaluated a transcriptomic dataset of PAHs along a range of carcinogenic potency, and adapted and refined novel transcriptional approaches toward biomarker identification and predictive classification.

In chapter 2, we comparatively evaluated the mechanisms of BAP and dibenzo[def,p]chrysene (DBC) in a primary 3D HBEC model to assess potential differences in mechanisms of toxicity. Current assumptions for assessing carcinogenic risk of PAHs is that they function through a common mechanism of action similar to BAP; however recent studies demonstrate that PAHs can act through unique mechanisms potentially contributing to cancer outcomes in a non-additive manner. In this study, we profiled the short-term gene signatures derived

from exposure to PAHs for 48 hrs. Specific gene targets were evaluated for BAP, DBC, and coal tar extracts (CTE) with quantitative PCR (qPCR), including CYP1A1, CYP1B1, and tight junction and gap junction barrier genes. Functional measurements of barrier integrity and gene signature profiling identified barrier disruption as a common mechanism of toxicity by the PAHs evaluated, and also identified over 1200 uniquely regulated genes between BAP and DBC. This work also identified novel transcriptional mechanisms of action for DBC, suggesting that the unique NRF2-mediated oxidative stress response gene networks regulated by DBC may mediate the enhanced carcinogenicity of DBC compared to BAP. Overall, these findings supported the utility of transcriptomic approaches in evaluating chemical-specific profiles of PAHs.

After evaluating chemical-specific gene signatures unique to each carcinogen, we expanded our transcriptional assessments to evaluate effects of exposure to a range of 6 carcinogenic and non-carcinogenic PAHs. In chapter 3, we selected dissimilarly affected gene pathways to develop a rapid classification approach that accurately predicts carcinogenic potency of PAHs using transcriptional gene signatures from HBECs. Previously, we developed an approach to use gene signatures generated from mouse skin after short-term chemical treatment to accurately predict cancer outcome [6]. Here, we demonstrated the successful translation of this approach into a 3D human bronchial epithelial model. Gene sets related to several biological pathways were evaluated for classification performance to differentiate PAHs by carcinogenic class, and integrated for an optimal classification accuracy of 91%. Individual endpoints and biomarkers, such as intracellular ROS generation and CYP450 gene regulation, were insufficient predictors of carcinogenicity in this study. Moreover, transcriptional benchmark dose modeling of BAP showed that the most sensitive pathway gene sets to BAP regulation were largely dissimilar from the pathways that best classified PAH carcinogenicity. Through applications of systems toxicology approaches, we analyzed global gene expression in 3D HBEC, developed classification approaches towards carcinogenic hazard assessment of

PAHs, and found evidence to challenge assumptions that BAP carcinogenicity (and subsequent MOAs) are reflective of overall PAH carcinogenicity.

In chapter 4, we set out to overcome pathway annotation limitations in transcriptional analyses by utilizing a weighted gene co-expression network analysis to identify co-modulated gene networks grouped by common expression patterns across the genes. We adapted the WGCNA approach in a novel manner to evaluate molecular mechanisms related to PAH cancer risk, as calculated by RPF estimates. Significantly regulated genes from HBEC exposed to 7 PAHs and PAH mixtures were analyzed using a two-tiered WGCNA approach. First to identify gene sets co-modulated to RPF and then to link the genes to a more comprehensive list of regulatory values, including inhalation-specific risk values. Over 3,000 genes were identified as significantly correlated and co-modulated to increasing cancer risk (RPF). Gene modules significantly correlated in common between RPF, oral cancer slope factors, and IARC cancer categorizations were also identified. Here, we demonstrated a novel manner of integrating gene sets with chemical toxicity equivalence estimates through WGCNA to understand potential mechanisms. Our findings support the usage of co-expression network analyses to identify links between chemical toxicity and high-dimensional transcriptional data in chemical MOA evaluations.

Taken together, studies demonstrate the utility of employing toxicogenomic approaches in organotypic airway epithelial models to assess the effects of carcinogenic air pollutants and mixtures. Through this work, we have demonstrated that early transcriptional signaling in response to PAH exposure can span a diverse range of mechanisms of toxicity. While these MOAs may have similarities and differences to BAP's, these studies have identified broader biomarkers linked to PAH cancer risk and utilized these different MOAs as an advantage in developing a classification model to predict chemical carcinogenic potency. Looking ahead, similar studies using organotypic human *in vitro* models could be used to further inform cancer risk evaluations and hazard assessments by combining transcriptional profiling with additional *in vitro* assay endpoints associated with chemical exposures. Gene sets found to be predictive of cancer risk (chapter 3) and correlated to increasing PAH cancer risk (chapter 4) could be further evaluated for common upstream regulators, including transcription factors, miRNA, or associated lncRNA. Additionally, gene modules correlated to cancer

risk (chapter 4) include several hundred miRNA and lncRNA that can be further evaluated as potential mediators of any mechanisms previously understood as linked to PAH carcinogenesis. The 3D HBEC also expresses xenobiotic metabolism enzymes capable of generating PAH metabolites. As future work continues to identify both chemical-specific mechanisms and broader cancer risk-associated mechanisms, it is necessary to link these back to various PAH metabolites and congeners that may be responsible for toxicity. As the environmental health sciences community continues to evaluate PAH toxicity within the context of mixtures, transcriptional profiling will be a valuable tool in understanding potential mixtures interactions, effects, and MOAs. Therefore, these advances in toxicogenomics have the potential to inform biomarker development, mechanistic evaluations, chemical hazard assessment, and future regulatory applications.

References

1. Ezzati, M., et al., *Comparative quantification of health risks : global and regional burden of disease attributable to selected major risk factors / edited by Majid Ezzati ... [et al.]*. 2004, World Health Organization: Geneva.
2. Smith, K., S. Mehta, and M. Maeusezahl-feuz, *Indoor Air Pollution from Household Use of Solid Fuels." Comparative Quantification of Health Risks 18:1435–1492*. 2004.
3. EPA, U.S. *Development of a relative potency factor (RPF) approach for polycyclic aromatic hydrocarbon (PAH) mixtures*. 2010 [cited EPA/635/R-08/012A; Available from: http://cfpub.epa.gov/ncea/cfm/recordisplay.cfm?deid=194584.
4. Siddens, L.K., et al., *Polycyclic aromatic hydrocarbons as skin carcinogens: comparison of benzo[a]pyrene, dibenzo[def,p]chrysene and three environmental mixtures in the FVB/N mouse*. Toxicol Appl Pharmacol, 2012. **264**(3): p. 377-86.
5. Courter, L.A., et al., *The influence of diesel exhaust on polycyclic aromatic hydrocarbon-induced DNA damage, gene expression, and tumor initiation in Sencar mice in vivo*. Cancer Lett, 2008. **265**(1): p. 135-47.
6. Tilton, S.C., et al., *Mechanism-Based Classification of PAH Mixtures to Predict Carcinogenic Potential*. Toxicol Sci, 2015. **146**(1): p. 135-45.
7. Chang, Y., et al., *Comparative mechanisms of PAH toxicity by benzo[a]pyrene and dibenzo[def,p]chrysene in primary human bronchial epithelial cells cultured at air-liquid interface*. Toxicology and Applied Pharmacology, 2019. **379**: p. 114644.
8. Siddens, L.K., et al., *Polycyclic aromatic hydrocarbons as skin carcinogens: Comparison of benzo[a]pyrene, dibenzo[def,p]chrysene and three environmental mixtures in the FVB/N mouse*. Toxicology and applied pharmacology, 2012. **264**(3): p. 377-386.
9. Samburova, V., B. Zielinska, and A. Khlystov, *Do 16 Polycyclic Aromatic Hydrocarbons Represent PAH Air Toxicity?* Toxics, 2017. **5**(3): p. 17.
10. Baird, W.M., L.A. Hooven, and B. Mahadevan, *Carcinogenic polycyclic aromatic hydrocarbon-DNA adducts and mechanism of action*. Environ Mol Mutagen, 2005. **45**(2-3): p. 106-14.
11. Gottmann, E., et al., *Data quality in predictive toxicology: reproducibility of rodent carcinogenicity experiments*. Environmental health perspectives, 2001. **109**(5): p. 509-514.

BIBLIOGRAPHY

Abdel-Shafy, Hussein I., and Mona S. M. Mansour. 2016. 'A review on polycyclic aromatic hydrocarbons: Source, environmental impact, effect on human health and remediation', *Egyptian Journal of Petroleum*, 25: 107-23.

Alam, Samina, Brian S. Bowser, Michael J. Conway, Mohd Israr, Eric J. Ryndock, Long Fu Xi, and Craig Meyers. 2010. 'Downregulation of Cdc2/CDK1 Kinase Activity Induces the Synthesis of Noninfectious Human Papillomavirus Type 31b Virions in Organotypic Tissues Exposed to Benzo[a]pyrene', *J Virol*, 84: 4630.

Alexander-Dann, Benjamin, Lavinia Lorena Pruteanu, Erin Oerton, Nitin Sharma, Ioana Berindan-Neagoe, Dezső Módos, and Andreas Bender. 2018. 'Developments in toxicogenomics: understanding and predicting compound-induced toxicity from gene expression data', *Molecular omics*, 14: 218-36.

Alexandrov, K., M. Rojas, and S. Satarug. 2010. 'The critical DNA damage by benzo(a)pyrene in lung tissues of smokers and approaches to preventing its formation', *Toxicol Lett*, 198: 63-8.

An, J., L. Yin, Y. Shang, Y. Zhong, X. Zhang, M. Wu, Z. Yu, G. Sheng, J. Fu, and Y. Huang. 2011. 'The combined effects of BDE47 and BaP on oxidatively generated DNA damage in L02 cells and the possible molecular mechanism', *Mutat Res*, 721: 192-8.

Andersson, Jan T., and Christine Achten. 2015. 'Time to Say Goodbye to the 16 EPA PAHs? Toward an Up-to-Date Use of PACs for Environmental Purposes', *Polycyclic Aromatic Compounds*, 35: 330-54.

Arey, Janet, and Roger Atkinson. 2003. 'Photochemical Reactions of PAHs in the Atmosphere', *PAHs: An Ecotoxicological Perspective*: 47-63.

Arlt, V. M., A. M. Krais, R. W. Godschalk, Y. Riffo-Vasquez, I. Mrizova, C. A. Roufosse, C. Corbin, Q. Shi, E. Frei, M. Stiborova, F. J. van Schooten, D. H. Phillips, and D. Spina. 2015. 'Pulmonary Inflammation Impacts on CYP1A1-Mediated Respiratory Tract DNA Damage Induced by the Carcinogenic Air Pollutant Benzo[a]pyrene', *Toxicol Sci*, 146: 213-25.

Arzayus, Krisa M., Rebecca M. Dickhut, and Elizabeth A. Canuel. 2001. 'Fate of Atmospherically Deposited Polycyclic Aromatic Hydrocarbons (PAHs) in Chesapeake Bay', *Environmental science & technology*, 35: 2178-83.

Astashkina, Anna, Brenda Mann, and David W. Grainger. 2012. 'A critical evaluation of in vitro cell culture models for high-throughput drug screening and toxicity', *Pharmacology & Therapeutics*, 134: 82-106.

ATSDR. 2017a. 'ATSDR's Substance Priority List: Agency for Toxic Substances and Disease Registry', *ATSDR*.

———. 2017b. 'ATSDR. ATSDR's Substance Priority List: Agency for Toxic Substances and Disease Registry', Accessed 11/18/2018. https://www.atsdr.cdc.gov/spl/#2017spl.

Bachir, Alexia I., Alan Rick Horwitz, W. James Nelson, and Julie M. Bianchini. 2017. 'Actin-Based Adhesion Modules Mediate Cell Interactions with the Extracellular Matrix and Neighboring Cells', *Cold Spring Harbor perspectives in biology*, 9: a023234.

Baird, W. M., L. A. Hooven, and B. Mahadevan. 2005. 'Carcinogenic polycyclic aromatic hydrocarbon-DNA adducts and mechanism of action', *Environ Mol Mutagen*, 45: 106-14.

Baird, William M., and Brinda Mahadevan. 2004. 'The uses of carcinogen-DNA adduct measurement in establishing mechanisms of mutagenesis and in chemoprevention', *Mutation Research/Fundamental and Molecular Mechanisms of Mutagenesis*, 547: 1-4.

Balharry, D., K. Sexton, and K. A. BeruBe. 2008. 'An in vitro approach to assess the toxicity of inhaled tobacco smoke components: nicotine, cadmium, formaldehyde and urethane', *Toxicology*, 244: 66-76.

Banni, M., S. Sforzini, V. M. Arlt, A. Barranger, L. J. Dallas, C. Oliveri, Y. Aminot, B. Pacchioni, C. Millino, G. Lanfranchi, J. W. Readman, M. N. Moore, A. Viarengo, and A. N. Jha. 2017. 'Assessing the impact of Benzo[a]pyrene on Marine Mussels: Application of a novel targeted low density microarray complementing classical biomarker responses', *PLoS One*, 12: e0178460.

Beagley, N., K. G. Stratton, and B. J. Webb-Robertson. 2010. 'VIBE 2.0: visual integration for bayesian evaluation', *Bioinformatics*, 26: 280-2.

Benbrahim-Tallaa, Lamia, Robert A. Baan, Yann Grosse, Béatrice Lauby-Secretan, Fatiha El Ghissassi, Véronique Bouvard, Neela Guha, Dana Loomis, and Kurt Straif. 2012. 'Carcinogenicity of diesel-engine and gasoline-engine exhausts and some nitroarenes', *The Lancet Oncology*, 13: 663-64.

Billiard, Sonya M., Joel N. Meyer, Deena M. Wassenberg, Peter V. Hodson, and Richard T. Di Giulio. 2007. 'Nonadditive effects of PAHs on Early Vertebrate Development: mechanisms and implications for risk assessment', *Toxicological Sciences*, 105: 5-23.

Birgersdotter, A., R. Sandberg, and I. Ernberg. 2005. 'Gene expression perturbation in vitro--a growing case for three-dimensional (3D) culture systems', *Semin Cancer Biol*, 15: 405-12.

Bláha, Luděk, Petra Kapplová, Jan Vondráček, Brad Upham, and Miroslav Machala. 2002. 'Inhibition of Gap-Junctional Intercellular Communication by Environmentally Occurring Polycyclic Aromatic Hydrocarbons', *Toxicological Sciences*, 65: 43-51.

Blasig, Ingolf E., Christian Bellmann, Jimmi Cording, Giovanna del Vecchio, Denise Zwanziger, Otmar Huber, and Reiner F. Haseloff. 2011. 'Occludin Protein Family: Oxidative Stress and Reducing Conditions', *Antioxidants & Redox Signaling*, 15: 1195-219.

Boffetta, Paolo, Nadia Jourenkova, and Per Gustavsson. 1997. 'Cancer risk from occupational and environmental exposure to polycyclic aromatic hydrocarbons', *Cancer Causes & Control*, 8: 444-72.

Bogaards, J. J. P., M. Bertrand, P. Jackson, M. J. Oudshoorn, R. J. Weaver, P. J. Van Bladeren, and B. Walther. 2000. 'Determining the best animal model for human cytochrome P450 activities: a comparison of mouse, rat, rabbit, dog, micropig, monkey and man', *Xenobiotica*, 30: 1131-52.

Bojes, Heidi K., and Peter G. Pope. 2007. 'Characterization of EPA's 16 priority pollutant polycyclic aromatic hydrocarbons (PAHs) in tank bottom solids and associated contaminated soils at oil exploration and production sites in Texas', *Regulatory Toxicology and Pharmacology*, 47: 288-95.

Boyle, J. O., Z. H. Gumus, A. Kacker, V. L. Choksi, J. M. Bocker, X. K. Zhou, R. K. Yantiss, D. B. Hughes, B. Du, B. L. Judson, K. Subbaramaiah, and A. J. Dannenberg. 2010. 'Effects of cigarette smoke on the human oral mucosal transcriptome', *Cancer Prev Res (Phila)*, 3: 266-78.

Burczynski, Michael E., Michael McMillian, Joe Ciervo, Li Li, James B. Parker, Robert T. Dunn, II, Sam Hicken, Spencer Farr, and Mark D. Johnson. 2000. 'Toxicogenomics-Based Discrimination of Toxic Mechanism in HepG2 Human Hepatoma Cells', *Toxicological Sciences*, 58: 399-415.

Cao, X., H. Lin, L. Muskhelishvili, J. Latendresse, P. Richter, and R. H. Heflich. 2015. 'Tight junction disruption by cadmium in an in vitro human airway tissue model', *Respir Res*, 16: 30.

Chang, Yvonne, Lisbeth K. Siddens, Lauren K. Heine, David A. Sampson, Zhen Yu, Kay A. Fischer, Christiane V. Löhr, and Susan C. Tilton. 2019. 'Comparative mechanisms of PAH toxicity by benzo[a]pyrene and dibenzo[def,p]chrysene in primary human bronchial epithelial cells cultured at air-liquid interface', *Toxicol Appl Pharmacol*, 379: 114644.

Chari, Raj, Kim M. Lonergan, Raymond T. Ng, Calum MacAulay, Wan L. Lam, and Stephen Lam. 2007. 'Effect of active smoking on the human bronchial epithelium transcriptome', *BMC Genomics*, 8: 297.

Chen, Xuefeng, Hengyao Niu, Yang Yu, Jingjing Wang, Shuangyi Zhu, Jianjie Zhou, Alma Papusha, Dandan Cui, Xuewen Pan, Youngho Kwon, Patrick Sung, and Grzegorz Ira. 2016. 'Enrichment of Cdk1-cyclins at DNA double-strand breaks stimulates Fun30 phosphorylation and DNA end resection', *Nucleic Acids Res*, 44: 2742-53.

Chepelev, N. L., I. D. Moffat, S. Labib, J. Bourdon-Lacombe, B. Kuo, J. K. Buick, F. Lemieux, A. I. Malik, S. Halappanavar, A. Williams, and C. L. Yauk. 2015a. 'Integrating toxicogenomics into human health risk assessment: lessons learned from the benzo[a]pyrene case study', *Crit Rev Toxicol*, 45: 44-52.

Chepelev, Nikolai L., Alexandra S. Long, Andrew Williams, Byron Kuo, Rémi Gagné, Dean A. Kennedy, David H. Phillips, Volker M. Arlt, Paul A. White, and Carole L. Yauk. 2016. 'Transcriptional Profiling of Dibenzo[def,p]chrysene-induced Spleen Atrophy Provides Mechanistic Insights into its Immunotoxicity in MutaMouse', *Toxicological Sciences*, 149: 251-68.

Chepelev, Nikolai, Ivy Moffat, Sarah Labib, Julie Bourdon-Lacombe, Byron Kuo, Julie Buick, France Lemieux, Amal Malik, Sabina Halappanavar, Andrew

Williams, and Carole Yauk. 2015b. 'Integrating toxicogenomics into human health risk assessment: Lessons learned from the benzo[a] pyrene case study', *Crit Rev Toxicol*, 45: 44-52.

Cho, H. Y., and S. R. Kleeberger. 2010. 'Nrf2 protects against airway disorders', *Toxicol Appl Pharmacol*, 244: 43-56.

Chorley, Brian N., Michelle R. Campbell, Xuting Wang, Mehmet Karaca, Deepa Sambandan, Fatu Bangura, Peng Xue, Jingbo Pi, Steven R. Kleeberger, and Douglas A. Bell. 2012. 'Identification of novel NRF2-regulated genes by ChIP-Seq: influence on retinoid X receptor alpha', *Nucleic Acids Res*, 40: 7416-29.

Courter, L. A., A. Luch, T. Musafia-Jeknic, V. M. Arlt, K. Fischer, R. Bildfell, C. Pereira, D. H. Phillips, M. C. Poirier, and W. M. Baird. 2008a. 'The influence of diesel exhaust on polycyclic aromatic hydrocarbon-induced DNA damage, gene expression, and tumor initiation in Sencar mice in vivo', *Cancer Lett*, 265: 135-47.

Courter, L. A., T. Musafia-Jeknic, K. Fischer, R. Bildfell, J. Giovanini, C. Pereira, and W. M. Baird. 2007. 'Urban dust particulate matter alters PAH-induced carcinogenesis by inhibition of CYP1A1 and CYP1B1', *Toxicol Sci*, 95: 63-73.

Courter, Lauren A., Andreas Luch, Tamara Musafia-Jeknic, Volker M. Arlt, Kay Fischer, Robert Bildfell, Cliff Pereira, David H. Phillips, Miriam C. Poirier, and William M. Baird. 2008b. 'The influence of diesel exhaust on polycyclic aromatic hydrocarbon-induced DNA damage, gene expression, and tumor initiation in Sencar mice in vivo', *Cancer Lett*, 265: 135-47.

Coyne, C. B., M. K. Vanhook, T. M. Gambling, J. L. Carson, R. C. Boucher, and L. G. Johnson. 2002a. 'Regulation of airway tight junctions by proinflammatory cytokines', *Mol Biol Cell*, 13: 3218-34.

Coyne, Carolyn B., Miriam K. Vanhook, Todd M. Gambling, Johnny L. Carson, Richard C. Boucher, and Larry G. Johnson. 2002b. 'Regulation of Airway Tight Junctions by Proinflammatory Cytokines', *Molecular Biology of the Cell*, 13: 3218-34.

Cui, Yuxia, and Richard S. Paules. 2010. 'Use of transcriptomics in understanding mechanisms of drug-induced toxicity', *Pharmacogenomics*, 11: 573-85.

Daston, George, and Pauline McNamee. 2005. 'Alternatives to Toxicity Testing in Animals: Challenges and Opportunities', *Environmental Health Perspectives - ENVIRON HEALTH PERSPECT*.

Devalia, J. L., H. Bayram, C. Rusznak, M. Calderon, R. J. Sapsford, M. A. Abdelaziz, J. Wang, and R. J. Davies. 1997. 'Mechanisms of pollution-induced airway disease: in vitro studies in the upper and lower airways', *Allergy*, 52: 45-51; discussion 57-8.

Devalia, J. L., H. Bayram, C. Rusznak, M. Calderón, R. J. Sapsford, M. A. Abdelaziz, J. Wang, and R. J. Davies. 1997. 'Mechanisms of pollution-induced airway disease: in vitro studies in the upper and lower airways', *Allergy*, 52: 45-51; discussion 57-8.

Di Toro, Dominic M., Joy A. McGrath, and David J. Hansen. 2000. 'Technical basis for narcotic chemicals and polycyclic aromatic hydrocarbon criteria. I. Water and tissue', *Environ Toxicol Chem*, 19: 1951-70.

Du, Jingjing, and Chuanyong Jing. 2018. 'Anthropogenic PAHs in lake sediments: a literature review (2002–2018)', *Environmental Science: Processes & Impacts*, 20: 1649-66.

EPA, U.S. 2010a. 'Development of a relative potency factor (RPF) approach for polycyclic aromatic hydrocarbon (PAH) mixtures'. http://cfpub.epa.gov/ncea/cfm/recordisplay.cfm?deid=194584.

———. 2010b. "Development of a Relative Potency Factor (Rpf) Approach for Polycyclic Aromatic Hydrocarbon (PAH) Mixtures (External Review Draft)." In, edited by U.S. Environmental Protection Agency. Washington, DC

Eun, Jung Woo, So Yeon Ryu, Ji Heon Noh, Min-Jae Lee, Ja-Jun Jang, Jae Chun Ryu, Kwang Hwa Jung, Jeong Kyu Kim, Hyun Jin Bae, Hongjian Xie, Su Young Kim, Sug Hyung Lee, Won Sang Park, Nam Jin Yoo, Jung Young Lee, and Suk Woo Nam. 2008. 'Discriminating the molecular basis of hepatotoxicity using the large-scale characteristic molecular signatures of toxicants by expression profiling analysis', *Toxicology*, 249: 176-83.

Ezzati, Majid, Alan D. Lopez, Anthony A. Rodgers, and Christopher J. L. Murray. 2004. "Comparative quantification of health risks : global and regional burden of disease attributable to selected major risk factors / edited by Majid Ezzati ... [et al.]." In. Geneva: World Health Organization.

Fan, X., and J. J. Chen. 2014. 'Role of Cdk1 in DNA damage-induced G1 checkpoint abrogation by the human papillomavirus E7 oncogene', *Cell Cycle*, 13: 3249-59.

Farmahin, R., A. Williams, B. Kuo, N. L. Chepelev, R. S. Thomas, T. S. Barton-Maclaren, I. H. Curran, A. Nong, M. G. Wade, and C. L. Yauk. 2017. 'Recommended approaches in the application of toxicogenomics to derive points of departure for chemical risk assessment', *Arch Toxicol*, 91: 2045-65.

Fei, L., Y. Ma, M. Zhang, X. Liu, Y. Luo, C. Wang, H. Zhang, W. Zhang, and Y. Han. 2017. 'RACK1 promotes lung cancer cell growth via an MCM7/RACK1/ Akt signaling complex', *Oncotarget*, 8: 40501-13.

Fei, Liangru, and Hongtao Xu. 2018. 'Role of MCM2–7 protein phosphorylation in human cancer cells', *Cell & Bioscience*, 8: 43.

Genualdi, Susan A., Robert K. Killin, Jim Woods, Glenn Wilson, David Schmedding, and Staci L. Massey Simonich. 2009. 'Trans-Pacific and Regional Atmospheric Transport of Polycyclic Aromatic Hydrocarbons and Pesticides in Biomass Burning Emissions to Western North America', *Environmental science & technology*, 43: 1061-66.

Goodale, Britton C., Susan C. Tilton, Margaret M. Corvi, Glenn R. Wilson, Derek B. Janszen, Kim A. Anderson, Katrina M. Waters, and Robert L. Tanguay. 2013. 'Structurally distinct polycyclic aromatic hydrocarbons induce

differential transcriptional responses in developing zebrafish', *Toxicology and applied pharmacology*, 272: 656-70.

Gottmann, E., S. Kramer, B. Pfahringer, and C. Helma. 2001. 'Data quality in predictive toxicology: reproducibility of rodent carcinogenicity experiments', *Environ Health Perspect*, 109: 509-14.

Guo, X., and N. Mei. 2018. 'Benchmark Dose Modeling of In Vitro Genotoxicity Data: a Reanalysis', *Toxicol Res*, 34: 303-10.

Gusenleitner, D., S. S. Auerbach, T. Melia, H. F. Gomez, D. H. Sherr, and S. Monti. 2014. 'Genomic models of short-term exposure accurately predict long-term chemical carcinogenicity and identify putative mechanisms of action', *PLoS One*, 9: e102579.

Hanzalova, Katerina, Pavel Rossner, and Radim J. Sram. 2010. 'Oxidative damage induced by carcinogenic polycyclic aromatic hydrocarbons and organic extracts from urban air particulate matter', *Mutation Research/Genetic Toxicology and Environmental Mutagenesis*, 696: 114-21.

Heijne, Wilbert H. M., Anne S. Kienhuis, Ben van Ommen, Rob H. Stierum, and John P. Groten. 2005. 'Systems toxicology: applications of toxicogenomics, transcriptomics, proteomics and metabolomics in toxicology', *Expert Review of Proteomics*, 2: 767-80.

Hsing, A., Douglas Faller, and C. Vaziri. 2000. 'DNA-damaging aryl hydrocarbons induce Mdm2 expression via p53-independent post-transcriptional mechanisms', *J Biol Chem*, 275: 26024-31.

Huang, Tzu-Hsuan, Longfei Huo, Ying-Nai Wang, Weiya Xia, Yongkun Wei, Shih-Shin Chang, Wei-Chao Chang, Yueh-Fu Fang, Chun-Te Chen, Jing-Yu Lang, Chun Tu, Yan Wang, Ming-Chuan Hsu, Hsu-Ping Kuo, How-Wen Ko, Jia Shen, Heng-Huan Lee, Pei-Chih Lee, Yun Wu, Chung-Hsuan Chen, and Mien-Chie Hung. 2013. 'Epidermal growth factor receptor potentiates MCM7-mediated DNA replication through tyrosine phosphorylation of Lyn kinase in human cancers', *Cancer cell*, 23: 796-810.

IARC. 2010a. 'Some non-heterocyclic polycyclic aromatic hydrocarbons and some related exposures', *IARC Monographs and the Evaluation of Carcinogenic Risks to Humans*, 92.

———. 2010b. 'Some non-heterocyclic polycyclic aromatic hydrocarbons and some related exposures. Monographs on the evaluation of carcinogenic risks to humans.', *IARC MONOGRAPHS ON THE EVALUATION OF CARCINOGENIC RISKS TO HUMANS*, 92.

———. 2010c. *Some non-heterocyclic polycyclic aromatic hydrocarbons and some related occupational exposures* (IARC Press ;

Distributed by World Health Organization: Lyon, France

Geneva).

———. 2013. 'Diesel and Gasoline Engine Exhausts and Some Nitroarenes', *IARC Monographs and the Evaluation of Carcinogenic Risks to Humans*, 105.

———. 2014. 'Diesel and gasoline engine exhausts and some nitrarenes', *IARC MONOGRAPHS ON THE EVALUATION OF CARCINOGENIC RISKS TO HUMANS*, 105.

———. 2015. 'Outdoor Air Pollution', *IARC Monographs and the Evaluation of Carcinogenic Risks to Humans*, 109.

IARC Working Group on the Evaluation of Carcinogenic Risks to Humans., World Health Organization., and International Agency for Research on Cancer. 2013. *Bitumens and bitumen emissions, and some N- and S-heterocyclic polycyclic aromatic hydrocarbons* (IARC Press: Lyon).

Incardona, J. P., H. L. Day, T. K. Collier, and N. L. Scholz. 2006. 'Developmental toxicity of 4-ring polycyclic aromatic hydrocarbons in zebrafish is differentially dependent on AH receptor isoforms and hepatic cytochrome P4501A metabolism', *Toxicol Appl Pharmacol*, 217: 308-21.

Innes, Anh L., Prescott G. Woodruff, Ronald E. Ferrando, Samantha Donnelly, Gregory M. Dolganov, Stephen C. Lazarus, and John V. Fahy. 2006. 'Epithelial Mucin Stores Are Increased in the Large Airways of Smokers With Airflow Obstruction', *Chest*, 130: 1102-08.

Iwabuchi, K., P. L. Bartel, B. Li, R. Marraccino, and S. Fields. 1994. 'Two cellular proteins that bind to wild-type but not mutant p53', *Proc Natl Acad Sci U S A*, 91: 6098-102.

Jarvis, I. W., K. Dreij, A. Mattsson, B. Jernstrom, and U. Stenius. 2014. 'Interactions between polycyclic aromatic hydrocarbons in complex mixtures and implications for cancer risk assessment', *Toxicology*, 321: 27-39.

Karp, P. H., T. O. Moninger, S. P. Weber, T. S. Nesselhauf, J. L. Launspach, J. Zabner, and M. J. Welsh. 2002. 'An in vitro model of differentiated human airway epithelia. Methods for establishing primary cultures', *Methods Mol Biol*, 188: 115-37.

Kensler, T. W., N. Wakabayashi, and S. Biswal. 2007. 'Cell survival responses to environmental stresses via the Keap1-Nrf2-ARE pathway', *Annu Rev Pharmacol Toxicol*, 47: 89-116.

Killin, Robert K., Staci L. Simonich, Daniel A. Jaffe, Cindy L. DeForest, and Glenn R. Wilson. 2004. 'Transpacific and regional atmospheric transport of anthropogenic semivolatile organic compounds to Cheeka Peak Observatory during the spring of 2002', *Journal of Geophysical Research: Atmospheres*, 109.

Kim, Ji-Young, Jung Kwon, Ja Eun Kim, Woo Suk Koh, Moon-Koo Chung, Seokjoo Yoon, Chang Woo Song, and Michael Lee. 2005. 'Identification of potential biomarkers of genotoxicity and carcinogenicity in L5178Y mouse lymphoma cells by cDNA microarray analysis', *Environmental and Molecular Mutagenesis*, 45: 80-89.

Kimlin, L., J. Kassis, and V. Virador. 2013. '3D in vitro tissue models and their potential for drug screening', *Expert Opin Drug Discov*, 8: 1455-66.

Kopec, A. K., L. D. Burgoon, D. Ibrahim-Aibo, A. R. Burg, A. W. Lee, C. Tashiro, D. Potter, B. Sharratt, J. R. Harkema, J. C. Rowlands, R. A. Budinsky, and T. R. Zacharewski. 2010. 'Automated dose-response analysis and comparative toxicogenomic evaluation of the hepatic effects elicited by TCDD, TCDF, and PCB126 in C57BL/6 mice', *Toxicol Sci*, 118: 286-97.

Kopec, A. K., M. L. D'Souza, B. D. Mets, L. D. Burgoon, S. E. Reese, K. J. Archer, D. Potter, C. Tashiro, B. Sharratt, J. R. Harkema, and T. R. Zacharewski. 2011. 'Non-additive hepatic gene expression elicited by 2,3,7,8-tetrachlorodibenzo-p-dioxin (TCDD) and 2,2',4,4',5,5'-hexachlorobiphenyl (PCB153) co-treatment in C57BL/6 mice', *Toxicol Appl Pharmacol*, 256: 154-67.

Krewski, Daniel, Daniel Acosta, Melvin Andersen, Henry Anderson, John C. Bailar, Kim Boekelheide, Robert Brent, Gail Charnley, Vivian G. Cheung, Sidney Green, Karl T. Kelsey, Nancy I. Kerkvliet, Abby A. Li, Lawrence McCray, Otto Meyer, Reid D. Patterson, William Pennie, Robert A. Scala, Gina M. Solomon, Martin Stephens, James Yager, Lauren Zeise, Testing Staff of Committee on Toxicity, and Agents Assessment of Environmental. 2010. 'Toxicity Testing in the 21st Century: A Vision and a Strategy', *Journal of Toxicology and Environmental Health, Part B*, 13: 51-138.

Kummer, V., J. Maskova, Z. Zraly, J. Neca, P. Simeckova, J. Vondracek, and M. Machala. 2008. 'Estrogenic activity of environmental polycyclic aromatic hydrocarbons in uterus of immature Wistar rats', *Toxicol Lett*, 180: 212-21.

Labib, S., A. Williams, C. H. Guo, K. Leingartner, V. M. Arlt, H. H. Schmeiser, C. L. Yauk, P. A. White, and S. Halappanavar. 2016. 'Comparative transcriptomic analyses to scrutinize the assumption that genotoxic PAHs exert effects via a common mode of action', *Arch Toxicol*, 90: 2461-80.

Labib, Sarah, Andrew Williams, Byron Kuo, Carole L. Yauk, Paul A. White, and Sabina Halappanavar. 2017. 'A framework for the use of single-chemical transcriptomics data in predicting the hazards associated with complex mixtures of polycyclic aromatic hydrocarbons', *Arch Toxicol*, 91: 2599-616.

Lafontaine, Scott, Jill Schrlau, Jack Butler, Yuling Jia, Barbara Harper, Stuart Harris, Lisa M. Bramer, Katrina M. Waters, Anna Harding, and Staci L. Massey Simonich. 2015. 'Relative Influence of Trans-Pacific and Regional Atmospheric Transport of PAHs in the Pacific Northwest, U.S', *Environmental science & technology*, 49: 13807-16.

Langfelder, P., and S. Horvath. 2008. 'WGCNA: an R package for weighted correlation network analysis', *BMC Bioinformatics*, 9: 559.

Larkin, A., L. K. Siddens, S. K. Krueger, S. C. Tilton, K. M. Waters, D. E. Williams, and W. M. Baird. 2013. 'Application of a fuzzy neural network

model in predicting polycyclic aromatic hydrocarbon-mediated perturbations of the Cyp1b1 transcriptional regulatory network in mouse skin', *Toxicol Appl Pharmacol*, 267: 192-9.

Lee, Seul Ji, Young Na Yum, Sang Cheol Kim, Yuneung Kim, Johan Lim, Won Jun Lee, Kyung Hye Koo, Joo Hwan Kim, Jee Eun Kim, Woo Sun Lee, Soojung Sohn, Sue Nie Park, Jeong Hill Park, Jeongmi Lee, and Sung Won Kwon. 2013. 'Distinguishing between genotoxic and non-genotoxic hepatocarcinogens by gene expression profiling and bioinformatic pathway analysis', *Sci Rep*, 3: 2783.

Liao, Y., G. K. Smyth, and W. Shi. 2014. 'featureCounts: an efficient general purpose program for assigning sequence reads to genomic features', *Bioinformatics*, 30: 923-30.

Libalova, Helena, Pavel Rossner, Kristyna Vrbova, Tana Brzicova, Jitka Sikorova, Michal Vojtisek-Lom, Vit Beranek, Jiri Klema, Miroslav Ciganek, Jiri Neca, Miroslav Machala, and Jan Topinka. 2018. 'Transcriptional response to organic compounds from diverse gasoline and biogasoline fuel emissions in human lung cells', *Toxicology in Vitro*, 48: 329-41.

Love, M. I., W. Huber, and S. Anders. 2014a. 'Moderated estimation of fold change and dispersion for RNA-seq data with DESeq2', *Genome Biol*, 15: 550.

Love, Michael I., Wolfgang Huber, and Simon Anders. 2014b. 'Moderated estimation of fold change and dispersion for RNA-seq data with DESeq2', *Genome Biology*, 15: 550.

Mackay, Donald, and Daryl Callcott. 1998. 'Partitioning and Physical Chemical Properties of PAHs.' in Alasdair H. Neilson (ed.), *PAHs and Related Compounds: Chemistry* (Springer Berlin Heidelberg: Berlin, Heidelberg).

Maertens, Alexandra, Thomas Luechtefeld, Andre Kleensang, and Thomas Hartung. 2015. 'MPTP's Pathway of Toxicity Indicates Central Role of Transcription Factor SP1', *Arch Toxicol*, 89: 743-55.

Maertens, Alexandra, Vy Tran, Andre Kleensang, and Thomas Hartung. 2018. 'Weighted Gene Correlation Network Analysis (WGCNA) Reveals Novel Transcription Factors Associated With Bisphenol A Dose-Response', *Frontiers in Genetics*, 9.

Magkoufopoulou, C., S. M. H. Claessen, M. Tsamou, D. G. J. Jennen, J. C. S. Kleinjans, and J. H. M. van Delft. 2012. 'A transcriptomics-based in vitro assay for predicting chemical genotoxicity in vivo', *Carcinogenesis*, 33: 1421-29.

Marston, C. P., C. Pereira, J. Ferguson, K. Fischer, O. Hedstrom, W. M. Dashwood, and W. M. Baird. 2001. 'Effect of a complex environmental mixture from coal tar containing polycyclic aromatic hydrocarbons (PAH) on the tumor initiation, PAH-DNA binding and metabolic activation of carcinogenic PAH in mouse epidermis', *Carcinogenesis*, 22: 1077-86.

Mathijs, Karen, Karen J. J. Brauers, Danyel G. J. Jennen, Andre Boorsma, Marcel H. M. van Herwijnen, Ralph W. H. Gottschalk, Jos C. S. Kleinjans, and

Joost H. M. van Delft. 2009. 'Discrimination for Genotoxic and Nongenotoxic Carcinogens by Gene Expression Profiling in Primary Mouse Hepatocytes Improves with Exposure Time', *Toxicological Sciences*, 112: 374-84.

Mathis, Carole, Carine Poussin, Dirk Weisensee, Stephan Gebel, Arnd Hengstermann, Alain Sewer, Vincenzo Belcastro, Yang Xiang, Sam Ansari, Sandra Wagner, Julia Hoeng, and Manuel C. Peitsch. 2013. 'Human bronchial epithelial cells exposed in vitro to cigarette smoke at the air-liquid interface resemble bronchial epithelium from human smokers', *American Journal of Physiology - Lung Cellular and Molecular Physiology*, 304: L489-L503.

McGarry, M. A., G. D. Charles, T. Medrano, M. R. Bubb, M. B. Grant, M. Campbell-Thompson, and K. T. Shiverick. 2002. 'Benzo(a)pyrene, but not 2,3,7,8-tetrachlorodibenzo-p-dioxin, alters cell adhesion proteins in human uterine RL95-2 cells', *Biochem Biophys Res Commun*, 294: 101-7.

McKim, J. M., Jr. 2010. 'Building a tiered approach to in vitro predictive toxicity screening: a focus on assays with in vivo relevance', *Comb Chem High Throughput Screen*, 13: 188-206.

Mezencev, R., and S. S. Auerbach. 2020. 'The sensitivity of transcriptomics BMD modeling to the methods used for microarray data normalization', *PLoS One*, 15: e0232955.

Moffat, Ivy, Nikolai L. Chepelev, Sarah Labib, Julie Bourdon-Lacombe, Byron Kuo, Julie K. Buick, France Lemieux, Andrew Williams, Sabina Halappanavar, Amal I. Malik, Mirjam Luijten, Jiri Aubrecht, Daniel R. Hyduke, Albert J. Fornace, Carol D. Swartz, Leslie Recio, and Carole L. Yauk. 2015. 'Comparison of toxicogenomics and traditional approaches to inform mode of action and points of departure in human health risk assessment of benzo[a]pyrene in drinking water', 45: 1-43.

Moorthy, B., C. Chu, and D. J. Carlin. 2015. 'Polycyclic aromatic hydrocarbons: from metabolism to lung cancer', *Toxicol Sci*, 145: 5-15.

Müllers, Erik, Helena Silva Cascales, Kamila Burdova, Libor Macurek, and Arne Lindqvist. 2017. 'Residual Cdk1/2 activity after DNA damage promotes senescence', *Aging cell*, 16: 575-84.

Nikolsky, Y., E. Kirillov, R. Zuev, E. Rakhmatulin, and T. Nikolskaya. 2009. 'Functional analysis of OMICs data and small molecule compounds in an integrated "knowledge-based" platform', *Methods Mol Biol*, 563: 177-96.

Nookaew, I., M. Papini, N. Pornputtapong, G. Scalcinati, L. Fagerberg, M. Uhlen, and J. Nielsen. 2012. 'A comprehensive comparison of RNA-Seq-based transcriptome analysis from reads to differential gene expression and cross-comparison with microarrays: a case study in Saccharomyces cerevisiae', *Nucleic Acids Res*, 40: 10084-97.

Oesterling, E., M. Toborek, and B. Hennig. 2008. 'Benzo[a]pyrene induces intercellular adhesion molecule-1 through a caveolae and aryl hydrocarbon receptor mediated pathway', *Toxicol Appl Pharmacol*, 232: 309-16.

Oliveira, Marta, Klara Slezakova, Cristina Delerue-Matos, Maria Carmo Pereira, and Simone Morais. 2019. 'Children environmental exposure to particulate matter and polycyclic aromatic hydrocarbons and biomonitoring in school environments: A review on indoor and outdoor exposure levels, major sources and health impacts', *Environment International*, 124: 180-204.

Olson, M. F., and E. Sahai. 2009. 'The actin cytoskeleton in cancer cell motility', *Clin Exp Metastasis*, 26: 273-87.

Park, Jong-Heum, Andrea B. Troxel, Ronald G. Harvey, and Trevor M. Penning. 2006. 'Polycyclic Aromatic Hydrocarbon (PAH) o-Quinones Produced by the Aldo-Keto-Reductases (AKRs) Generate Abasic Sites, Oxidized Pyrimidines, and 8-Oxo-dGuo via Reactive Oxygen Species', *Chem Res Toxicol*, 19: 719-28.

Penning, Trevor M., Michael E. Burczynski, Chien-Fu Hung, Kirsten D. McCoull, Nisha T. Palackal, and Laurie S. Tsuruda. 1999. 'Dihydrodiol Dehydrogenases and Polycyclic Aromatic Hydrocarbon Activation: Generation of Reactive and Redox Active o-Quinones', *Chem Res Toxicol*, 12: 1-18.

Pereira, Wilfred E., Frances D. Hostettler, Samuel N. Luoma, Alexander van Geen, Christopher C. Fuller, and Roberto J. Anima. 1999. 'Sedimentary record of anthropogenic and biogenic polycyclic aromatic hydrocarbons in San Francisco Bay, California', *Marine Chemistry*, 64: 99-113.

Pezzulo, A. A., T. D. Starner, T. E. Scheetz, G. L. Traver, A. E. Tilley, B. G. Harvey, R. G. Crystal, P. B. McCray, Jr., and J. Zabner. 2011. 'The air-liquid interface and use of primary cell cultures are important to recapitulate the transcriptional profile of in vivo airway epithelia', *Am J Physiol Lung Cell Mol Physiol*, 300: L25-31.

Phillips, David H., Volker M. Arlt, Dagmar Aimová, Marie Stiborová, C. Roland Wolf, Colin J. Henderson, Markus Thiemann, Oliver J. Schmitz, Eva Frei, Peter B. Farmer, Rajinder Singh, and Gonçalo Gamboa da Costa. 2008. 'Metabolic activation of benzo[a]pyrene in vitro by hepatic cytochrome P450 contrasts with detoxification in vivo : experiments with hepatic cytochrome P450 reductase null mice', *Carcinogenesis*, 29: 656-65.

Phillips, Jason R., Daniel L. Svoboda, Arpit Tandon, Shyam Patel, Alex Sedykh, Deepak Mav, Byron Kuo, Carole L. Yauk, Longlong Yang, Russell S. Thomas, Jeff S. Gift, J. Allen Davis, Louis Olszyk, B. Alex Merrick, Richard S. Paules, Fred Parham, Trey Saddler, Ruchir R. Shah, and Scott S. Auerbach. 2019. 'BMDExpress 2: enhanced transcriptomic dose-response analysis workflow', *Bioinformatics*, 35: 1780-82.

Piberger, Ann Liza, Christopher T. Krüger, Bettina M. Strauch, Beatrice Schneider, and Andrea Hartwig. 2018. 'BPDE-induced genotoxicity: relationship between DNA adducts, mutagenicity in the in vitro PIG-A assay, and the transcriptional response to DNA damage in TK6 cells', *Arch Toxicol*, 92: 541-51.

Plíšková, Martina, Jan Vondráček, Bořivoj Vojtěšek, Alois Kozubík, and Miroslav Machala. 2004. 'Deregulation of Cell Proliferation by Polycyclic

Aromatic Hydrocarbons in Human Breast Carcinoma MCF-7 Cells Reflects Both Genotoxic and Nongenotoxic Events', *Toxicological Sciences*, 83: 246-56.

Rager, Julia E., Scott S. Auerbach, Grace A. Chappell, Elizabeth Martin, Chad M. Thompson, and Rebecca C. Fry. 2017. 'Benchmark Dose Modeling Estimates of the Concentrations of Inorganic Arsenic That Induce Changes to the Neonatal Transcriptome, Proteome, and Epigenome in a Pregnancy Cohort', *Chemical Research in Toxicology*, 30: 1911-20.

Ramesh, A., A. Archibong, D.B. Hood, Z. Guo, and B.G. Loganathan. 2011. *Global environmental distribution and human health effects of polycyclic aromatic hydrocarbons* (CRC Press: Boca Raton, FL).

Ravindra, Khaiwal, Ranjeet Sokhi, and René Van Grieken. 2008. 'Atmospheric polycyclic aromatic hydrocarbons: Source attribution, emission factors and regulation', *Atmospheric Environment*, 42: 2895-921.

Rengarajan, Thamaraiselvan, Peramaiyan Rajendran, Natarajan Nandakumar, Boopathy Lokeshkumar, Palaniswami Rajendran, and Ikuo Nishigaki. 2015. 'Exposure to polycyclic aromatic hydrocarbons with special focus on cancer', *Asian Pacific Journal of Tropical Biomedicine*, 5: 182-89.

Ross, J. A., G. B. Nelson, K. H. Wilson, J. R. Rabinowitz, A. Galati, G. D. Stoner, S. Nesnow, and M. J. Mass. 1995. 'Adenomas induced by polycyclic aromatic hydrocarbons in strain A/J mouse lung correlate with time-integrated DNA adduct levels', *Cancer Res*, 55: 1039-44.

Saeed, A. I., V. Sharov, J. White, J. Li, W. Liang, N. Bhagabati, J. Braisted, M. Klapa, T. Currier, M. Thiagarajan, A. Sturn, M. Snuffin, A. Rezantsev, D. Popov, A. Ryltsov, E. Kostukovich, I. Borisovsky, Z. Liu, A. Vinsavich, V. Trush, and J. Quackenbush. 2003. 'TM4: a free, open-source system for microarray data management and analysis', *Biotechniques*, 34: 374-8.

Samburova, Vera, Barbara Zielinska, and Andrey Khlystov. 2017. 'Do 16 Polycyclic Aromatic Hydrocarbons Represent PAH Air Toxicity?', *Toxics*, 5: 17.

Samuels-Lev, Y, DJ O'Connor, D Bergamaschi, G Trigiante, JK Hsieh, S Zhong, I Campargue, L Naumovski, T Crook, and X Lu. 2001. 'ASPP proteins specifically stimulate the apoptotic function of p53', *Molecular cell*, 8: 781-94.

Schamberger, A. C., N. Mise, J. Jia, E. Genoyer, AÖ Yildirim, S. Meiners, and O. Eickelberg. 2014a. 'Cigarette smoke-induced disruption of bronchial epithelial tight junctions is prevented by transforming growth factor-β', *Am J Respir Cell Mol Biol*, 50: 1040-52.

Schamberger, Andrea C., Nikica Mise, Jie Jia, Emmanuelle Genoyer, Ali Ö. Yildirim, Silke Meiners, and Oliver Eickelberg. 2014b. 'Cigarette Smoke–Induced Disruption of Bronchial Epithelial Tight Junctions Is Prevented by Transforming Growth Factor-β', *American Journal of Respiratory Cell and Molecular Biology*, 50: 1040-52.

Schwermer, Melanie, Sangkyun Lee, Johannes Köster, Tom van Maerken, Harald Stephan, Angelika Eggert, Katharina Morik, Johannes H. Schulte, and

Alexander Schramm. 2015. 'Sensitivity to cdk1-inhibition is modulated by p53 status in preclinical models of embryonal tumors', *Oncotarget*, 6: 15425-35.

Shannon, P., A. Markiel, O. Ozier, N. S. Baliga, J. T. Wang, D. Ramage, N. Amin, B. Schwikowski, and T. Ideker. 2003. 'Cytoscape: a software environment for integrated models of biomolecular interaction networks', *Genome Res*, 13.

Shao, K., and A. J. Shapiro. 2018. 'A Web-Based System for Bayesian Benchmark Dose Estimation', *Environ Health Perspect*, 126: 017002.

Shi, Q., R. R. Fijten, D. Spina, Y. Riffo Vasquez, V. M. Arlt, R. W. Godschalk, and F. J. Van Schooten. 2017. 'Altered gene expression profiles in the lungs of benzo[a]pyrene-exposed mice in the presence of lipopolysaccharide-induced pulmonary inflammation', *Toxicol Appl Pharmacol*, 336: 8-19.

Shi, Q., R. W. L. Godschalk, and F. J. van Schooten. 2017. 'Inflammation and the chemical carcinogen benzo[a]pyrene: Partners in crime', *Mutat Res*, 774: 12-24.

Siddens, L. K., K. L. Bunde, T. A. Harper, Jr., T. J. McQuistan, C. V. Lohr, L. M. Bramer, K. M. Waters, S. C. Tilton, S. K. Krueger, D. E. Williams, and W. M. Baird. 2015. 'Cytochrome P450 1b1 in polycyclic aromatic hydrocarbon (PAH)-induced skin carcinogenesis: Tumorigenicity of individual PAHs and coal-tar extract, DNA adduction and expression of select genes in the Cyp1b1 knockout mouse', *Toxicol Appl Pharmacol*, 287: 149-60.

Siddens, L. K., A. Larkin, S. K. Krueger, C. A. Bradfield, K. M. Waters, S. C. Tilton, C. B. Pereira, C. V. Lohr, V. M. Arlt, D. H. Phillips, D. E. Williams, and W. M. Baird. 2012. 'Polycyclic aromatic hydrocarbons as skin carcinogens: comparison of benzo[a]pyrene, dibenzo[def,p]chrysene and three environmental mixtures in the FVB/N mouse', *Toxicol Appl Pharmacol*, 264: 377-86.

Siddens, Lisbeth K., Kristi L. Bunde, Tod A. Harper, Tammie J. McQuistan, Christiane V. Löhr, Lisa M. Bramer, Katrina M. Waters, Susan C. Tilton, Sharon K. Krueger, David E. Williams, and William M. Baird. 2015. 'Cytochrome P450 1b1 in polycyclic aromatic hydrocarbon (PAH)-induced skin carcinogenesis: Tumorigenicity of individual PAHs and coal-tar extract, DNA adduction and expression of select genes in the Cyp1b1 knockout mouse', *Toxicology and applied pharmacology*, 287: 149-60.

Siddens, Lisbeth K., Andrew Larkin, Sharon K. Krueger, Christopher A. Bradfield, Katrina M. Waters, Susan C. Tilton, Cliff B. Pereira, Christiane V. Löhr, Volker M. Arlt, David H. Phillips, David E. Williams, and William M. Baird. 2012. 'Polycyclic aromatic hydrocarbons as skin carcinogens: Comparison of benzo[a]pyrene, dibenzo[def,p]chrysene and three environmental mixtures in the FVB/N mouse', *Toxicology and applied pharmacology*, 264: 377-86.

Sievers, Chelsie K., Erin K. Shanle, Christopher A. Bradfield, and Wei Xu. 2013. 'Differential action of monohydroxylated polycyclic aromatic hydrocarbons with estrogen receptors α and β', *Toxicol Sci*, 132: 359-67.

Sigal, Alex, and Varda Rotter. 2000. 'Oncogenic Mutations of the p53 Tumor Suppressor: The Demons of the Guardian of the Genome', *Cancer Res*, 60: 6788.

Smith, Dennis A. 1991. 'Species Differences in Metabolism and Pharmacokinetics: Are We Close to an Understanding?', *Drug Metabolism Reviews*, 23: 355-73.

Smith, Kirk, Sumi Mehta, and Mirjam Maeusezahl-feuz. 2004. 'Indoor Air Pollution from Household Use of Solid Fuels." Comparative Quantification of Health Risks 18:1435–1492'.

Smith, Maren L., Marcelo F. Lopez, Kellie J. Archer, Aaron R. Wolen, Howard C. Becker, and Michael F. Miles. 2016. 'Time-Course Analysis of Brain Regional Expression Network Responses to Chronic Intermittent Ethanol and Withdrawal: Implications for Mechanisms Underlying Excessive Ethanol Consumption', *PLoS One*, 11: e0146257.

Song, M. K., Y. J. Kim, M. Song, H. S. Choi, Y. K. Park, and J. C. Ryu. 2011. 'Polycyclic aromatic hydrocarbons induce migration in human hepatocellular carcinoma cells (HepG2) through reactive oxygen species-mediated p38 MAPK signal transduction', *Cancer Sci*, 102: 1636-44.

Song, M. K., M. Song, H. S. Choi, Y. J. Kim, Y. K. Park, and J. C. Ryu. 2012. 'Identification of molecular signatures predicting the carcinogenicity of polycyclic aromatic hydrocarbons (PAHs)', *Toxicol Lett*, 212: 18-28.

Spies, R. B., and D. W. Rice. 1988. 'Effects of organic contaminants on reproduction of the starry flounder Platichthys stellatus in San Francisco Bay', *Marine Biology*, 98: 191-200.

Sridhar, S., F. Schembri, J. Zeskind, V. Shah, A. M. Gustafson, K. Steiling, G. Liu, Y. M. Dumas, X. Zhang, J. S. Brody, M. E. Lenburg, and A. Spira. 2008. 'Smoking-induced gene expression changes in the bronchial airway are reflected in nasal and buccal epithelium', *BMC Genomics*, 9: 259.

Staal, Yvonne C. M., Marcel H. M. van Herwijnen, Frederik J. van Schooten, and Joost H. M. van Delft. 2006. 'Modulation of gene expression and DNA adduct formation in HepG2 cells by polycyclic aromatic hydrocarbons with different carcinogenic potencies', *Carcinogenesis*, 27: 646-55.

Sullivan, A., and X. Lu. 2007. 'ASPP: a new family of oncogenes and tumour suppressor genes', *British Journal of Cancer*, 96: 196-200.

Sun, Tao, Simon Jackson, John W. Haycock, and Sheila MacNeil. 2006. 'Culture of skin cells in 3D rather than 2D improves their ability to survive exposure to cytotoxic agents', *Journal of Biotechnology*, 122: 372-81.

Sutherland, J. J., Y. W. Webster, J. A. Willy, G. H. Searfoss, K. M. Goldstein, A. R. Irizarry, D. G. Hall, and J. L. Stevens. 2018. 'Toxicogenomic module associations with pathogenesis: a network-based approach to understanding drug toxicity', *The Pharmacogenomics Journal*, 18: 377-90.

Sutherland, Jeffrey J., Robert A. Jolly, Keith M. Goldstein, and James L. Stevens. 2016. 'Assessing Concordance of Drug-Induced Transcriptional Response in Rodent Liver and Cultured Hepatocytes', *PLOS Computational Biology*, 12: e1004847.

Sverdrup, Line E., Torben Nielsen, and Paul Henning Krogh. 2002. 'Soil Ecotoxicity of Polycyclic Aromatic Hydrocarbons in Relation to Soil Sorption, Lipophilicity, and Water Solubility', *Environmental science & technology*, 36: 2429-35.

Tarantini, A., A. Maitre, E. Lefebvre, M. Marques, A. Rajhi, and T. Douki. 2011. 'Polycyclic aromatic hydrocarbons in binary mixtures modulate the efficiency of benzo[a]pyrene to form DNA adducts in human cells', *Toxicology*, 279: 36-44.

Team, AEGIS Study. 2017. 'Shared Gene Expression Alterations in Nasal and Bronchial Epithelium for Lung Cancer Detection', *J Natl Cancer Inst*, 109.

Thyssen, J., J. Althoff, G. Kimmerle, and U. Mohr. 1981. 'Inhalation studies with benzo[a]pyrene in Syrian golden hamsters', *J Natl Cancer Inst*, 66: 575-7.

Tilton, S. C., L. K. Siddens, S. K. Krueger, A. J. Larkin, C. V. Lohr, D. E. Williams, W. M. Baird, and K. M. Waters. 2015. 'Mechanism-Based Classification of PAH Mixtures to Predict Carcinogenic Potential', *Toxicol Sci*, 146: 135-45.

Topinka, J., L. R. Schwarz, F. Kiefer, F. J. Wiebel, O. Gajdoš, P. Vidová, L. Dobiáš, M. Fried, R. J. Šrám, and T. Wolff. 1998. 'DNA adduct formation in mammalian cell cultures by polycyclic aromatic hydrocarbons (PAH) and nitro-PAH in coke oven emission extract', *Mutation Research/Genetic Toxicology and Environmental Mutagenesis*, 419: 91-105.

Trapnell, C., L. Pachter, and S. L. Salzberg. 2009. 'TopHat: discovering splice junctions with RNA-Seq', *Bioinformatics*, 25: 1105-11.

Trapnell, C., A. Roberts, L. Goff, G. Pertea, D. Kim, D. R. Kelley, H. Pimentel, S. L. Salzberg, J. L. Rinn, and L. Pachter. 2012. 'Differential gene and transcript expression analysis of RNA-seq experiments with TopHat and Cufflinks', *Nat Protoc*, 7: 562-78.

Trapnell, C., B. A. Williams, G. Pertea, A. Mortazavi, G. Kwan, M. J. van Baren, S. L. Salzberg, B. J. Wold, and L. Pachter. 2010. 'Transcript assembly and quantification by RNA-Seq reveals unannotated transcripts and isoform switching during cell differentiation', *Nat Biotechnol*, 28: 511-5.

Tung, E. W., N. A. Philbrook, C. L. Belanger, S. Ansari, and L. M. Winn. 2014. 'Benzo[a]pyrene increases DNA double strand break repair in vitro and in vivo: a possible mechanism for benzo[a]pyrene-induced toxicity', *Mutat Res Genet Toxicol Environ Mutagen*, 760: 64-9.

Turpeinen, M., C. Ghiciuc, M. Opritoui, L. Tursas, O. Pelkonen, and M. Pasanen. 2007. 'Predictive value of animal models for human cytochrome P450 (CYP)-mediated metabolism: A comparative study in vitro', *Xenobiotica*, 37: 1367-77.

Upham, B. L., S. J. Masten, B. R. Lockwood, and J. E. Trosko. 1994a. 'Nongenotoxic effects of polycyclic aromatic hydrocarbons and their

oxygenation by-products on the intercellular communication of rat liver epithelial cells', *Fundam Appl Toxicol*, 23: 470-5.

Upham, Brad L., Susan J. Masten, Beth R. Lockwood, and James E. Trosko. 1994b. 'Nongenotoxic Effects of Polycyclic Aromatic Hydrocarbons and Their Ozonation By-Products on the Intercellular Communication of Rat Liver Epithelial Cells', *Toxicological Sciences*, 23: 470-75.

van Delft, J. H. M., E. van Agen, S. G. J. van Breda, M. H. Herwijnen, Y. C. M. Staal, and J. C. S. Kleinjans. 2004. 'Discrimination of genotoxic from non-genotoxic carcinogens by gene expression profiling', *Carcinogenesis*, 25: 1265-76.

———. 2005. 'Comparison of supervised clustering methods to discriminate genotoxic from non-genotoxic carcinogens by gene expression profiling', *Mutation Research/Fundamental and Molecular Mechanisms of Mutagenesis*, 575: 17-33.

Vondráček, Jan, Alois Kozubík, and Miroslav Machala. 2002. 'Modulation of Estrogen Receptor-Dependent Reporter Construct Activation and G0/G1–S-Phase Transition by Polycyclic Aromatic Hydrocarbons in Human Breast Carcinoma MCF-7 Cells', *Toxicological Sciences*, 70: 193-201.

Wang, J., B. J. Webb-Robertson, M. M. Matzke, S. M. Varnum, J. N. Brown, R. M. Riensche, J. N. Adkins, J. M. Jacobs, J. R. Hoidal, M. B. Scholand, J. G. Pounds, M. R. Blackburn, K. D. Rodland, and J. E. McDermott. 2013. 'A semiautomated framework for integrating expert knowledge into disease marker identification', *Dis Markers*, 35: 513-23.

Watanabe, Takashi, Takayoshi Suzuki, Masakatsu Natsume, Madoka Nakajima, Kazunori Narumi, Shuichi Hamada, Tomohiro Sakuma, Akiko Koeda, Keiyu Oshida, Yohei Miyamoto, Akihisa Maeda, Michiasa Hirayama, Hisakazu Sanada, Hiroshi Honda, Wakako Ohyama, Emiko Okada, Yohei Fujiishi, Shizuyo Sutou, Ayami Tadakuma, Yasuyoshi Ishikawa, Mahoko Kido, Rina Minamiguchi, Izumi Hanahara, and Chie Furihata. 2012. 'Discrimination of genotoxic and non-genotoxic hepatocarcinogens by statistical analysis based on gene expression profiling in the mouse liver as determined by quantitative real-time PCR', *Mutation Research/Genetic Toxicology and Environmental Mutagenesis*, 747: 164-75.

Webb-Robertson, Bobbie-Jo M., Thomas O. Metz, Katrina M. Waters, Qibin Zhang, and Marian Rewers. 2017. 'Bayesian Posterior Integration for Classification of Mass Spectrometry Data.' in Susmita Datta and Bart J. A. Mertens (eds.), *Statistical Analysis of Proteomics, Metabolomics, and Lipidomics Data Using Mass Spectrometry* (Springer International Publishing: Cham).

Webster, A. F., N. Chepelev, R. Gagne, B. Kuo, L. Recio, A. Williams, and C. L. Yauk. 2015. 'Impact of Genomics Platform and Statistical Filtering on Transcriptional Benchmark Doses (BMD) and Multiple Approaches for Selection of Chemical Point of Departure (PoD)', *PLoS One*, 10: e0136764.

White, Paul A. 2002. 'The genotoxicity of priority polycyclic aromatic hydrocarbons in complex mixtures', *Mutation Research/Genetic Toxicology and Environmental Mutagenesis*, 515: 85-98.

WHO. 2018. 'World Health Statistics 2016 data visualizations dashboard: Ambient and household air pollution attributable death rate (2016)', *World Health Organization Global Health Observatory*.

Wignall, J. A., E. Muratov, A. Sedykh, K. Z. Guyton, A. Tropsha, I. Rusyn, and W. A. Chiu. 2018. 'Conditional Toxicity Value (CTV) Predictor: An In Silico Approach for Generating Quantitative Risk Estimates for Chemicals', *Environ Health Perspect*, 126: 057008.

Williams, Andrew, Julie K. Buick, Ivy Moffat, Carol D. Swartz, Leslie Recio, Daniel R. Hyduke, Heng-Hong Li, Albert J. Fornace, Jiri Aubrecht, and Carole L. Yauk. 2015. 'A predictive toxicogenomics signature to classify genotoxic versus non-genotoxic chemicals in human TK6 cells', *Data in Brief*, 5: 77-83.

Williams, Antony J., Christopher M. Grulke, Jeff Edwards, Andrew D. McEachran, Kamel Mansouri, Nancy C. Baker, Grace Patlewicz, Imran Shah, John F. Wambaugh, Richard S. Judson, and Ann M. Richard. 2017. 'The CompTox Chemistry Dashboard: a community data resource for environmental chemistry', *Journal of Cheminformatics*, 9: 61.

Witt, Gesine, and Herbert Siegel. 2000. 'The Consequences of the Oder Flood in 1997 on the Distribution of Polycyclic Aromatic Hydrocarbons (PAHs) in the Oder River Estuary', *Marine Pollution Bulletin*, 40: 1124-31.

Witter, Barbara, Marcus Winkler, and Kurt Friese. 2003. 'Depth Distribution of Chlorinated and Polycyclic Aromatic Hydrocarbons in Floodplain Soils of the River', *Acta hydrochimica et hydrobiologica*, 31: 411-22.

Xia, Pu, Hanxin Zhang, Ying Peng, Wei Shi, and Xiaowei Zhang. 2020. 'Pathway-based assessment of single chemicals and mixtures by a high-throughput transcriptomics approach', *Environ Int*, 136: 105455.

Xiao, Hui, and Shivendra V. Singh. 2005. 'Cellular response to benzo[a]pyrene-7,8-diol-9,10-epoxide exposure in human lung cancer cells', *Cancer Res*, 65: 275.

Xuan, Botai, Deepraj Ghosh, Emily M. Cheney, Elizabeth M. Clifton, and Michelle R. Dawson. 2018. 'Dysregulation in Actin Cytoskeletal Organization Drives Increased Stiffness and Migratory Persistence in Polyploidal Giant Cancer Cells', *Sci Rep*, 8: 11935.

Yamaya, M., W. E. Finkbeiner, S. Y. Chun, and J. H. Widdicombe. 1992. 'Differentiated structure and function of cultures from human tracheal epithelium', *Am J Physiol*, 262: L713-24.

Yang, Longlong, Bruce C. Allen, and Russell S. Thomas. 2007. 'BMDExpress: a software tool for the benchmark dose analyses of genomic data', *BMC Genomics*, 8: 387.

Yang, Wan-Xia, Yun-Yan Pan, and Chong-Ge You. 2019. 'CDK1, CCNB1, CDC20, BUB1, MAD2L1, MCM3, BUB1B, MCM2, and RFC4 May Be

Potential Therapeutic Targets for Hepatocellular Carcinoma Using Integrated Bioinformatic Analysis', *Biomed Res Int*, 2019: 1245072.

Yu, C. H., F. Y. Xing, J. Y. Zhang, J. Q. Xu, and Y. C. Li. 2018. 'A combination of mRNA expression profile and miRNA expression profile identifies detection biomarkers in different tumor stages of laryngeal squamous cell carcinoma', *Eur Rev Med Pharmacol Sci*, 22: 7296-304.

Zavala, Jose, Bridget O'Brien, Kim Lichtveld, Kenneth G. Sexton, Ivan Rusyn, Ilona Jaspers, and William Vizuete. 2016. 'Assessment of Biological Responses of EpiAirway(™) 3-D Cell Constructs vs. A549 Cells for Determining Toxicity of Ambient Air Pollution', *Inhalation toxicology*, 28: 251-59.

Zhang, B., and S. Horvath. 2005. 'A general framework for weighted gene co-expression network analysis', *Stat Appl Genet Mol Biol*, 4: Article17.